Det Kgl. Danske Videnskabernes Selskab
Mathematisk-fysiske Meddelelser. I, 11.

ON THE LICHTENBERG FIGURES

PART I. A PRELIMINARY INVESTIGATION

BY

P. O. PEDERSEN

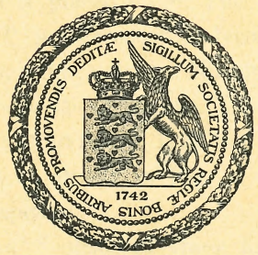

KØBENHAVN
HOVEDKOMMISSIONÆR: ANDR. FRED. HØST & SØN, KGL. HOF-BOGHANDEL
BIANCO LUNOS BOGTRYKKERI
1919

Chapter I.

Introduction and Historical Remarks.

THE LICHTENBERG dust figures can be made in many ways; one of the simplest is as follows: An electrically neutral plate P of ebonite (Fig. 1) is placed on a metal disk B. From the knob K of a Leyden jar L a spark is passed to the

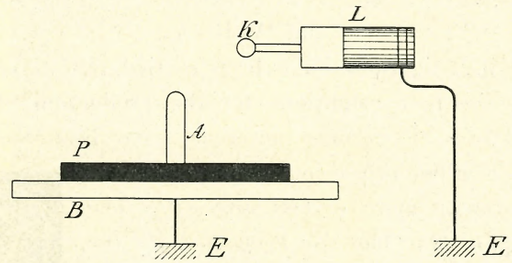

Fig. 1. Simple Lichtenberg Arrangement.

small metal rod A placed on P. The rod A is then removed and the plate P powdered with lycopodium, flour sulphur, or some other suitable powder. Mixtures of different powders may also be used with advantage. The dust settled on P then forms a LICHTENBERG figure. If K has been positive the shape of the figure is as shown in Fig. 2, while Fig. 3 shows the result for K negative.

LICHTENBERG[1,2] observed these figures for the first time in the year 1777*; since then they have formed the subject of a long series of investigations. And naturally so: the figures are beautiful and the difference between the positive and negative ones very striking. It may therefore be expected that a

* For references see the bibliography at the end of the paper.

closer study of this phenomenon would give valuable information on the nature of electricity, and the history of these figures is also very closely connected with the history of the theories of electricity — one fluid and two fluid theories —. At present the corresponding literature is mainly of historical interest and we shall therefore only call attention to the papers of P. F. Riess, E. Reitlinger, A. v. Waltenhofen, W. v. Bezold, W. G. Armstrong, A. Oberbeck, and W. Holtz.

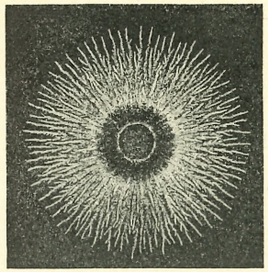

Fig. 2. Positive Lichtenberg Dust Figure. (Air; $p = 760$; $m = 0.8$*)

Many investigations have been carried out in order to ascertain the best conditions for the production of these figures. Plates of various materials have been tried and mixtures of differently coloured powders have been used with more or less success.** The photographic plate has also been used for the recording of transient electrical discharges by J. Brown (1888),[1] E. T. Trouvelot (1888),[1] K. Hansen (1916),[1] and others. These authors have, however, used such high voltages that rather complicated figures, like those in Figs. 4 and 5, have been obtained. Just recently M. Toepler (1917)[1] has published some beautiful photographs of »sliding« electrical discharges (Gleitfunken). All these figures are, however, so complicated that they do not invite a closer study of their features.

Fig. 3. Negative Dust Figure. (Air; $p = 760$; $m = 0.8$).

* In the following p denotes the gas pressure in millimetres of mercury, l the spark length in millimeters (see Fig. 10), D the diameter of the electrode A, d_0 thickness of insulating plate both in millimeters. m stands for magnification.

** v. Villarsy proposed 1788 the use of a mixture of red lead and flour sulphur. A mixture of 3 powders, viz Carnine, lycopodium, and sulphur has been used by K. Bürker[1].

W. G. Armstrong in 1897 published some simple photographic Lichtenberg figures. Especially some of his positive figures are remarkably pure and simple and many of his plates show very interesting features. The beautiful illustrations — partly in colours — of dust figures, which W. G. Armstrong and H. Stroud[1] published in 1899 also give much valuable information about the Lichtenberg figures.*

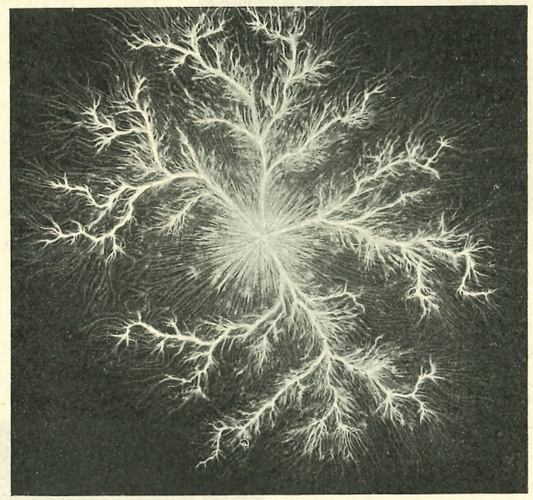

Fig. 4. Positive Discharge with High Voltage. (Air; $p = 760$; $l = 7$; $D = 0$; $d_0 = 1.4$; $m = 0.7$).

S. Mikola (1917) recently published some beautiful photographs of simple Lichtenberg figures — positive and negative — obtained direct on photographic plates. These figures are very regular and characteristical and exhibit very fine details. The photographical method of Mikola has been used almost exclusively throughout this investigation and this method is also — contrary to Mikola's own observation — applicable to Lichtenberg figures in hydrogen,

* This work of Lord Armstrong seems to be but little known; S. Mikola f. inst. does not mention it.

oxygen, and carbon dioxide, but the figures obtained in these gases are rather faint, especially at lower pressures.

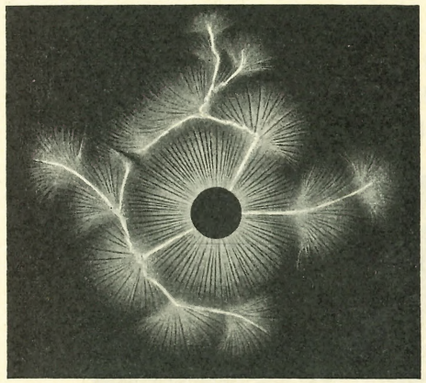

Fig. 5. Negative Discharge with High Voltage. (Air; $p = 760$: $l = 7$; $D = 10$; $d_0 = 1.4$; $m = 0.7$).

Examples of such figures in air are shown in Figs. 6 and 7. In nitrogen and argon the figures are still brighter than in air. In cases where the photographic method gives too faint figures, the ordinary dust method may be used with advantage even if it does not give such delicate details as the photographic one.

Many investigations have formerly been carried out in the hope of getting an explanation of the origination of these figures and of the very remarkable difference between the positive and negative ones. On the whole very little progress has, however, been made. With regard to the former experiments and speculations it is sufficient to refer to the papers mentioned on page 4, which contain ample information on this question.

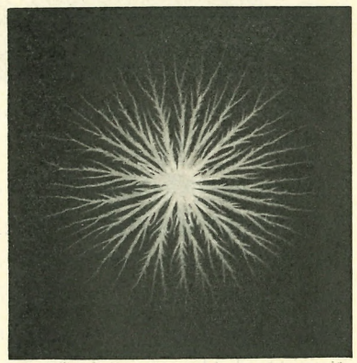

Fig. 6. Normal Positive Figure. (Air; $p=760$; $l=3$; $D=0$; $d_0=1.4$; $m=1$).

E. Reitlinger[1,2], in 1860-61, tried to explain the figures on the hypothesis that electrical particles during the discharge travel from the electrode outwards through the

surrounding gas. The positive and negative particles move in different manners, this being the cause for the difference between the positive and negative figures. Even if Reitlinger was — and necessarily must have been — unable to give a satisfactory explanation of the phenomenon, his ideas were remarkably sound and his proofs of the close connection between these figures and the electrical properties of the gas seem conclusive. He had, in fact, solved this intricate question as far as it could be solved at that time. His views were, however, in the main only supported by A. v. Waltenhofen[1], and later investigators have worked along other lines. As late as 1905 W. Holtz[1] even comes to the conclusion that the nature of the gas, nay even gas altogether, is of little importance with regard to the Lichtenberg figures.

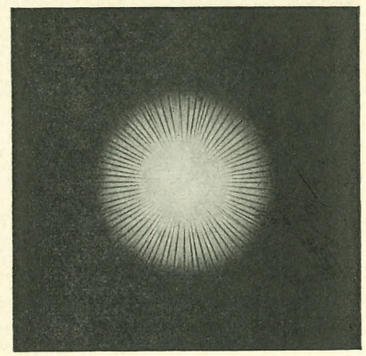

Fig. 7. Normal Negative Figure. (Air; $p=760$; $l=7$; $D=0$; $d_0=1.4$; $m=1$).

According to W. v. Bezold[1,2,3,4], who had carried out a series of important investigations on this subject, the figures are due to air currents. He supposes — rather arbitrarily — that the negative figure is formed by air currents going outwards from the electrode while air currents in the opposite direction produce the positive ones. He tried to prove this hypothesis by experiments on powdered water. By means of a tube, the end of which was just at the surface of the powdered water, a small amount could suddenly be either added to or drawn away from the bulk of water. In the first case a »negative« and in the last a »positive« figure appeared. The resemblance is, however, not very striking. As a conclusive proof he considered the following circumstance: He found,

that the exterior part of the figure formed from a positive, ring-shaped electrode had the normal positive appearance, but the interior part was of negative character, and similarly for negative discharges. E. Mach and S. Doubrava[1] denied the correctness hereof, and Figs. 8 and 9 show that these authors were right: the exterior and the interior part of the figures are either both of positive or both of negative character. The mistake made by v. Bezold is, however, very excusable; it would be almost impossible to settle this question by the dust method. We shall later see that the Lichtenberg figures are formed with such great velocity that air currents cannot have any appreciable influence.

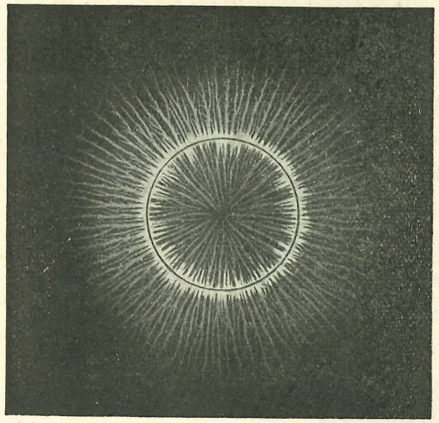

Fig. 8. Positive Figure obtained with Ringshaped Electrode. (Air; $p = 760$; $l = 3$; $m = 0.9$).

G. Quincke[1] sees in the often mentioned figures an interaction of different sorts of rays: positive rays able to penetrate millimetres of insulators, negative rays, and retrograde rays of two different kinds. His positive and negative rays even seem to be of composite nature — consisting of both quickly moving particles and electromagnetic radiation. This explanation of the Lichtenberg figures will hardly be accepted as satisfactory.

S. Mikola[1] in his above mentioned paper also gives some new and rather startling hypotheses. His views may be summarized as follows: Electromagnetic impulses are emitted from the edge of the condenser, when impulsively discharged. These impulses, travelling along the conductor, produce positive and negative ions of great velocity, which move rapidly along the conductor and with certain intervals of time cause the emission of electromagnetic impulses, which in turn liberate ions from the conductor. Even accepting all these rather strange hypotheses it is not easy to see how they can afford a satisfactory explanation of the great differences between the positive and negative figures.

Notwithstanding the great amount of work which has been spent in order to elucidate this question, we know, up to the present, little more about the origination of these figures than Lichtenberg did. This fact will probably explain the present lack of interest in this question. Neither in J. J. Thomson: Conduction of Electricity through Gases (1906), nor in J. S. Townsend: Electricity in Gases (1915), nor in A. Winkelmann: Handbuch der Physik (1908), is the name of Lichtenberg to be found.

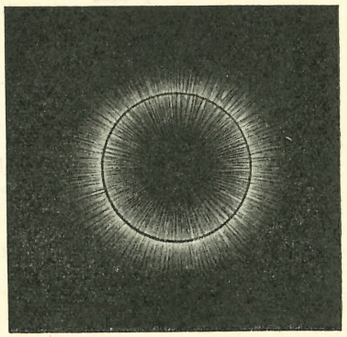

Fig. 9. Negative Figure obtained with Ringshaped Electrode. (Air; $p = 760$; $l = 6$; $m = 0.9$).

The aim of the present investigation is to throw some light on the main features of the origination of the Lichtenberg figures. The results obtained seem to indicate that the elucidation of the origination of these figures will probably prove to be of great importance for the study of the process of ionization of gases and for the molecular and atomic dynamics.

The present paper deals only with a preliminary investigation of the general features of the Lichtenberg figures and the numerical results are to be considered as provisional. Several more detailed investigations connected with this problem are being carried out at present.

Chapter II.

General Remarks on the Origination of the Lichtenberg Figures.

1. Most of the experiments described in the following are carried out with the arrangement shown in Fig. 10. The condenser C can be charged through the great resistances R_1

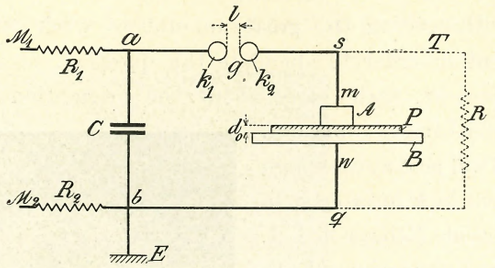

Fig. 10. Diagram of Circuit for ordinary Lichtenberg Figures.

and R_2 from a small influence machine connected to M_1 and M_2. The resistance R_1 is a slate pencil, and R_2 either a slate pencil or a thin piece of wood. The spark gap g has 4 cm. brass balls, k_1 and k_2. The small electrode A generally rests on the sensitive film of the dry plate P placed on the metal disk B which is connected through the wire nqb and resistance R_2 with one pole of the electric machine. The connecting wire is earthed at b. Electrode A, plate P, and electrode B form what we will call the Lichtenberg gap (L. G.). When working with other gases than air and in rarefied gases the L. G. was enclosed in a bell jar, the wire m being carried air-tight through the side of the jar. The figures are said to be positive when k_1 is positive before the spark passes over. The electrical machine must be rotated very slowly, especially when working with short spark lengths, in order to get a definite sparking voltage and to avoid the passage of more than one spark each time.

The L. G. was generally shunted by a slate pencil R or some other great resistance. This shunt increases the damping of the oscillations in the circuit $CgAPBC$, but its main object is to bring about that the potential of the electrode A before and after a discharge is equal to that of the earth connection E. Otherwise the removal af A may cause a new discharge, and other complications may arise.

Different dry plates have been tried; the most satisfactory results have been obtained with Hauff's Roentgen plates.

The figures only appear if the P. D. across the L. G. is altered in an impulsive or sudden manner and not if the potential of A is raised gradually — the spark gap g being short circuited and the shunt R removed. This observation was made by T. P. Reiss (1864)[1]; S. Mikola[1] herefrom draws the conclusion that the formation of these figures is due to the rapid variation in the potential across the L. G., and does not take place because and when the P. D. has reached a certain value. He considers that this form of discharge is produced when the innermost ends of the lines of force travelling along the electrode A are suddenly stopped; the sharp bends thereby produced on these lines then travel out along them with the velocity of light, and constitute an electromagnetic radiation of the same kind as Roentgen rays.

It is, however, not necessary to introduce new and rather doubtful hypotheses in order to explain the necessity of a very steep rise in the P. D. across the L. G. in order to obtain Lichtenberg figures. We need only consider the circumstances connected with the commencement of a Lichtenberg discharge a little closer. The spark in g (see Fig. 10) starts an electric wave along the wire k_2m. The maximum voltage of this wave is partially reflected at A and the reflected wave travels back along mk_2. The potential at A is the sum of the potential of the incident and of the reflected wave, and if the capacity of A is small, the maximum potential

at A will be almost equal to twice the sparking voltage. In comparing the effect of a stationary voltage across the L. G. with that of an impulsive voltage caused by a spark as in Fig. 10, the former must be about twice the sparking voltage. But a statical voltage however great does not produce Lichtenberg figures. So far Mikola is right. A static voltage in this connection means a voltage which has been raised very slowly. At a certain stage of this charging of the electrode A the intensity of the electric field between A and the plate P reaches a value at which ionization by collision commences. But no disruptive discharge takes place because the ionization current is charging the surface of the insulating plate P and thus automatically keeping the intensity of the electric field between A and P below a certain value, a value too low to produce sparking. Simultaneously with the process of charging of P a diffusion of this charge along the surface of the plate is going on, but the electric field nowhere attains a value sufficiently high to produce disruptive discharges of any kind. It is not before the diffused charge in sufficient quantity has reached the edge of the plate that the electric field there becomes sufficiently intense to produce a spark, which increases in length until it connects A and B. Photographs of such sliding sparks are reproduced in Armstrong's work, and these sparks have been very carefully investigated by Toepler.

The reason why the Lichtenberg figures do not appear with slowly varying potentials is simply that the intensity af the electric field in this case does not attain the necessary high value. With a rapidly varying potential there is, however, a possibility of obtaining sufficiently strong fields because it takes some time to establish the compensating charge on the plate P.

At the edge of the coatings of leyden jars and similar condensers analogous conditions are to be found. If the potential varies slowly, the ionization which takes place at the edge causes the electric charges to be distributed in such a way that the electric field nowhere attains a value high enough to produce strong ionization, and a quasi-stationary state is established, during which a feeble current leaks from one electrode to the other. If the potential changes very rapidly there is not sufficient time for effecting this distribution of the charge, and the field may attain such high values that a figure appears. If the condenser is subjected to high frequency voltages, such Lichtenberg discharges appear twice every period, and the heat caused hereby will often crack the glass.

As pointed out it is necessary to apply rapidly varying potentials in order to get the necessary intensity of the electric field. On the other hand the P. D. across the L. G. must not be kept too long or with too high a value after the Lichtenberg discharge has been started. Otherwise, in addition to the first formed, regular Lichtenberg figure, there will appear other more complicated ones and, if the P. D. is kept on for say about 1.10^{-6} second, a spark generally occurs. In order to obtain pure and simple Lichtenberg figures the L. G. must be subjected to a very high impulsive voltage of very short duration. And to this very impulsivity the Lichtenberg figures owe the great importance they undoubtedly have for the study of discharges in gases. They show the effect of a very strong field of extremely short duration. The field may be so strong that it cannot be sustained for say 10^{-6} second without resulting in a disruptive discharge in which most of the effects of the initial or Lichtenberg state of the discharge would be altogether lost. It seems difficult to imagine any other method by which this initial state of ionization could be investigated — and so easily and conveniently investigated — the Lichtenberg figures affording an almost instantaneous picture of what is going on during this initial ionization.

The duration of a Lichtenberg discharge is about 1.10^{-8} second as will be shown later on. W. v. Bezold and others working with dust figures state that the origination of these figures takes a comparatively long time. They have probably been led to this mistake by the relatively slow movements which are to be seen in the dust even several minutes after the formation of the figures. These movements are due to electrostatic forces on the dust particles and have nothing to do with the origination of the Lichtenberg figures.

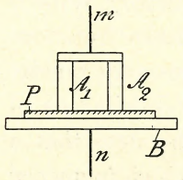

Fig. 11. Lichtenberg Figures from several Parallel Electrodes.

The Lichtenberg figures originate and develop with great regularity and exactness. This is easily shown by placing

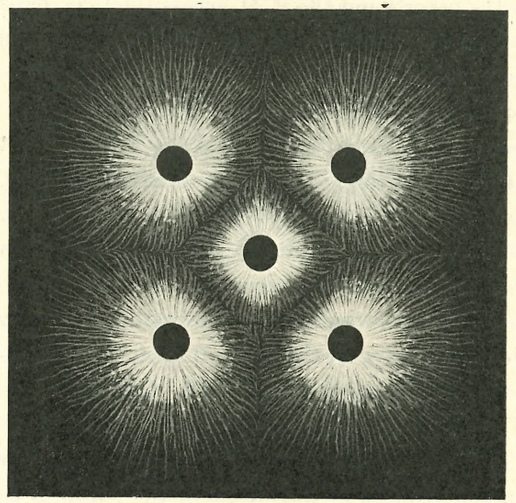
Fig- 12. Positive Figure from five Electrodes. (Air; $p = 760$; $l = 6$; $d_0 = 1.3$; $m = 0.8$).

several electrodes connected in parallel on the same plate as indicated in Fig. 11, where the electrodes A_1 and A_2 are connected to a metal plate and rest on the photographic

plate P. Separate Lichtenberg figures then start simultaneously from the different electrodes, and the boundary lines between the different figures are very regular, showing the great precision with which the figures originate. Fig. 12 shows a positive and Fig. 13 a negative figure of this kind.

W. v. Bezold and S. Mikola have proved that the shape and the size of the figures are independent of the nature of the electrode, provided only it is a good conductor. This may be easily confirmed by the fact that the electrodes in the Figures 12 and 13 may be made of different metals without thereby in any way altering the shape and size of the combined figure. If on the other hand a very bad conductor is used as electrode, the appearance of the figures is altered as pointed out by W. v. Bezold and S. P. Thompson[1]. These irregular figures have not been included in our investigation.

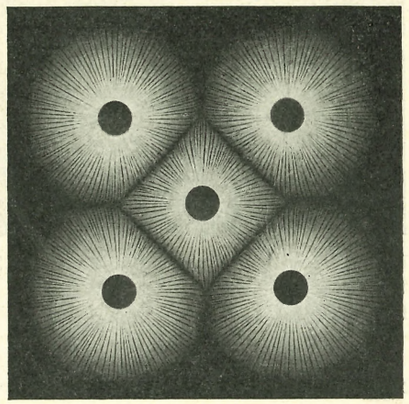
Fig. 13. Negative Figure from five Electrodes. (Air; $p = 760$; $l = 6$; $d_0 = 1.3$; $m = 0.8$).

Even if the metal electrode is put in a shoe of insulating material, for instance ebonite, say 1 millimetre thick, a regular Lichtenberg figure may be formed. The effect of the shoe is a reduction in size of the figure and some retardation in the discharge. In Fig. 14 and Fig. 15 the right electrode is with, the left one without, shoe and both electrodes are connected to the same metal plate (see Fig. 11).

A similar effect is produced by placing a plate of insulating material across the path of the figure as shown in Fig. 16. A

glass plate 0.77 mm. thick was cemented to the sensitive film by means of picein. It is seen that the figure is not cut off by the vertical glass plate but its range is somewhat reduced.

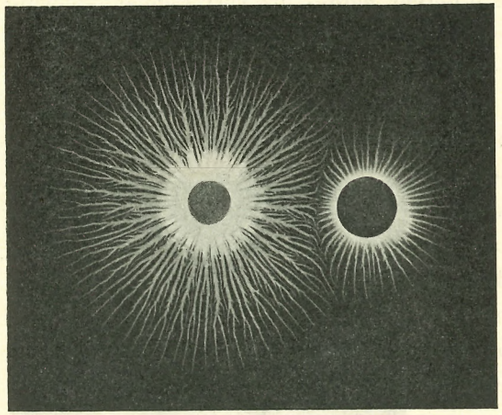

Fig. 14. Positive Figure from two Parallel Brass Electrodes, the Right one with a Shoe of Ebonite, 1 mm. thick. (Air; $p = 760$; $l = 8$; $d_0 = 1.4$; $m = 1$).

G. Quincke explains this behaviour of the Lichtenberg figures by postulating that these figures are due to some specific kind of rays which are able to pass through insulators. A closer study of Fig. 16 does not lend support to Quincke's view: the »rays« outside the plate are not extensions of the inside »rays«, but start from the outer surface of the glass plate and in a direction very nearly normal to this plate. The outside part of the figure is no doubt due to the electric field just outside the glass plate caused by the sudden accumulation of charge on the inner side of this plate.

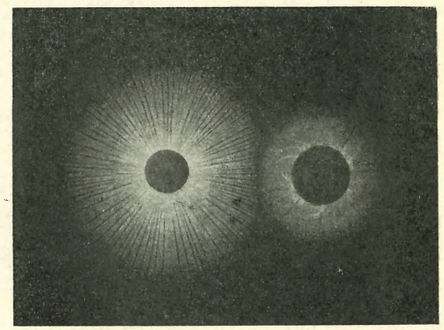

Fig. 15. Negative Figure corresponding to Fig. 14.

The size and shape of the L. F. are to a remarkably high degree independent of the nature of the insulating plate and of the condition of its surface. Plates of glass, quartz, ebonite, and pitch give exactly the same figures. As shown by E. W. Blake (1870)[1] L. F. may also be obtained on pitch which is heated to its melting point. Even on a water surface the regular figures may be observed, as pointed out by E. Reitlinger (1860)[1]. The shape and character of the figures is exactly the same whether the plate is powdered before or after the discharge has taken place. The dust figures and the photographic figures have also the same shape and character, the entire difference being that the dust figures are somewhat coarser and consequently do not show such fine details as the photographic ones.

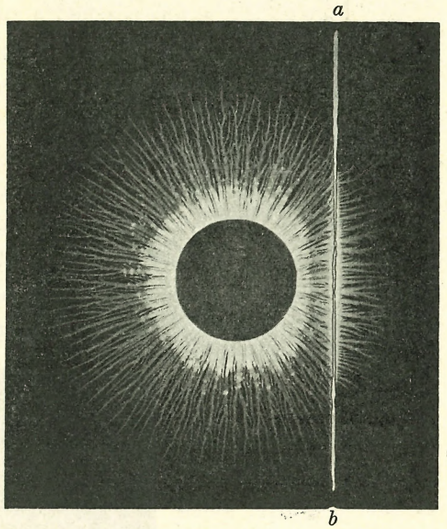

Fig. 16. Positive Figure. *ab* Screen of *a* 0.77 mm. Glassplate cemented to the Film of the Photographic Plate. (Air; $p = 760$; $l = 5$; $D = 17$; $d_0 = 1.4$; $m = 1$).

If the conductivity of the surface of the insulating plate is too great, the intensity of the electric field along the plate will not attain the necessary high value and no Lichtenberg figure will appear, but the discharge will take some other form. In as far as the conductivity does not attain such a high value, the Lichtenberg figures are entirely independent of the state of ionization at the surface of the plate. This has been shown in many ways of which I shall only mention the following.

A spark gap g' was inserted between R_1 and the point a (see Fig. 10), and a condenser C' between the point b and a point between g' and R_1. C' had a greater capacity than C. When the p. d. across g' has reached a sufficiently high value a spark passes in g', the condenser C begins to be charged and a spark passes through g causing a Lichtenberg figure to be formed on the plate P. The spark in g' precedes the Lichtenberg figure by about 1×10^{-6} second. The spark gap g' was placed above and at some distance from the photographic plate, a perforated screen being inserted between them. The distance between the spark and the photographic plate was varied within wide limits; with the greatest distance the blackening of the exposed parts of the plate could barely be seen, while with the shortest distance the exposed spots were completely opaque. In all cases the size, shape, and character of the figures were the same in the exposed and in the unexposed parts of the figures, and no peculiarity was to be seen at the places where the Lichtenberg figures passed from an exposed to an unexposed spot or vice versa.

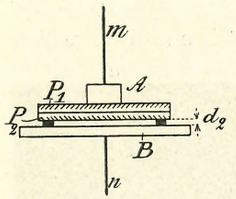

Fig. 17. Arrangement for Primary and Secondary Figures.

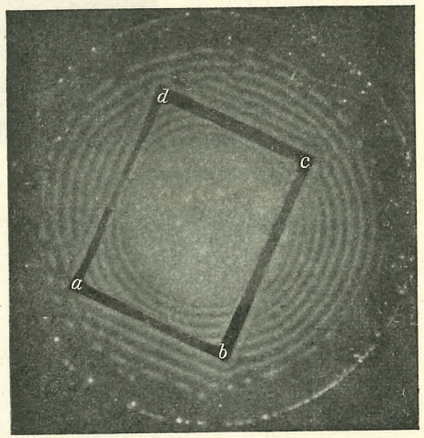

Fig. 18. Negative Secondary Figure corresponding to Primary in Fig. 19. *abcd* rectangular Frame of Mica cut between *a* and *d*. Thickness about 0.2 mm.

Other experiments were carried out with ionization produced by γ-rays from radium enclosed in a platinum tube. The arrangement for the producing of the Lichtenberg figures was the normal one shown in Fig. 10, and the radium tube was placed on a sheet of ebonite at a distance of from 2 to 6 mm. above the photographic plate. The ebonite plate was 1 mm. thick and had a hole just below the tube. The plate was exposed to the γ-rays for 15 to 60 seconds before the Lichtenberg discharge took place, and the exposed spots were accordingly more or less blackened. Many experiments were made, but it was in no case possible to ascertain any influence whatever of these spots of ionization upon the Lichtenberg figures, whether they were positive or negative.

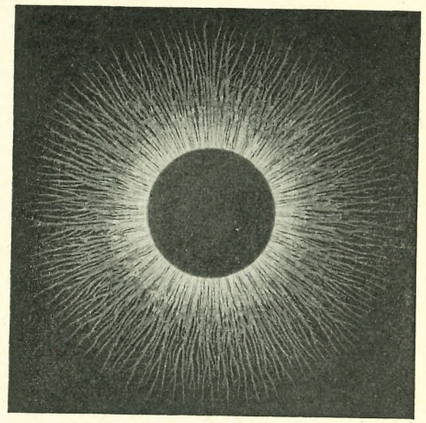

Fig. 19. Positive Primary Figure corresponding to Secondary in Fig. 18. (Air; $p = 760$; $l = 7$; $D = 24$; $d_0 = 2 \times 1.4$; $m = 0.8$).

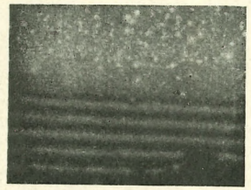

Fig. 20. Part of Negative Secondary Figure. The Electrode had a straight Edge and covered the homogeneous Part of the Figure. ($d_2 = 0.2$ mm).

Fig. 21. Part of Positive Secondary Figure starting from below a straight Edge *aa* of the Upper Electrode ($d_2 = 0.2$ mm).

On the other hand we have also tried to remove all chance

ions from the surface on which the Lichtenberg figure is formed. In order to do this a ring-shaped electrode was placed on the photographic plate concentric with the electrode A (see Fig. 10), and a battery in series with an induction coil was inserted between A and the ring electrode. The E. M. F. of the battery was varied within wide limits and any natural ionization was, no doubt, either completely removed or at least greatly reduced. The discharges took place with the battery inserted, and the Lichtenberg figures thus formed were in no way different from the others.

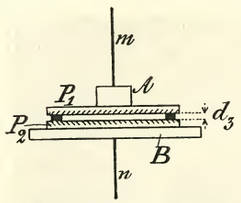

Fig. 22. Arrangement for Tertiary Figures.

It appears from these and other experiments that the Lichtenberg figures within extremely wide limits are independent of the state of ionization at the surface of the plate. These figures are thus in a very high degree independent of the nature of the plate and the mechanical and physical condition of its surface. We shall later on see that size, shape, and character of the Lichtenberg figures depends almost exclusively on the nature and pressure of the surrounding gas.

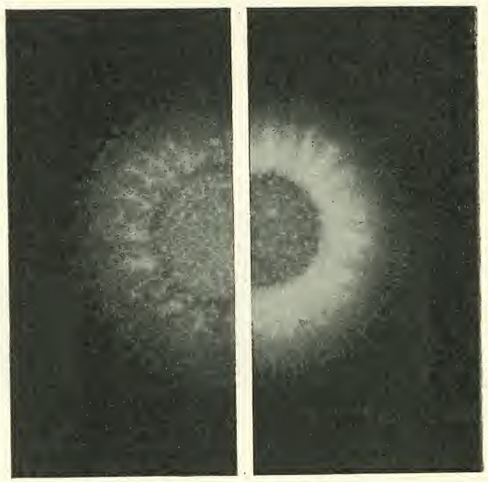
a b

Fig. 23. a Lower and b Upper Tertiary Figure for Negative Discharge. (Air; $p = 760$; $l = 8$; $D = 17.5$; $d_3 = 0.1$; $m = 1$).

2. We have so far only considered figures which start from the small electrode. W. G. Armstrong and H. Stroud

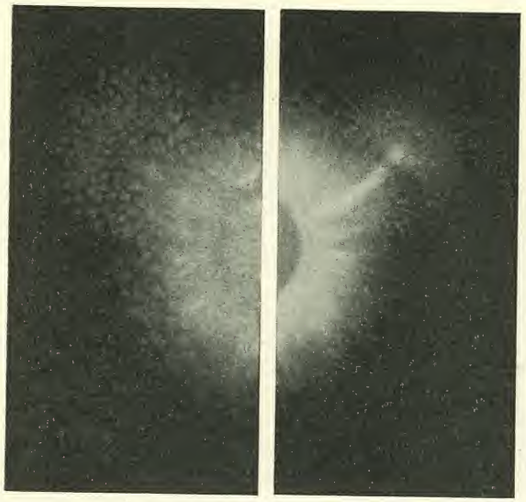
a b

Fig. 24. a Lower and b Upper Tertiary Figure for Negative Discharge. (Air; $p = 760$; $l = 8$; $D = 17.5$; $d_3 = 0.1$; $m = 1$).

(1899)[1] and S. Mikola (1917)[1] have shown that very remarkable figures may be obtained in front of the great electrode B on a sensitive film at a little distance (P_2 Fig. 17). S. Mikola calls these secondary figures and those formed from the electrode A primary Lichtenberg figures. A secondary figure is shown in Fig. 18, while Fig. 19 shows the corresponding primary figure. Parts of secondary figures are also shown in Fig. 20 and 21. We call these secondary figures negative (positive) when the simultaneous primary figure is positive (negative).

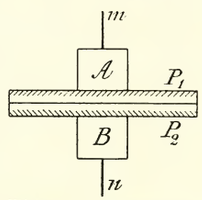

Fig. 25. Arrangement for Simultaneous Positive and Negative Figures.

A third kind of figures are obtained if two photographic plates are placed between the electrodes with the sensitive

films against each other. We call these tertiary figures. If the distance d_3 (see Fig. 22) between the films is small, very remarkable and finely shaped figures may be obtained. Examples of such figures are shown in Figs. 23 and 24. The explanation of these figures will hardly offer any greater difficulty when the problems of the primary and secondary Lichtenberg figures have been solved.

Fig. 26. Positive Figure. (N_2; $p = 760$; $l = 5$; $D = 17.5$; $d_0 = 1.4$; $m = 1$).

If the two electrodes A and B are of approximately the same size (see Fig. 25) there is simultaneously formed two primary figures of opposite polarity, say a positive from A and a negative from B. This observation was made by Lichtenberg.

Fig. 27. Negative Figure. (N_2; $p = 760$; $D = 17.5$; $d_0 = 1.4$; $m = 1$).

We have so far only considered the effect of a single impulse. The discharge of the condenser C through the circuit $gmABnb$ will generally, however, be oscillatory (see Fig. 10). The Lichtenberg gap APB forms a small condenser of a capacity C'' which increases as the size of the figure starting from A increases. The period T of the oscillation is determined by

$$T = 2\pi \sqrt{L_0 \frac{CC''}{C + C''}},$$

where L_0 is the coefficient of selfinduction of the circuit $CagsqbC$ and C the capacity of the condenser C.

The damping of these oscillations depends upon the resistance of the wires, the dielectric losses in the condensers, the loss in the spark gap, but especially upon the losses caused by the shunt R and by the Lichtenberg discharge itself. In cases where the combined effect of these losses does not give a sufficiently high damping the first impulse will, half a period later, be followed by an impulse of opposite polarity, and this latter impulse will create a new discharge superposed on the previous one. Without the shunt R (see Fig. 10) the damping of a positive discharge at atmospheric pressure will generally be so small that the effect of the succeeding negative impulse is rather great. The inner part of the positive figure is then covered by the following negative discharge as shown in Figs. 12, 16, 19, and 26. It is seen that this negative discharge mainly follows the paths of the preceeding positive one. By

Fig. 28. Negative Figure. (93 % N_2 + 1 % O_2; $p = 150$; $D = 17.5$; $d = 1.4$; $m = 0.8$).

use of a suitable shunt the negative impulse may be sufficiently reduced; the positive figure then appears pure as in Fig. 6.

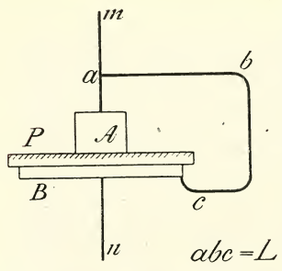

Fig. 29. Arrangement for Oscillating Discharges.

At lower pressure the positive figures will often be pure even if no shunt is used. The negative discharge at atmospheric pressure is generally so highly damped that the succeeding positive impulse is without any appreciable effect; the negative figure therefore generally appears pure as in Figs. 7 and 27. At lower pressures the negative discharge is apparently less damped and the succeeding positive impulse therefore able to effect a positive discharge superposed on the preceeding negative one. Fig. 28 shows a positive discharge of this kind; its appearance is very remarkable, but the further discussion of this question will be taken up later on.


Fig. 30. Oscillating Discharge, first Half-wave Positive.
$L = 133$ cm. (Air: $p = 760$; $l = 10$; $D = 9.5$; $d_0 = 1.3$; $m = 1$).

If the L. G. is shunted by a wire *abc* (see Figs. 29 and 10) the period of the circuit *CgmabcnqbC* is increased and the damping reduced so much that an ordinary, slightly damped oscillation is created in this circuit when a spark passes at *g*. In this case each of a number of succeeding half-waves of opposite polarity will cause discharges to take place, and the figure made during the first discharge is overlapped by the

succeeding figures and it is rather indifferent whether the first discharge was positive or negative. Fig. 30 shows a "positive" figure of this kind and Fig. 31 a "negative" one, but there is hardly any difference between them. We have not found opportunity to investigate the properties of these figures.

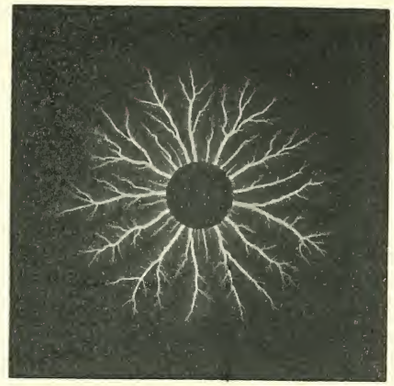
Fig. 31. As Fig. 30, but first Half-wave Negative.

Chapter III.

General Features of the Lichtenberg Figures.

a. Negative Figures.

1. General Character of the Negative Figures. With the exception of some thin dark lines which we shall consider later on, the pure negative figure appears as a white disk with nearly equal brightness over the whole area, except the external boundary though, where the brightness gradually dies away (see Figs. 7, 27, and 28). In all works dealing with Lichtenberg dust figures the negative figures are only characterized by their external boundaries, being marked by a strong dust ring, generally appearing just outside the negative disk (see Fig. 3). The above mentioned dark lines are so fine that they are unable to manifest themselves clearly with the dust method.

Using the photographic method it is clearly seen that the negative figure is broken up in separate parts by a number

of dark lines (see Figs. 7, 27, and 28). We will call each of these bright parts a negative flow or stream. The width of the negative flows varies in the same figure within wide limits, while the dark lines are very nearly all of the same width. The boundary between the dark lines and the negative streams is, however, not very sharply defined, the transition from the white parts to the dark ones being more or less gradual, and there is an uncertainity of about $\pm$ 0.005 mm. in the determination of the boundary line.

The mean width of the negative flows in Fig. 27 (measured at a distance of 8 mm. from the electrode) is 0.68 mm., the broadest being 1.10 mm. and the narrowest 0.18 mm. wide. In other instances the variation is even greater (see f. inst. Fig. 28). Strongly contrasted with this is the great constancy in the width of the dark lines*.

The mean value of the width of 16 consecutive dark lines in Fig. 27 was 0.095 mm., and the greatest deviation $\pm$ 0.009 mm. The width of the different dark lines is thus at least nearly constant, and for the same line its width is nearly the same over its whole length, with the exception of the part in the neighbourhood of the electrode where the dark lines are sometimes much broader (see f. inst Fig. 28). We shall later on return to this point.

The width of the dark lines is apparently independent of the spark length and of the size of the electrode. To show this we quote in Table 1 some figures obtained in air at atmospheric pressure.

For short spark lengths it is difficult to measure the width of the dark lines. The figures in the table give the limits within which the width was estimated to fall.

The mean value of the width of the negative flows also

* This constancy of the width of the dark lines seems to have escaped the attention of S. Mikola, probably because he preferably used rather thick plates, with which these lines are broader and less regular.

Table 1. Width of Dark Lines in Air (p = 760 mm. hg).

Length of spark l in mm.	1.	2.	3.	5.	7.	9.
Width of dark lines in mm. — electrode: D = 40 mm.	0.09—0.11	0.09—0.11	0.09—0.11	0.92	0.10	0.092
Width of dark lines in mm. — electrode: point	0.09—0.11				0.10	0.091

seems to be independent of the spark length, in other words, the number of negative flows is nearly independent of the spark length.

The width of the dark lines depends also very little on the nature of the gas, as shown by the following figures.

Table 2.

	Mean Value of Width of Dark Lines	Mean Value of Width of Negative Streams
Air p = 760 mm. hg	0.095 mm.	0.68 mm.
N_2 —	0.095 -	0.68 -
H_2 —	0.100 -	0.58 -
CO_2 (from flask) —	0.11 -	1.25 -
O_2 (—) —	0.18 -	0.50 -

With the exception of oxygen the width of the dark lines is practically the same for all gases investigated. Also in other respects oxygen behaves differently from air, nitrogen, hydrogen and carbon dioxide. The average width of the negative flows is also nearly the same with the exception of carbon dioxide for which gas it is nearly twice as great as for the other four gases.

In Fig .32 are shown some enlarged photographs* of parts of negative figures in different gases. It is seen that there is no great difference between figures in nitrogen (Fig. 32 a), air (*h*), hydrogen (*d*), and carbon dioxide (*f*). While the lines are straight in the three first mentioned gases, they are, however, somewhat bent in carbon dioxide. In oxygen (*e*) the figures are not so regular as in the other gases.

* The width of the dark lines has been measured directly on the Lichtenberg plates. On copies the dark lines will often appear broader or thinner according to circumstances. Fig. 32 is therefore not to be used for a measurement of the width of the dark lines.

The width of the dark lines and the flows increases with decreasing pressure, this increase being especially pro-

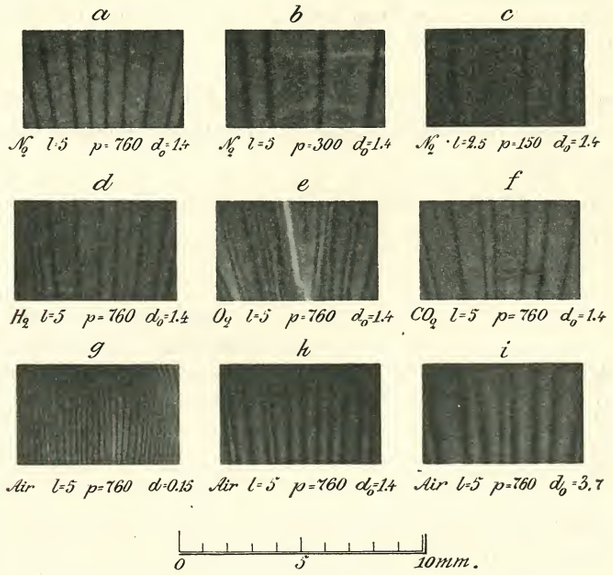

Fig. 32. Parts of Negative Figures in various Gases and at various Pressures.

nounced in case of the flows as shown in the following table.

Table 3. Width of Dark Lines and Negative Flows for Different Pressures.

Gas: — Nitrogen (from steel flask, 93 % N_2 + 7 % O_2).

Pressure	760	300	150	75 mm. hg.
Width of dark lines	0.095	0.154	0.173	0.25—0.30 mm
Average width of negative flows.	0.68	0.93	1.6	2.8 mm.
Maximum — — ..	1.10	4.5	12.0	11.0 -
Minimum — — ..	0.18	0.3	1.4	1.0 -

The influence of varying pressure in the case of nitrogen is shown in Fig. 32 a, b, c.

The width of the dark lines and the average width of the negative flows decreases with decreasing thickness of the photographic plate as shown in the following table.

Table 4. Width of Dark Lines and Negative Flows for Different Thicknesses of Plate.

Thickness d_0 of plate P (see Fig. 10)...	0.15	1.4	3.7 mm.
Width of dark lines	0.055	0 10	0 25 mm.
Average width of negative flows.....	0.18	0.68	0.82 -

This feature is illustrated by Fig. 32 g,h,i. When d_0 is small both the dark lines and the negative flows are very narrow. The greater the value of d_0 the greater is also the width of the dark lines while there seems to be a limit value of the average width of the negative flows. With great value of d_0 the constancy of the width of the dark lines is not so pronounced and the whole figure becomes less regular.

On very thin plates the dark lines have a tendency to be bent but are otherwise very regular.

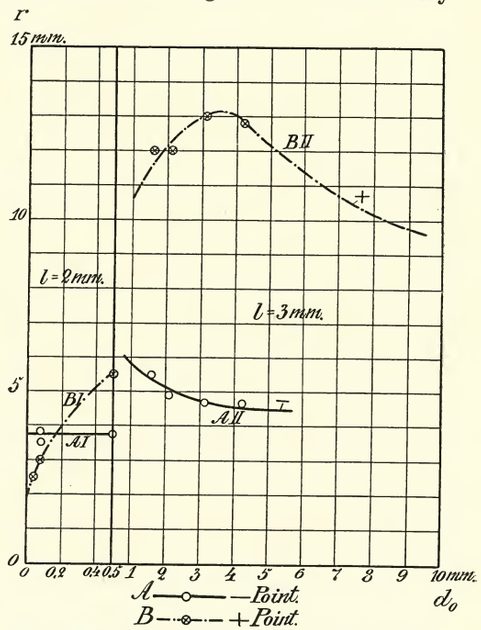

Fig. 33. Effect of Thickness of Plate (d_0) on the Range (r) of Dust Figures.

2. Size or Range of the Negative Figures. The size may be measured in different ways; as the size we shall

take the range or the length r of the negative flow reckoned from the electrode to the outermost end. It is to be expected that the size will be dependent upon a good many things. We shall in the following investigate the influence of some of the most important of these factors.

W. v. Bezold (1871)[4] proved that the dielectric constant of the plate P (see Fig. 10) has little or no influence

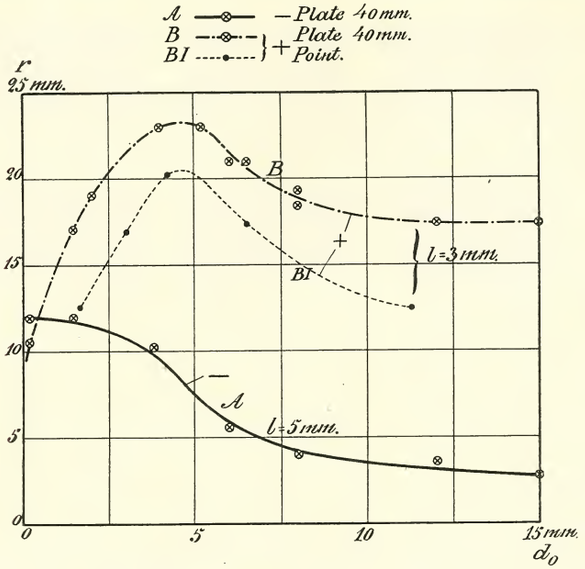

Fig. 34. Relation between Range and Thickness of Plate for Photographic Figures.

on the size of the figure, and our experiments, as far as they go, are in agreement herewith.

The thickness d_0 of the plate is of little importance so long as the plate is thin, but for thicker plates there is a marked decrease in size with increasing thickness. This is evident from Fig. 33 which shows the results of W. v. Bezold's measurement for dust figures, and Fig. 34, containing some of our results for photographic Lichtenberg figures. For

very great values of d_0 the range very slowly approaches the value of r corresponding to $d = \infty$.

The influence of the spark length was investigated by W. v. Bezold (1871)[4], S. Mikola (1917) and others. Bezold's

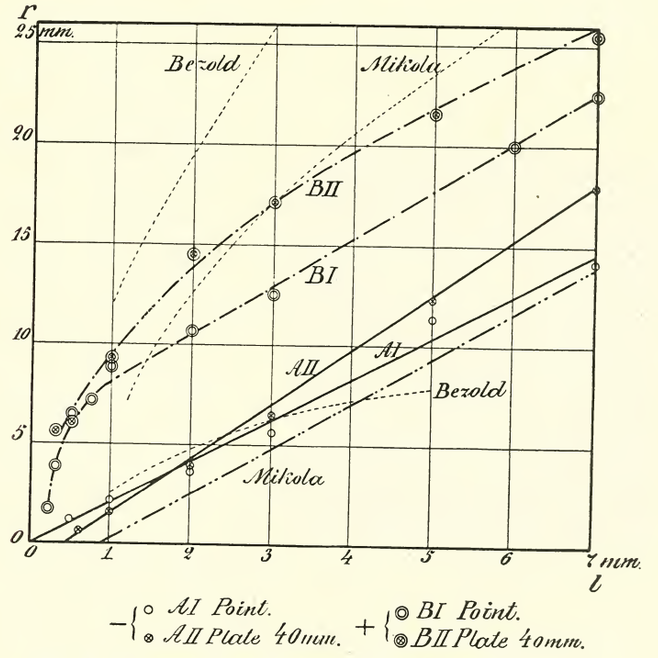

Fig. 35. Effect of Spark Length (l) on the Range (r) of Positive and Negative Figures. (Air; $p = 760$; Bezold's values are for Dust Figures, the others refer to Photographic Figures. $d_0 = 1.4$ in A and B-curves, by Mikola about 3 to 4 mm. D is about 20 mm. by Mikola).

and Mikola's results are shown in the lower part of Fig. 35 which also contains the results of our measurements. Both Mikola's and our own measurements give a linear relation between spark length and size, while v. Bezold's curve is bent with the concavity against the l-axis. v. Bezold's results refer to dust figures, and the size of negative dust

figures is generally taken as the radius of the dust ring enclosing the negative figure. Such rings do not appear in the photographic Lichtenberg figures, and it is therefore difficult to compare the size of these two kinds of figures. It ought to be mentioned, however, that at lower pressure the (l, r)-curves for photographic figures become bent in the same way as v. Bezold's curve.

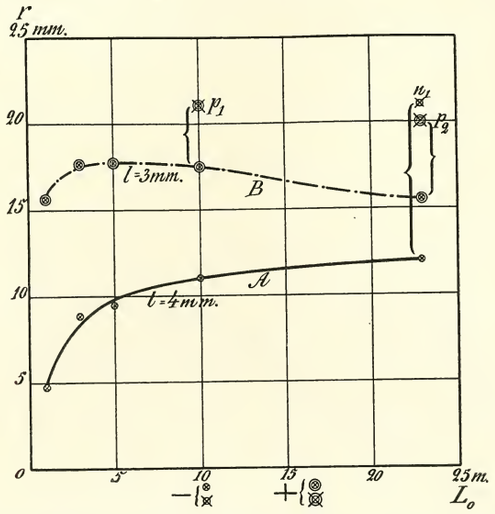

Fig. 36. Effect of Duration of Impulse on the Range of Positive and Negative Photographic Figures.

For point-electrode the (l, r)-line seems to pass through the origin (AI in Fig. 35), while the (l, r)-lines for greater electrodes starts from the l-axis to the right of the origin (AII), and the more so the greater the diameter of the electrode and the thickness of the plate is. These results are in complete agreement with the investigations of M. Toepler[1].

Another point to be noted is that the angle, which the (l, r)-line makes with the l-axis, increases with increasing size of the electrode, being smallest for a point-electrode. S. Mikola generally uses much thicker plates than we do, and

his electrode seems to have had a diameter of about 20 mms., intermediate between our point-electrode (AI) and plate-electrode (AII), which had a diameter of 40 mms. Considering all these points it appears from Fig. 35 that the agreement between Mikola's measurements and ours is very good.

Effect of duration of the impulse on the size of the negative figure. In order to investigate this point we have altered the lengths of the wires k_2s and bq (Fig. 10) keeping all other circumstances as far as possible constant. In Fig. 36 we have plotted the value of r as a function of the length L_0 of each of the wires k_2s and bq. For short wires (up to about 10 metres) r is very nearly proportional to the square root of L_0, for longer wires the increase of r is very slow. But here a new phenomenon sets in, consisting in the formation of fan shaped extensions outside or nearly outside the range of the normal figure (see Fig. 37). The greatest lengths of these are in Fig. 36 marked n_1. This form of discharge is very similar to that caused by too high tension and both are closely connected with the sliding sparks investigated by M. Toepler.

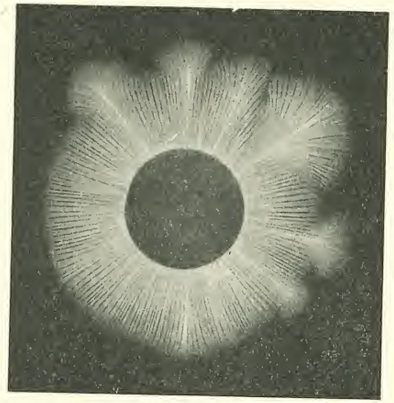

Fig. 37. Negative Figure. (Wire $k_2s = bq = 23$ m., see Fig. 10. (Air; $p = 760$; $l = 4$; $D = 17.5$; $d_0 = 1.4$; $m = 1$).

Effect of gas pressure on the range. W. v. Bezold (1871)[4] found that

$$p \cdot r = \text{constant},$$

while S. Mikola (1917) expresses the results of his measurements in the empirical formula:

$$r = \frac{r_0}{(p+k)^{9/2}},$$

r_0 and k being constants.

The full curve in Fig. 38 shows the results of our measurements and in the same figure curves are drawn corresponding to Bezold's and Mikola's formulae. The constant in the first is chosen so that Bezold's formula agrees with our

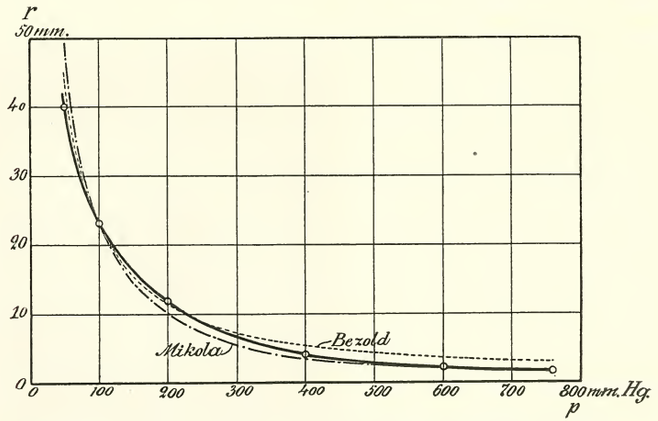

Fig. 38. Relation between Gas Pressure and Range of the Negative Figures. (Air; $l = 2$; $D = 10$; $d_0 = 1.4$).

value of r for $p = 100$ mm. hg., while r_0 and k in Mikola's formula are given such values that his curve agrees with ours for $p = 100$ and $p = 600$ mm. hg.

The differences between the three curves are not great, and the measurements cannot be made sufficiently accurate to determine with certainty which of the two curves is the best representative of our experiments. There is, however, hardly any doubt that the product $p \cdot r$ increases with decreasing pressure.

The dependence of the range on the nature of the gas has not yet been sufficiently investigated. We shall therefore only quote the results of a few provisional measurements.

Table 5. Range of Negative Figures in Various Gases. ($l = 5$ mm.; $p = 760$ mm. hg.).

Gas:	Range:
Air	13.0 mm.
Nitrogen from steel flask (93 % N_2 + 7 % O_2)	13.0 -
Hydrogen —	13.5 -
Oxygen —	8.5 -
Carbon dioxide —	10.0 -

b. Positive Figures.

1. General Character of the Positive Figures. The positive figures will later on be subjected to a more detailed investigation, we shall therefore at present only consider their general appearance.

The positive figures consist of sharply defined stems or trunks with short, well defined branches or offshoots, see Figs. 6, 14, 16, and 19. The appearance of the figures, and especially the ramification, depends on the nature of the gas, and we shall later on return to this point; for the present we shall only deal with some general features of positive figures in atmospheric air or in nitrogen.

Effect of gas pressure on the appearance of the figures. It has been found that the number of branches per centimetre of trunks is proportional to the pressure. To illustrate this point some of our results are quoted in Table 6.

Table 6. Effect of Gas Pressure on the Number of Branches. Nitrogen from steel flask (93 % N_2 + 7 % O_2).

Pressure p mm. hg.	Number N of branches on 1 cm. of trunk	$100 \frac{N}{p}$
760	7.7	1.0
300	3.0	1.0
150	1.14	0.76
75	0.64	0.85
34	0.36	1.1
	Mean value..	0.94

The values of N quoted in the table are mean values for at least 10 different trunks, and there is, and necessarily must be, a rather great uncertainty in the determination of N. The figures in Table 6, however, strongly support the view that the average number of branches per centimetre of trunk is proportional to the pressure.

We have further found that the product of gas pressure and width of trunks is constant. This relation, however, only holds good at the free ends of the trunks; close to the electrode, where the different trunks cannot find sufficient space to develop, this relation does not hold good and cannot be expected to do so. The width of the trunks generally decreases from the electrode outwards, and the width ought to be measured in corresponding points. As such we have taken points whose distance from the top of the trunks is inversely proportional to the gas pressure. The results of such a series of measurements are quoted in the following table.

Table 7. Effect of Gas Pressure on the Width of the Trunks. Nitrogen from steel flask (93 % N_2 + 7 % O_2).

Pressure p mm. hg.	Width of trunks t mm.	Distance from test point to top of trunk mm.	$p \cdot t$
760	0.12	0.5	91
300	0 29	1.3	87
150	0.59	2 6	89
75	1.42	5.2	106
34	3.60	11.0	119
		Mean value..	98

In order to illustrate this point we have also taken a series of microphotographs of the top end of trunks in the same gas but at different pressures, making the magnification proportional

to the pressure. Fig. 39 shows such a series of microphotographs. It appears from Table 7 and Fig. 39 that the product of gas pressure and width of trunks or branches is very nearly constant in the interval from atmospheric pressure down to about 75 mm. hg. For pressures below 75 mm. hg. the width of the trunks is greater than according to this rule.

2. The range of the positive figures is mainly dependent upon the same physical constants as the range of the

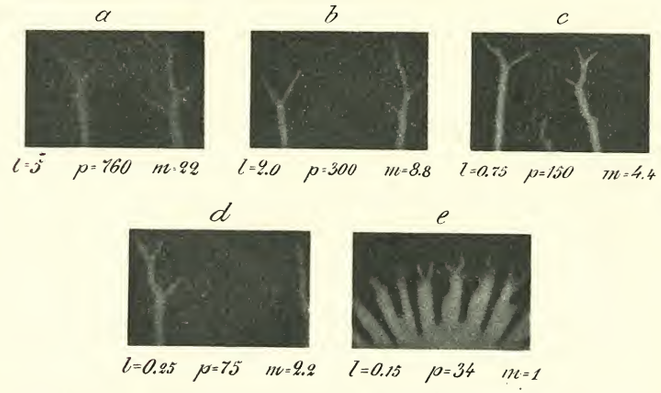

Fig. 39. Microphotographs of Top Ends of Trunks, the Magnification being equal to $\frac{p}{34}$.

negative figures but the influences of some of these constants show very characteristical differences in the two cases. The range r is, as shown by W. v. Bezold (1871)[4], independent of the value of the dielectric constant for isotropic plates. For crystalline plates the range may be different in different directions, a fact first discovered by E. Wiedemann (1849)[1]. We shall, however, in this paper confine ourselves to the discussion of isotropic plates.

The range depends very much on the thickness of the plate. W. v. Bezold's results for dust figures at atmospheric

pressure are indicated in Fig. 33, while Fig. 34 shows some of our measurements for photographic Lichtenberg figures. An example of a (d_0,r)-curve at lower pressure is shown in Fig. 40. While the range of the negative figures attains its maximum value for very small values of d_0 (see Fig. 33 and 34), the range of the positive figure on the contrary is very small for small values of d_0, and attains large values for greater values of d_0. At atmospheric pressure the range is maximum

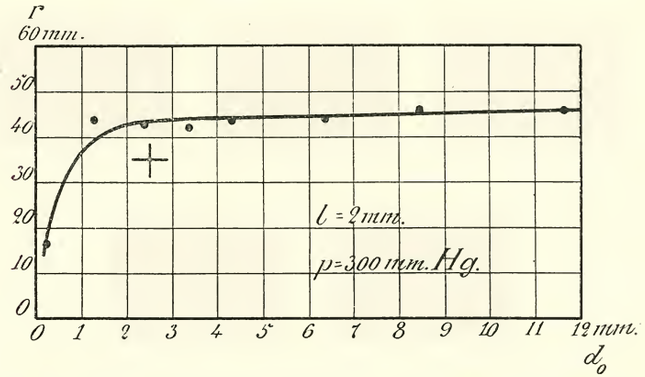

Fig. 40. Effect of Thickness of Plate on the Range of the Positive Figure. (Air; $p = 300$; $l = 2$; $d_0 = 1.4$).

for d_0 about 5 mm.; at lower pressure the range seems to be maximum for $d_0 = \infty$ (see Fig. 40.).

The relation between range and length of spark for air at atmospheric pressure is shown in Fig. 35. W. v. Bezold's measurements refer to dust figures, S. Mikola's and ours to photographic figures. The agreement between the three sets of measurements is not very good. The rather great ranges found by W. v. Bezold are probably due to the fact that his voltages varied too rapidly, the sparking voltages thereby attaining too high values. The difference between S. Mikola's and our measurements is — partially at least — due to difference in the thicknesses of the plates, by Mikola about

3 or 4 mm. in our experiments about 1.4 mm. For small spark lengths the character of the (l,r)-curves differs very much for positive and negative figures. While the (l,r)-curves for negative figures approximate straight lines, which for point electrodes apparently start from the origin, the corresponding curves for positive figures all start from some points of the positive l-axis and in a direction approximately normal to this axis; this is even true for point electrodes. For greater spark lengths the curves bend towards the l-axis and become approximately straight and parallel to the corresponding lines for negative figures.

S. Mikola gives the following formulae for the range of the positive and negative figures

$$r = a_1 \sqrt{V - V_0} \quad \text{for positive figures} \qquad (a)$$

and

$$r = a_2 (V - V_0) \quad \text{for negative figures.} \qquad (b)$$

V being the actual spark potential and V_0 the smallest P. D. capable of producing a figure.

According to Mikola V_0 has the same value in (a) and (b), that is to say that the positive and negative (l,r)-curves start from the same point. This is, however, as we have seen, only true in special cases. With point electrodes the negative (l,r)-curve always seems to start from the origin while the positive curve starts from a positive point of the l-axis. The following experiment is also in accordance with this view. A point electrode suddenly connected to a P. D. of 440 volts gave small but well defined negative Lichtenberg figures at atmospheric pressure. Of a positive figure no trace was obtained even with 730 volts, the largest constant P. D. at our disposal. The formulae (a) and (b) are thus no doubt only approximate ones and can only be used within certain limits, and V_0 will in general have different values in (a) and (b).

The effect of the duration of the impulse on

the range was tested in the same way as the similar question for negative figures, and the results are plotted in Fig. 36. The range of the positive figures seems to be rather independent of the duration of the impulse, while for negative figures the range is approximately proportional to this duration. A positive figure of normal size and character appears when the P. D. across the L. G. has reached a certain value even if the P. D. is only kept on during an extremely short time.

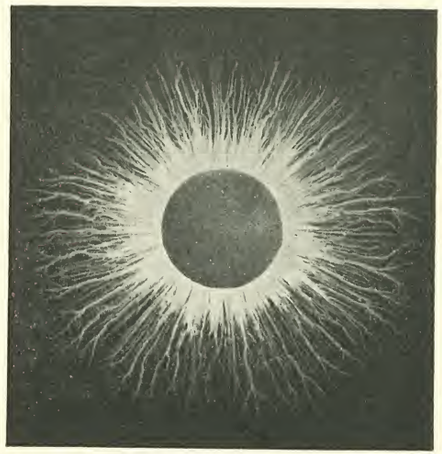

Fig. 41. Positive Figure. (Wire $k_2 s = bq = 23$ m.; Air; $p = 760$; $l = 3$; $D = 17.5$; $d_0 = 1.4$; $m = 1$).

If the P. D. is applied during a relatively long time, a new discharge takes place, the range of which is indicated by points marked p_1 and p_2 in Fig. 36. In so far there is a close analogy between the behaviour of the positive and negative figures. But while the negative fanshaped discharges seem to start from the ends of individual small sparks (see Fig. 37), the second positive discharge seems to have exactly the same character as the first one (see Fig. 41). The only difference between the first and second discharge seems to be that the trunks of the last are confined to the free spaces between the trunks of the first discharge. The trunks of the second discharge are therefore comparatively narrow in the neighbourhood of the electrode and expand as soon as they find sufficient space to do so. (Some of the details mentioned have been lost in the reproduction of Figs. 37 and 40).

W. v. Bezold (1871)[4] and S. Mikola (1917)[1] investigated how the range of the positive figures depends upon the pressure in the gas.

v. Bezold found the following formula

$$r = \frac{a_1}{p},$$

while S. Mikola found that

$$r = \frac{a_2}{(p + k)^{3/2}}$$

was in better agreement with his measurements. a_1, a_2, and k are constants.

One of our series of measurements is plotted in Fig. 42. It does not agree with any of the above formulae; but with suitable values of the constants the discrepancies are only small in both cases. Both formulae are to be considered as empirical and, as v. Bezold's only contains one arbitrary constant and Mikola's two, it would be natural to prefer the first of the two formulae, at least until further evidence is available.

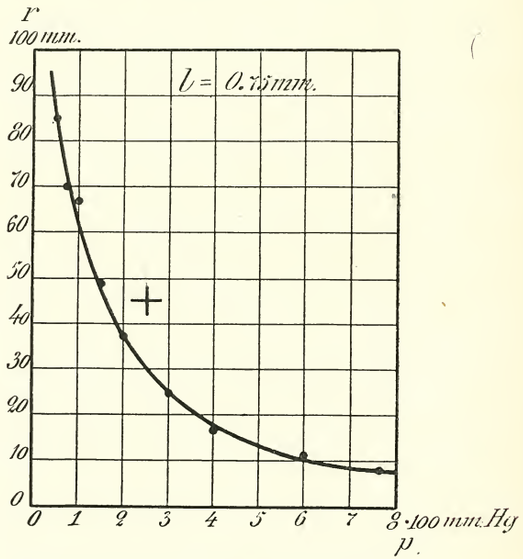

Fig. 42. Relation between Gas Pressure and Range of Positive Figure. (Air; $l = 0.75$; $d_0 = 1.4$).

The range depends also upon the nature of the gas, but we have not yet made any definite measurements. The following table contains some of our provisional results.

Table 8. Ranges of Positive Figures in Various Gases.
($l = 5$ mm.; $p = 760$ mm. hg.).

Gas:	Range:
Air	23 mm.
Nitrogen from steel flask (93 % N_2 + 7 % O_2)	23 -
Hydrogen —	28 -
Oxygen — (the positive figure is very faint)	20 -
Carbon dioxide —	11 -

c. Secondary Figures.

1. General Features. These figures have been observed by W. G. Armstrong and H. Stroud (1899, plates III and IV of Supplement), and reproductions of very fine specimens of them are to be found in S. Mikola's paper (1917). The secondary figures start on the plate P_2 (see Fig.17) a little outside the edge of the upper electrode A, and continue for some distance outwards. The negative figures consist of a series of soft, hazy lines, while in the positive ones the lines are more sharply defined, and from each line a great number of sharp offshoots project outwards, almost reaching the next line (see Fig. 20 and 21). The distance between consecutive lines increases with increasing distance from the edge of the upper electrode and with increasing distance between the lower plate P_2 and the electrode B (see Fig. 17). Below the upper electrode the plate P_2 shows a rather uniform light, while the outermost part of the negative secondary figure shows a tendency to disintegrate into round, hazy spots (see Figs. 18 and 20), and the positive figure into sharply defined but very irregular spots (see Fig. 21).

S. Mikola states that the secondary figure always forms a system of lines orthogonal to the discharge lines of the simultaneous primary figure. This is, however, not always true, as an inspection of Figs. 18 and 19 will prove. Fig. 18 shows a secondary and Fig. 19 the simultaneous primary figure. The plate P_2 rested on a rectangular frame *abcd* of mica which had no influence whatever on the primary figure (Fig.

19) but caused very marked alterations in the lines of the secondary figure (Fig. 18). A comparison between the two figures shows that the two sets of lines are not always orthogonal to each other, but it shows also that there is some tendency towards this orthogonality.

Chapter IV.

Velocity of the Positive and Negative Lichtenberg Discharge.

1. Method of Measurement. For the elucidation of the origination of these figures it is of great importance to

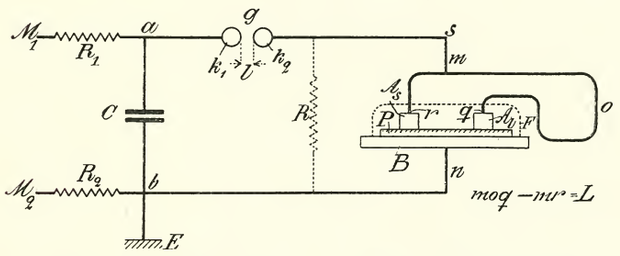

Fig. 43. Circuit Connections in Velocity Measurements.

determine the manner in which they attain their final shape and size. The figures may possibly originate in either of two ways: They may almost at once attain their final shape and size while the intensity increases during the time it takes to form the figure; or the figures may spread out from the electrode attaining, more or less, the final intensity as far as the discharge has reached while there is no alteration outside the instantaneous boundary of the figure. In the latter case the velocity of the spreading out becomes of great interest, and if this velocity can be determined, it is thereby proved that the figures originate by spreading out from the electrodes.

In the following we shall describe a method for the measure-

ments of this velocity, together with the results of a number of such measurements under different conditions and for different gases.

The main principles of the measurements are indicated in Figs. 43 and 44, of which the first shows the diagram of connections and the second the form and the position of the two upper electrodes used in the measurements. When a spark passes through g, an electric wave starts herefrom and travels from k_2 along the wire leading to m. Here it parts in two separate waves, one running along the wire mr to the electrode A_s and the other along moq to the electrode A_l. The velocity of the wave fronts will very nearly be equal to the velocity of light $v = 3 \times 10^{10}$, and if the wire moq is L cm. longer than mr, the wave travelling along moq will reach A_l τ seconds later than the other wave reaches A_s, where $\tau = \frac{L}{v}$.

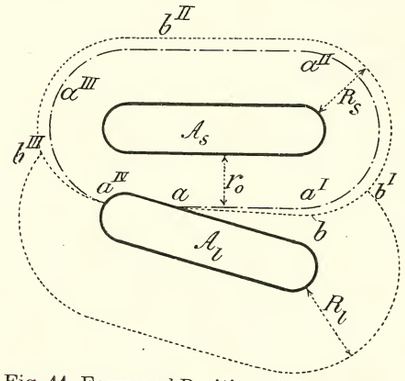

Fig. 44. Form and Position of Eleotrodes in Velocity Measurements.

Both electrodes being alike, their potentials will increase in the same manner, the only difference being that the potential of A_l lags τ seconds behind that of A_s. The discharge will therefor start τ seconds later from A_l than from A_s, and if the discharge travels a distance r_0 cm. from A_s before the electric wave reaches A_l, the mean velocity u of the discharge is determined by

$$u = \frac{r_0}{\tau} = \frac{r_0}{L} v = \frac{r_0}{L} \cdot 3 \cdot 10^{10} \text{ cm/sec.}$$

It is of great importance to chose the shape, size, and positions of A_s and A_l in such a manner that the value of r_0 may

be determined without ambiguity. Electrodes of the form shown in Fig. 44, and placed as indicated, have proved to answer very well and have been used in almost all our experiments.

The electrodes are placed in such a way that the shortest distance between them is slightly less than r_0. The discharge from A_s will then have reached A_l at the moment the electric wave through the wire moq reaches A_l. The boundary of the discharge from A_s at this moment is in Fig. 44 indicated by aa^I a^{II} a^{III} a^{IV}. A discharge then starts from A_l while at the same time the discharge from A_s pushes on further outward. The result hereof is, that the two discharges meet in a line abb_1 passing through the point a. A part, ab, of this line is nearly straight. The behaviour of the discharges at the meeting line is different under different conditions: In positive figures at atmospheric pressure both discharges push beyond the meeting line, the offshoots from one side making their way for some distance into the free spaces on the other side and vice versa. An example hereof is shown in Fig. 45. In this case the meeting line is not very sharp and cannot be determined with any great accuracy. At lower pressure there is either no trespassing

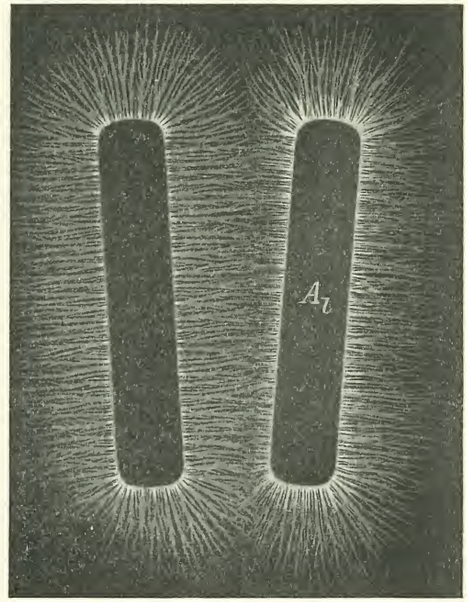

Fig. 45. Positive Velocity Figure. $L = 10$ m. (Air; $p = 300$; $l = 2.5$; $d_0 = 1.4$; $m = 0.8$).

at all or at least only very little, and the meeting line is accordingly very well defined. Examples of such figures are shown in Fig. 46—49. For negative discharges the meeting line is rather well marked at atmospheric pressure (see Fig. 50) while at lower pressures it often becomes less sharp.

As mentioned above the meeting line starts from the point a on A_l (see Fig. 44) reached by the discharge from A_s at the moment the electric impulse reaches the electrode A_l. The first part, ab, is in most cases nearly a straight line making only a small angle with the edge of A_s. That this is so, is easily understood. Before the electric impulse reaches A_l, the electric force in the space between A_s and A_l is due to the charge on A_s and on the area covered by the electric figure which surrounds A_s. As soon as the electric impulse reaches A_l, the electric force exerted by the charge on A_l at points between A_l and aa^{I} will predominate over the force due to the charge on A_s and its figure. As we shall see later on, the velocity increases with increasing force and the figure starting from A_l will therefore spread with greater velocity than that with which the figure belonging to A_s progresses further from the line aa^{I}.

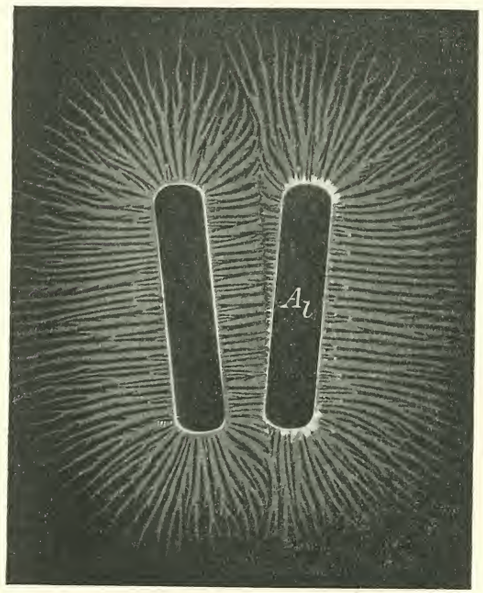

Fig. 46. Positive Velocity Figure. $L = 6$ m. (Air; $p = 300$; $l = 1$; $d_0 = 1.4$; $m = 0.8$).

We have until now supposed the front of the waves travelling along the wires mr and moq (Fig. 43) to be so steep that the rise in potential at the wave front could be considered as instantaneous. The wave front is, however, in general not so steep, and we will have to consider what difference it makes that the potential of A_s and A_l increases gradually instead of instantaneously. The result of this gradual rise in potential of A_s is that the discharge does not start immediately when the wave reaches A_s but a little later when the potential has attained the necessary value. There will, however, be the same retardation at the electrode A_l, and the measurement of the velocity is so far not affected. But another effect of the gradual rise of potential ought to be considered. During the short interval from the moment the wave front just reaches A_l to the moment the discharge starts from A_l the electric field due to the charge on A_l tends to reduce the

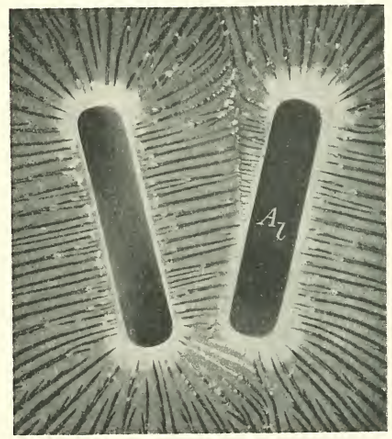

Fig. 47. Part of Positive Velocity Figure. $L = 6$ m. (Air; $p = 300$; $l = 2.5$; $d_0 = 1.4$; $m = 0.8$).

Fig. 48. Part of Positive Velocity Figure. $L = 6$ m. (Air; $p = 150$; $l = 2.8$; $d = 1.4$; $m = 0.8$).

velocity of the discharge from A_s. The result hereof is that the velocity as measured comes out a little too small.

Another possible source of error may conveniently be discussed here. If the discharge does not start immediately when the potential reaches the necessary value but is retarded a certain time τ', this retardation will be the same at A_s and A_l and will therefore only affect the measurements by reducing the velocity of the discharge from A_s during the interval τ'. The measured velocity will therefore in this case be too small. It ought to be remarked, however, that we have no indications whatever of such a retardation.

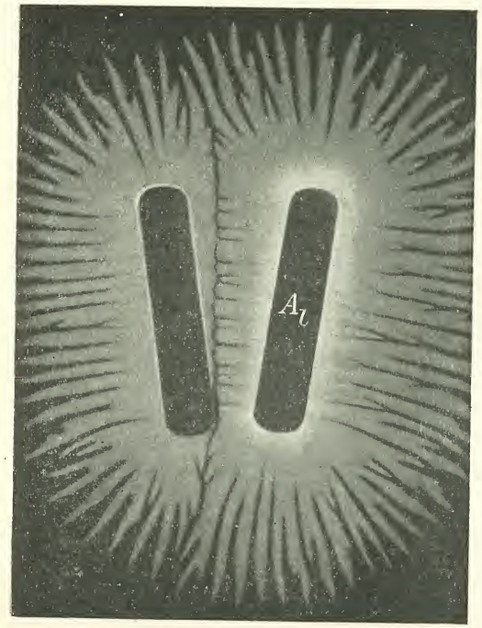

Fig. 49. Reversed Positive Velocity Figure. $L = 6$ m. (Air; $p = 75$; $l = 0.25$; $d_0 = 1.4$; $m = 0.8$).

A slowly rising wave front may influence the velocity measurements in another way. If the wire *mr* (Fig. 43) is short compared with the increasing frontal part of the wave, the increase of voltage by reflection at A_s will not attain its normal maximum value, while this will be the case at the electrode A_l, the wire *moq* being considerably longer than *mr*. The maximum voltage in this case is therefore greater at A_l than at A_s. The result hereof is that the velocity measured is too small and that the final range R_1 from A_l is greater than the range R_s from A_s (see Figs. 44, 46, and 50).

If the maximum voltage attainable by reflection from the end of the long wire *moq* is but little more than just sufficient to start the discharge, the above mentioned effect of a rather short wire *mr* may result in a — at least at first sight — rather strange phenomenon: When the wave for the first time reaches A_s the voltage does not attain such a value that a discharge takes place from A_s. At A_l, on the other hand, the voltage becomes sufficiently high and a discharge starts from this electrode. The wave reflected from A_l then travels back along *qom* and in the mean time the spark at *g* is extinguished. The wire msk_2 is in reality rather short, and the increase of voltage by reflection at A_l is now sufficient to start a discharge from A_s. The result hereof is a velocity figure exactly similar to the ordinary ones, with the sole exception that the rôles of A_s and A_l have changed. An example of such a velocity figure is shown in Fig. 49. In accordance with the explanation given the insertion of a longer wire between *m* and A_s does away with this irregularity.

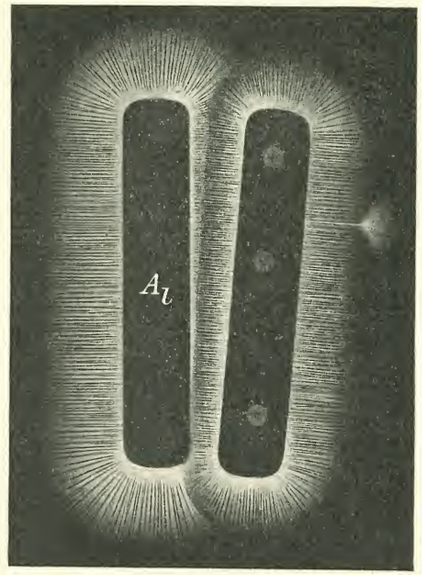

Fig. 50. Negative Velocity Figure used in the Measurement of Spark Retardation, compare Ch. VII, Fig. 72. (A_l on left Electrode should be A_2; $l_1 = 6$; $l_2 = 0.2$; no Ionization of g_2).

2. Results of the Velocity Measurements. A great

number of velocity measurements have been carried out in order to ascertain the effect of spark length, gas pressure, thickness of plate, and nature of the gas on the velocity.

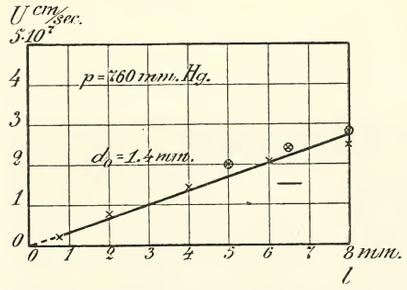

Fig. 51. Relation between Velocity U and Spark Length l for Negative Figures. (Air; $p = 760$; $d_0 = 1.4$).

Velocity of negative discharge. At atmospheric pressure the velocity U is nearly proportional to the spark length l (see Fig. 51) and the (l, U)-curve seems to pass through the origin. With a 3 mm. spark the velocity is about 1×10^7 cm/sec. At lower pressure the (l, U)-curve still starts from the origin but it is bent with the concavity against the l-axis (see the lower curves in Figs. 52 and 57).

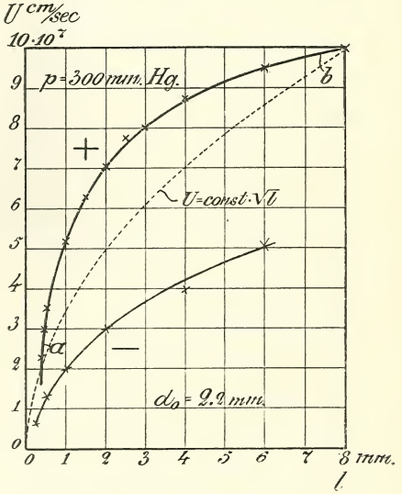

Fig. 52. Effect of Spark Length on the Positive and Negative Velocity (Air; $p = 300$; $d_0 = 2.2$).

The effect of pressure on the velocity is seen from Fig. 53. The velocity increases rapidly with decreasing pressure. As shown in the figure the experimental values fit in between the curves $U \cdot \sqrt{p}$ = constant and $U \cdot p$ = constant. The last mentioned seems to give the best approximation.

The relation between velocity and thickness of the plate is at atmospheric pressure shown in Fig. 54. For lower pressure the velocity does not decrease so rapidly with increasing

value of d_0. In all cases the velocity seems to be greatest for very small values of d_0.

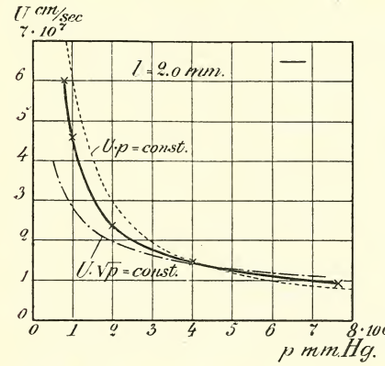

Fig. 53. Effect of Pressure on the Negative Velocity. (Air; $l = 2$; $d_0 = 1.4$).

We may summarize the main results as follows:

1. The (l, U)-curves start from the origin.
2. The (p, U)-curves are approximately hyperbolae giving very great values for the velocity at small pressures.
3. The velocity is greatest with very thin plates.

There is a very close analogy between the dependency of the velocity upon the constants l, p, and d_0 and the dependency of the range upon the same constants. In order to illustrate this anology we have in Fig. 55 shown two sets of curves, the upper one giving the relations between range and p, d_0, and l, the lower one the corresponding curves for the velocity.

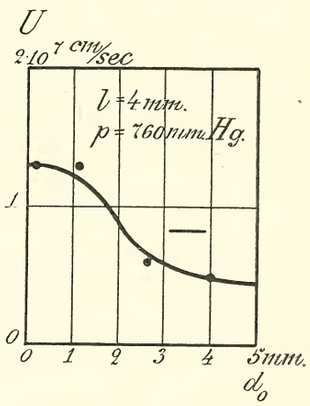

Fig. 54. Effect of Thickness of Plate on the Negative Velocity. (Air; $p = 760$; $l = 4$).

The negative velocity is very nearly the same in nitrogen and in air. For other gases measurements have not yet been made.

Velocity of the positive discharge. In air at atmospheric pressure and for spark lengths between 1.5 and 8 mm. the velocity is nearly proportional to the square root of the spark length, (see Fig. 56). At small spark lengths the velocity is, however, much smaller than according to this rule and the

velocity seems to be zero for a spark length of about .5 mm. This agrees well with the fact that no positive figure is formed

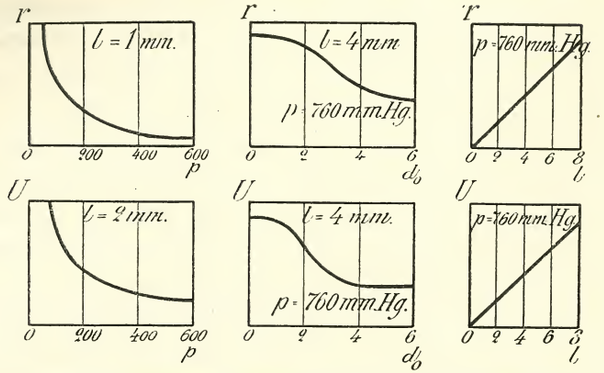

Fig. 55. Comparison between Range r and Velocity U for Negative Figures.

unless the spark length exceeds a certain value. Fig. 52 shows a (l, U)-curve corresponding to a pressure of 300 mm. hg. and Fig. 57 a similar curve for $p = 150$ mm. hg. In all three cases the general shape of the curves is the same and they all seem to start with zero velocity at some definite spark length l', where l' is roughly proportional to the pressure.

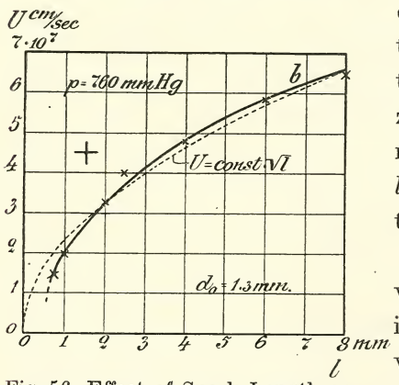

Fig. 56. Effect of Spark Length on the Positive Velocity. (Air; $p = 760$; $d_0 = 1.3$).

The relation between velocity and gas pressure is shown in Fig. 58. The velocity increases with decreasing pressure but seems to attain a definite value for very small pressures, a value which does not differ appreciably from the value for $p = 100$ mm. hg. (Fig. 58 contains only measurements

down to $p = 50$ mm. hg.; later measurements have been carried out down to $p = 20$ mm. hg. where the velocity was found to be about 5.2×10^7 cm/sec in very good agreement with the results recorded in Fig. 58).

The relation between velocity and thickness of plate is shown in Fig. 59 for a pressure of 300 mm. hg. and a spark length of 2 mm. At atmospheric pressure the (d_0, U)-curve has a similar shape; the measurements have been carried out, however, at the lower pressure, which gives a better determination of the velocity. The characteristic feature of the (d_0, U)-curve is the relatively very small values of U for small values of d_0. It seems as if U converges to zero together with d_0. The velocity curve has besides a rather marked maximum for values of d_0 about 2 to 3 mm. For great values of d_0 the velocity becomes rather small.

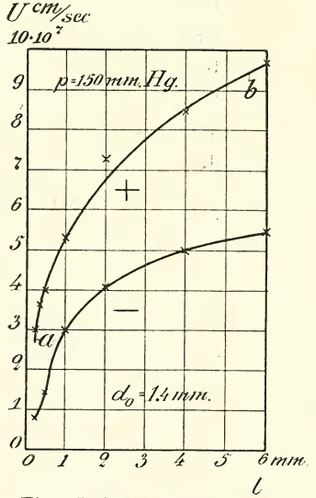

Fig. 57. Effect of Spark Length on the Positive and Negative Velocity. (Air; $p = 150$; $d_0 = 1.4$).

An examination of the different sets of measurements shows that the velocity depends upon the ratio of the pressure to the spark length, but not on these two constants separately. This relation is illustrated by the figures in Table 9, giving the results of a series of measurements in which the rate $\frac{p}{l}$ has a value of about 300. The mean value of U is 4.1×10^7 cm/sec, the highest being 4.5×10^7 and the lowest 3.8×10^7 cm/sec, that is a deviation of about $\pm$ 10 per cent from the mean value.

We may summarize the main results of our measurements of the positive velocity as follows:

Table 9. Positive Velocity in Air. p/l about 300.

Length of Spark l mm.	Air Pressure p mm. hg.	r_0 mm.	L mm.	$U = \frac{r_0}{L} \cdot 3 \times 10^{10}$ cm/sec
0.14	40	7.6	6000	3.8×10^7
0.25	75	7.8	6000	3.9 -
0.5	150	7.8	6000	3.9 -
0.5	150	8.4	6000	4.2 -
0.5	150	24.0	16000	4.5 -
1.0	300	9.0	6000	4.5 -
1.0	300	8.4	6000	4.2 -
2.5	760	8.2	6000	4.1 -
			Mean value..	4.1×10^7

1. The (l,U)-curves do not start from the origin, the velocity being zero until the spark length has attained a certain value which increases with increasing pressure.
2. For very small pressures the velocity converges to a limiting value, which is not very different from the value corresponding to $p = 100$ mm. Hg.
3. The (d_0,U)-curves seem to start from the origin and the velocity has a maximum value for d_0 between 2 and 3 mms.
4. $U = F\left(\frac{p}{l}\right)$.

For negative figures we found a very close analogy between range and velocity in their dependency upon the constants l, p, and d_0. This analogy is, for the positive figures, violated in one important point: the (p,r)-curves and (p,U)-curves having an essentially different shape. This is the greatest difference, but the (d_0,r)-curves and the (d_0,U)-curves also show marked differences (see Fig. 60).

The positive velocity in different gases has not yet been sufficiently investigated. We have in Table 10 quoted a few quite preliminary results.

Table 10. Positive Velocities in various Gases.

Spark Length mm.	Pressure mm. hg.	Gas	U cm/sec.
4.0	760	Air	4.8×10^7
—	—	H_2	4.5 -
0.5	150	Air	4.2 -
—	—	N_2	3.0 -
—	—	H_2	3.9 -

3. Preliminary Discussion of the Results.

The negative velocity. We have seen that the negative figures spread out from the electrode and it is therefore probable that these figures are due to electrons moving from the electrode outward under the influence of the electric field

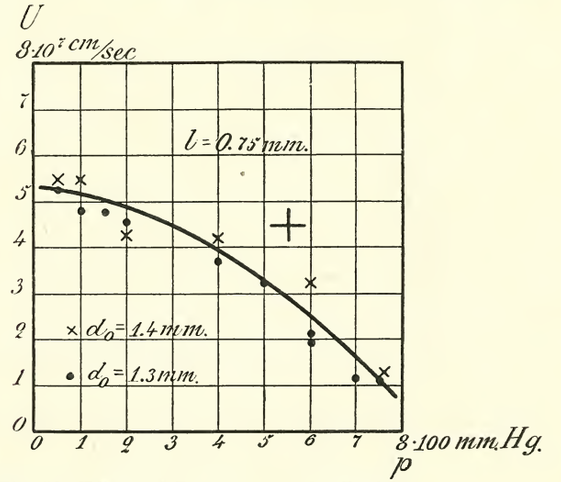

Fig. 58. Effect of Pressure on the Positive Velocity. (Air; $l = 0.75$)

each causing ionization by collision along its path. For the velocity of an electron moving in air under an electric force E the velocity U is determined by*)

$$U = \sqrt{2.04 \times 10^{-2} \cdot \frac{e}{m} \cdot \frac{E}{p}}, \qquad (a)$$

where E and e are in *e. s. u.* Putting $\frac{e}{m} = 5.3 \times 10^{17}$ and measuring E in volt per centimetre, this formula becomes

$$U = 6 \times 10^6 \sqrt{\frac{E}{p}} \cdot (\text{cm/sec.}). \qquad (b)$$

By the deduction of this formula it has been assumed that the velocity of an electron in the direction of the electric

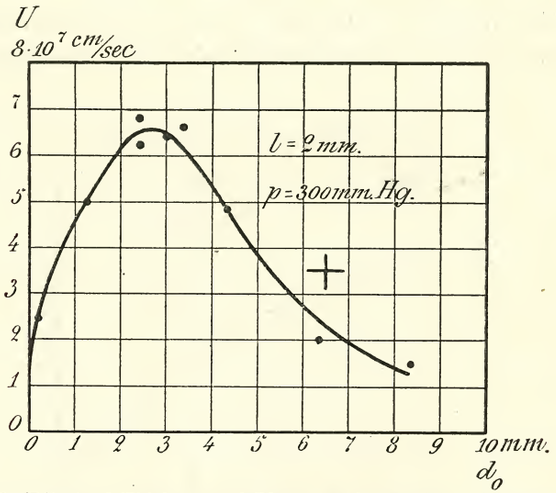

Fig. 59. Effect of Thickness of Plate on the Positive Velocity. (Air; $p = 300$; $l = 2.0$).

force greatly exceeds its velocity of agitation. These two velocities are, however, in this case approximately equal, and the above formula therefore gives too great values of U. We may write

* J. S. Townsend: Electricity in Gases. p. 343. (Oxford 1915).

$$U = \mu \cdot 6 \times 10^6 \sqrt{\frac{E}{p}}, \qquad (c)$$

where μ is a coefficient which is less than unity.

If we put $p = 760$ and $U = 2 \times 10^7$ cm/sec., corresponding to a spark length of about 6 mm. (see Fig. 51), the electric

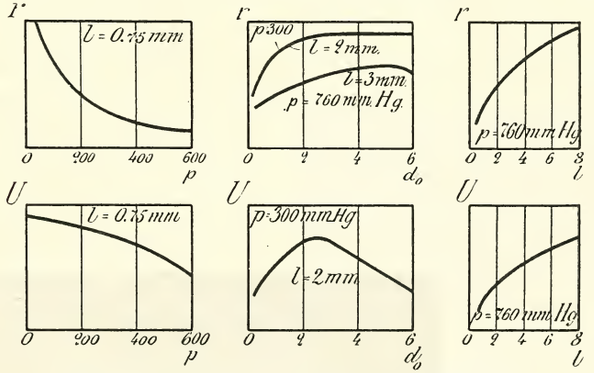

Fig. 60. Comparison of Range r and Velocity U for Positive Figures.

force is, according to formula (*c*), $E = \frac{1}{\mu^2}$ 8450 volts per centimetre.

This value is, no doubt, of the right order of magnitude. According to formula (*c*) the velocity should be proportional to the square root of the electric force and inversely proportional to the square root of the pressure. At lower pressure the velocity is nearly proportional to the square root of the spark length (see Figs. 52 and 57) while at atmospheric pressure there seems to be a straight line relation between U and l (see Fig. 51). With varying pressure the values of U fall between the values determined by $U \cdot \sqrt{p} =$ constant and by $U \cdot p =$ constant (see Fig. 53).

In view of the complicated nature of the phenomenon and in consideration of the fact that the coefficient μ depends on the ratio $\frac{E}{p}$ the above facts must be said to agree fairly well

with the supposition that the negative figures are due to electrons moving from the electrode outwards. A closer investigation of this question can, however, not be taken up with advantage before a detailed theory of the origination of these figures has been established.

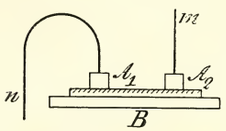

Fig. 61. Wire m and n connected to m and n in Fig. 10.

The positive velocity. If the positive figures are due to positive ions moving outwards from the electrodes, one should expect the positive velocity to be much smaller than the negative one. If, on the other hand, the positive figures as the negative are due to the movement of electrons, which in this case are drawn inwards to the electrode, it would be reasonable to expect about the same velocity for positive and negative figures and especially that the general character of the relations between the velocity and the constants l, p, and d_0 would be the same in both cases. Neither of these assumptions agree with the experimental results referred to in section 2. The positive velocity is in general found to be about 2 to 3 times greater than the negative, and the dependence of the velocities upon l, p, and d_0 shows principal differences for positive and negative figures.

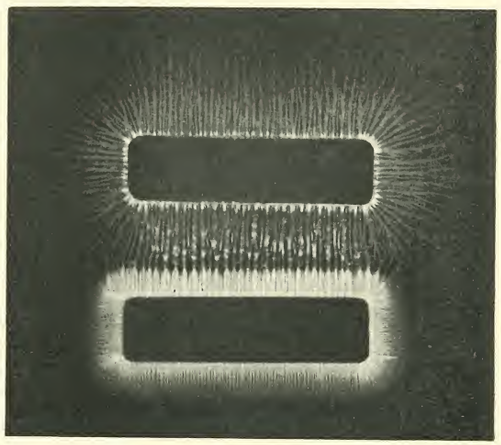
Fig. 62. Positive-Negative Figure. (Air; $p = 760$; $l = 5$; $d_0 = 1.4$; $m = 1$).

We shall not here take up the discussion of the origination of the positive figure, we have only stated the above mentioned difficulties in order to point out the desirability of some control of our velocity measurements. One way of doing this is as follows: Two equal electrodes A_1 and A_2 were placed on the film of the photographic plate (see Fig. 61), A_1 connected to the wire n (see Fig. 10) and A_2 to m, while the electrode B was insulated by being placed on an ebonite stand. The two small and equal capacities A_2-plate-B and B-plate-A_1 are thus in series in the discharge circuit and will at the moment the discharge starts be subjected to the same voltage. For positive discharges the figure at A_2 will be positive and the A_1-figure negative, and for negative discharges the polarity of the figures will be reversed, but apart from this change in polarity the two pairs of figures are identical.

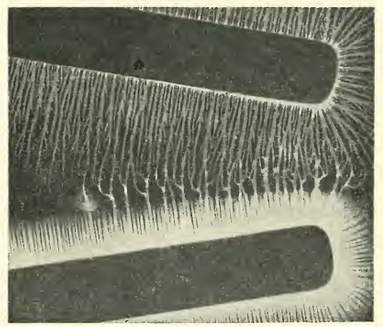
Fig. 63. Part of Positive-Negative Figure. (Air; $p = 760$; $l = 9$; $d_0 = 1.4$; $m = 0.8$).

Fig. 62 shows such a pair of figures, the two electrodes being parallel to each other. In the space between the electrodes neither the positive nor the negative figure has attained its final extension, the two figures having met each other before they were completed. In the space, where they meet, the two figures are connected by a third kind of discharge which we shall call the neutral discharge. This neutral discharge consists of a number of lines or bands of different broadness and with a soft or foggy appearance. They all form extensions of the positive trunks but differ from these by having no branches and by their foggy appearance. (These differences

are very clearly seen on the original photographs but have partly been lost in the reproduction. These neutral discharges show some other peculiarities, but we must defer the description hereof to a later occassion). Supposing the two figures start simultaneously the ratio of the distances from the electrodes to the neutral discharge will be equal to the ratio of their velocities. It will generally be more convenient to place the two electrodes at a small angle with each other, the velocity-ratio may then be measured at different points (see Fig. 63). There may be some uncertainty in measuring these distances and this method therefore only gives an approximate value of the velocity-ratio. The results obtained in this way agree, however, fairly well with those obtained with the former method as will be seen from the following table containing some of our measurements.

Table 11. Ratio of Positive and Negative Velocities Determined by Means of Simultaneous Figures.

Spark Length mm.	Pressure mm. hg.	$r_{pos.}$ mm.	$r_{neg.}$ mm.	$\frac{U_{pos.}}{U_{neg.}}$	Remarks
9.0	760	15.0	6 4	2 35	$d_0 = 2.8$ mm.
9.0	—	14.0	8 0	1 75	$d_0 = 1.3$ -
7.0	—	14.4	6.6	2.18	
5.0	—	11.0	4.5	2.45	
3.0	—	10.0	2.5	4.0	d_0 about 1.4 mm.
3.0	400	20.0	5.6	3.6	
2.0	—	18.0	3.7	4.9	
2.0	300	17.5	5.3	3.3	

Another question of some importance is whether the velocity along the surface of the plate is greater than the velocity of a sudden discharge in free air. In order to test this point we have made the following experiments: One of the electrodes in Fig. 12 was removed to a distance of 1 to 2 mm. from the plate, the other electrodes resting directly thereon.

The boundary lines between the figure around the elevated electrode and the figures from the other electrodes were thereby displaced somewhat toward the elevated electrode, but not appreciably more than what was to be expected on account of the greater distance. Even if this method does not allow anything like an exact comparison between the velocity in free air and along a plate, the experiment nevertheless indicates that there is no very great difference between the two velocities.

Chapter V.

Preliminary Theory of the Lichtenberg Figures.

1. Theory of the Negative Figures. In Chapter IV. 3. we supposed the negative figures to be due to ionization by collision produced by electrons moving outwards from the electrode. We shall now develop this working theory a little more and try to explain some of the characteristic features of the negative figures by means of it.

The very steep rise in potential caused by the electric impulse arriving at and being reflected from the electrode produces such a strong electric field in the neighbourhood of the electrode that ionization by collision sets in. This initial ionization will generally go on along the whole circumference of the electrode but with greater intensity at some points than at others. From those favourite points the negative discharge, carried by the swiftly moving electrons, will spread rapidly over the adjoining parts of the plate and thereby automatically reduce the electric force in the adjacent points at the edge of the electrode to such an extent that ionization by collision ceases to take place at these points. In this manner we get the negative discharge broken up in a number of separate flows starting from points at the edge of the electrode and distributed more or less at random along it. This question

is best illustrated by photographs taken at rather low pressure (see Fig. 28) where the distances between the starting points are greater than at higher pressure.

At some distance from the electrode the different flows have spread to such an extent that they cover the whole circumference with the exception of the thin black parting lines which we shall consider a little later. The exterior boundary of the figure will then be a circle — we suppose the electrode to be circular — the radius of which increases until the figure has attained its final size. We will now, for the sake of simplicity, suppose that the ionization is so intense in the already formed part of the figure that the drop of potential from the electrode to the front part of the figure may be neglected. In this case the density of the electric charge will be the same over the entire covered area and equal to

$$-q' = V \cdot \frac{\varepsilon}{4\pi d_0}, \qquad \text{(a)}$$

where V is the P. D. between the electrodes A and B, ε the dielectric constant of the plate and d_0 the thickness of same in centimetres. A corresponding surface density equal to $+q'$, is found on the electrode B. The free charge on the two surfaces will, however, only have a density of $-q$ and $+q$, where

$$q = \frac{V}{4\pi d_0}. \qquad \text{(b)}$$

The electric force at the edge of the figure depends on the free negative charge on the electrode A and on the developed part of the figure and the free positive charge on the electrode B. If A is not too great and if we only consider points in considerable distances from A, we may as a first approximation neglect the influence of the charge on A and only take account of the homogeneous circular charge distribution of intensity $-q$ on the surface of the plate and the corresponding charge distribution $+q$ on B. We may further

simplify our considerations by supposing that the thickness of the plate is very much smaller than the range of the figure. In this case the electric force at the edge of the figure will approximately be the same as if the figure was infinite with

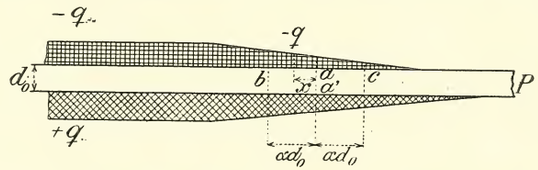

Fig. 64. Sketch of Distribution of Charge at the Edge of a Negative Figure.

a straight edge. Fig. 64 represents a cross section of such a straight edge and shows schematically the two charge distributions.

As the electric force only depends upon the free charges and as these are independent of the dielectric constant of the plate, the forces which are active in the formation of the figure and consequently also the size of the figure are independent of this constant, a result proved experimentally by W. v. Bezold.

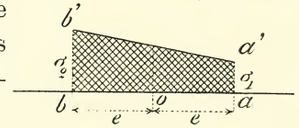

Fig. 65.

In Fig. 65 ab represents the cross section of a long rectilinear strip with a surface density of free electricity equal to σ_2 at b and to σ_1 at a and varying linearly from a to b. The electric force at a point o in the middle of the strip has a component in the direction oa equal to $4l \cdot \frac{\sigma_2 - \sigma_1}{2l} = -4l\frac{d\sigma}{dl}$, where $2l$ is the width of the strip and $\frac{d\sigma}{dl}$ the gradient of the charge density. We shall now consider the conditions at the edge of a figure while this figure is increasing in size due to the edge moving outwards from the electrode (see Fig. 64). The plate P rests upon the large plane metal electrode B (see Fig. 10); the horizontal component of the electric force at f. inst. the

point a' on the lower surface of P is therefore very small and may be neglected. At the point a on the upper surface of P and just opposite a' there will, however, be a considerable horizontal component, E. The effect of such parts of the charge being at a distance from aa', which is great compared with the thickness of the plate, will very nearly be the same in these two points, and the horizontal component in a must therefore mainly be due to the charges in the neighbourhood of that point, say, to the charges on the strip bc, the width of the strip being equal to $2\alpha d_0$ where the coefficient α is considerably greater than unity, say equal to 2. If the plate is so thin that the variation in the charge can be considered as linear over the distance bc, the horizontal component will be

$$E = \mu d_0 \frac{dq}{dx}. \qquad (c)$$

where $\frac{dq}{dx}$ is the gradient of the charge density on the upper surface of P, while μ is a coefficient, which is independent of d_0. The value of q in the homogeneous part of the figure inside the edge is inversely proportional to d_0 and we may reasonably suppose the same to be the case within the edge where the density is variable. If this is so, the product $d_0 \frac{dq}{dx}$ will be independent of d_0. As the size of the figure must be determined by the intensity of the force at the edge of the figure, our theory therefore leads to the conclusion that the size with thin plates is independent of their thinness, a result which is in complete agreement with our experiments (see Fig. 33 and 34). For greater values of d_0 the distance bc in Fig. 64 becomes so great that the charge does not even approximately vary linearly between these points. The result hereof will evidently be that E diminishes. According to this theory we may therefore expect that the range decreases with increasing thickness of the plate, slowly at first with thin plates but more rapidly with thicker ones until the distance bc becomes so great as to be comparable to the range of the figures. In this case our suppositions do not apply any longer, but it is easily seen that the range will approach a certain limit when d_0 becomes very great. All these deductions agree with the experimental results.

The diffusion of the electrons along the surface of the plate must also depend on the horizontal component of the electric force. We may therefore expect that the velocity will

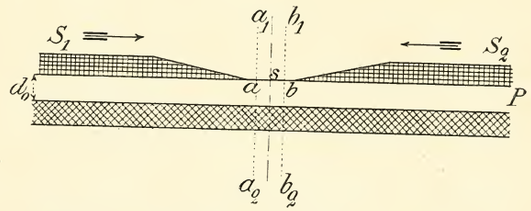

Fig. 66. Sketch of Cross Section of a Dark Line.

depend on the thickness of the plate in a similar manner as the range, a result also borne out by the experiments (see Figs. 34, 54, and 55).

We shall now consider the formation of the dark lines. The negative flow from a starting point at the edge of the electrode spreads outwards on the surface of the plate. The velocity is greatest in the radial direction but a sidewards spreading out — due to the mutual repulsion of the charge in the flow — also takes place. This lateral movement continues until the adjoining flow — moving in the opposite direction — is met. Fig. 66 is a sketch of two such flows, S_1 moving to the right and S_2 to the left. At the point s halfway between S_1 and S_2 the horizontal component E of the force is necessarily always zero, and no ionization by collision will take place there. At points to the right and left of s, E will be different from zero and varying with the time, the maximum value of E increasing with increasing distance from s. At two points

a and b, this maximum value is just sufficient to produce ionization, while between a and b no ionization will take place. The charge will diffuse over the whole surface, but no photographic impression is made between a and b, a—b thus being a cross section of a dark line. A little consideration shows that the distance between a and b, i. e. the width of the dark lines, will be very small when d_0 is very small and will increase with increasing value of d_0. This conclusion agrees with the experimental facts referred to in Chapter III.

The present theory also leads to the conclusion that the range ought to be proportional to the duration of the impulse. This is, to a certain extent, in agreement with the experiments described in Chapter III. a. and illustrated by the Figs. 36 and 37. When the voltage is kept on too long, more complicated forms of discharges appear, but we shall not at present enter into any further discussion of this point.

The present theory is certainly only a preliminary and approximative one. It does not take into account the P. D. which no doubt exists between the electrode and a point of the figure just inside the boundary region, and it does not say anything about the distribution of charge within this region. Besides, some of the approximations made are not very good. But crude as the theory is, it gives a fairly satisfactory explanation of the origination of the negative figure and of its qualities, and all the experimental facts seem to agree with our fundamental hypothesis that the negative figures are due to electrons moving outwards from the electrode and causing ionization along their path.

2. Theory of the Positive Figure. By a careful examination of all the experimental data we have collected about the positive figures, we have been led to the conclusion that these figures are due to positive particles moving outwards from the electrode. There are, however, some rather great difficulties in the way of the acceptance of this view. Some

of these difficulties have been removed while others are still outstanding. The whole question is, however, so important and its discussion will occupy so much space that it must be deferred to a later paper, where some other peculiarities of the positive discharge will also be discussed.

3. Theory of the Secondary Figure. In the sketch, Fig. 67, A and B denote as usual the electrodes, P the photographic plate with the film downwards. The line a_0ab represents diagrammatically a momentary distribution of the

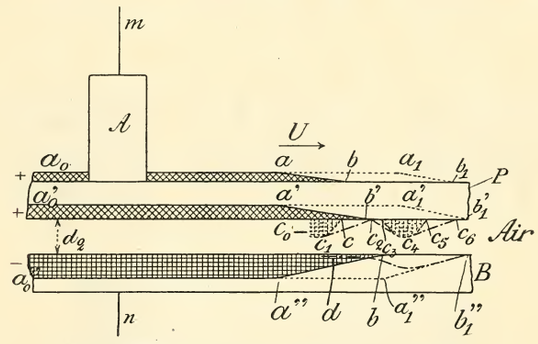

Fig. 67. Sketch of Formation of a Negative Secondary Figure.

free charge in the positive figure spreading out from A. $a_0'a'b'$ shows the corresponding induced charge at the lower surface of P, while $a_0''a''b$ represents the negative charge on the electrode B. During the formation of the primary positive figure the free charge at the upper surface of P and the induced charge on its lower surface move outwards with the velocity U of the positive discharge. If the distance between P and B is very small, so small that no considerable ionization takes place between them, the charge on B will spread in a similar manner, and no secondary figure appears. The plate P in this case, when developed, shows a more or less homogeneous blackening over the whole area below the positive figure while the intensity outside the boundary of this figure gradually

dies away. This effect on the film is due to the feeble ionization taking place in the layer of air between the plate and B.

If the distance between P and B is somewhat greater, but on the other hand not too great, say up to about 1 mm., the ionization taking place in the layer of air between P and B gives rise to certain complications, and a secondary figure generally appears. We shall now consider this process a little closer. At a certain moment the charge distribution may be as indicated in Fig. 67. The vertical component of the electric force at c_2 will then be very small while to the left of c_2 this component will have values which increase with increasing distance from c_2. At some point c this vertical force may be just great enough to give ionization by collision. The intensity of this ionization will rapidly increase if we go further to the left of the point c, and will result in a negative charge c_0c_1c being deposited on P. This charge produces a rather strong horizontal component of the electric field at c, resulting in a diffusion — generally combined with ionization — of the charge towards c_2. The new charge distribution may be represented by the line c_1c_2. In the meantime the front of the charge on the surface of P has reached the position a_1b_1, and the induced charge at the lower surface of P the position $a_1'b_1'$. The charge on the electrode B will not now be represented by the line $a_0''a_1''b_1''$ but rather by the dotted line shown between d and b_1'', and the vertical component of the electric force in the space between P and B will attain its greatest value somewhere in the neighbourhood of the point c_4. This force will cause a new ionization by collision between B and P, resulting in a negative charge $c_3c_4c_5$ being deposited on P. This charge will again diffuse especially towards c_6. And so on. For the explanation of the positive secondary figure it is only necessary to reverse the sign of all charges.

It follows from this explanation that the lines of the negative secondary figures should have the same soft and foggy

appearance which characterises the boundary of the negative figure. On the outer side of the lines of the positive secondary figures we may, on the other hand, expect to find offshoots of a positive character being due to lateral diffusion of the accumulated positive charges. The secondary lines will evi-

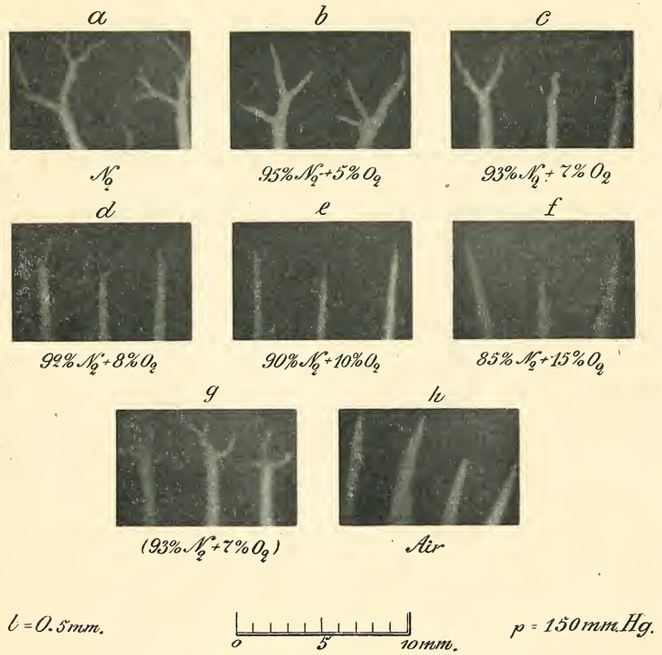

Fig. 68. Tops of Trunks of Positive Figures in Mixtures of Nitrogen and Oxygen. Part g in Nitrogen from Steel Flask.

dently have a tendency to be parallel with the simultaneous boundary of the primary figure, but if some obstacle is placed in the space between P and B, it is easily conceived that a secondary line will often start from the boundary of such an obstacle. It is to be expected that the distance between the secondary lines will increase with increasing distance between P and B and with decreasing charge. On all these points theory

and experiment agree completely with each other. This theory also explains why there are no secondary figures directly below the electrode A.

Chapter VI.

Positive Lichtenberg Figures in Various Gases.

Very few observations have been published about positive figures in other gases than air. E. Reitlinger (1861)[2] noted that

Table 12. Statistical Data of Figures in Mixtures of Nitrogen and Oxygen.
(l = 0.5 mm.; p = 150 mm. hg. D = 18 mm.; d_0 = 1.4 mm.).

Gas		Range r	Number of trunks	Number of branches on each trunk	a^1	b^1	c^1	Remarks
N_2	O_2							
per cent		mm.				mm.	mm.	
100	0	35	34	2.9 *	4.4	13.5	9.5	* Branches in the top not counted
95	5	35	30	2.6	2.6	7.9	12.5	
93	7	37	30	2.8	1.7	3.0	12.0	
92	8	37	34	2.8	1.0	1.1	12.2	
90	10	42	32	2.9	0.9	0.5	13.0	
85	15	40	36	3.0	0	0	12.0	
80	20	35	37	2.9	0	0	12.0	
67	33	32	28	3.1	0	0	11.5	
50	50	40	35	2.7	0	0	8.0	
33	67	31	25	2.7	0	0	6.0	
Mean value..		36.4	32.1	2.74				

[1] Column a contains the average number of branches in the top, only branches exceeding 1 mm. in length being counted. A pointed end of a trunk is counted as a branch. Column b contains the average value of the total length of all the branches per top. Column c the average length of branch-free trunk just below the top.

a figure in hydrogen has more branches than a figure in air. W. Holtz (1905)[1] is of the opinion that the nature of the gas is of very little importance. S. Mikola (1917)[1] states, that the figures in air and in nitrogen of atmospheric origin are similar and that figures in oxygen, hydrogen, carbon dioxide

and coal gas are so faint as to be almost invisible. We have taken some series of positive figures in nitrogen, oxygen, hydrogen, and different mixtures of these gases. Occasionally a figure has been taken in carbon dioxide and in a mixture of argon and air. All these experiments have been of a wholly

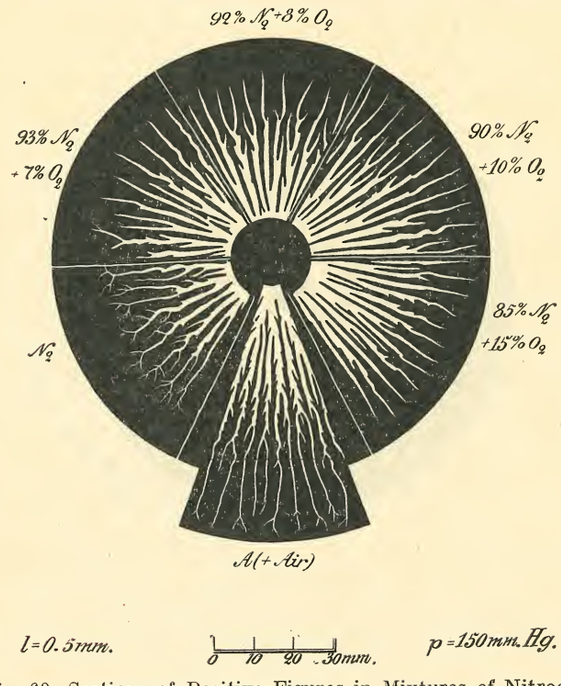

Fig. 69. Sections of Positive Figures in Mixtures of Nitrogen and Oxygen. (Lower Section in Argon + Air).

preliminary nature, but some of the obtained results may be of sufficient interest to be quoted here.

Mixture of nitrogen and oxygen. In pure nitrogen the figures are very clear and intense, the trunks and the thick branches being almost black on the developed plate, the top branches being somewhat »weaker« and not so sharply defined. With increasing percentage of oxygen the figure be-

comes fainter and with 1 per cent nitrogen and 99 per cent oxygen it is just visible.*) But other and more striking alterations take place. In pure nitrogen there is a well developed top consisting of a system of branches at the end of each trunk. With increasing percentage of oxygen this is greatly reduced. With 5 percent of oxygen the top is reduced to about

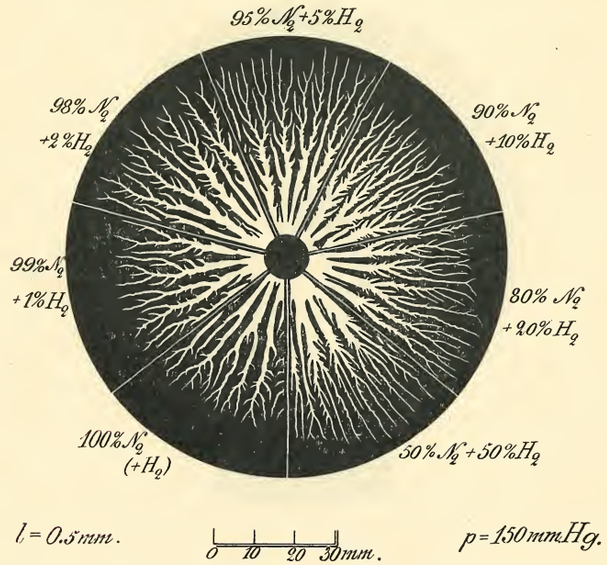

Fig. 70. Sections of Positive Figures in Mixtures of Nitrogen and Hydrogen.

half size and the remaining branches are stouter and more trunk like (see Fig. 68). With 7 per cent oxygen many of the trunks have no top at all but only some short irregular branches at the end of each trunk. With 10 per cent oxygen the trunks have a pointed end but no branches, and with still more oxygen the trunks are but ended. An increase in the percentage of oxygen beyond 15 does not seem to cause any great alteration in the shape of the figure with the exception that the

* All figures refer to per cent of volume.

outermost branchless part of the trunks becomes shorter. Neither the number of trunks nor the number of branches en each trunk — the branches in the top not being counted — seems to depend on the composition of the mixture; the whole offect of the oxygen is that it cuts away the top of the pure

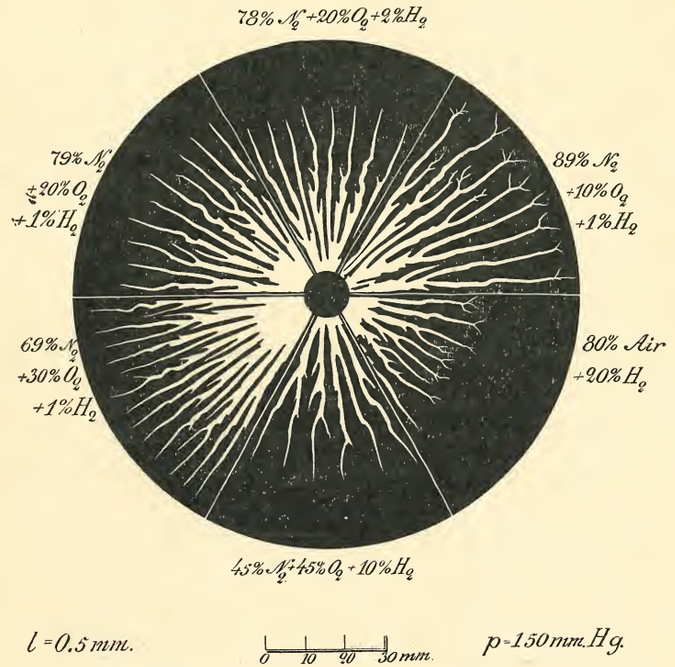

Fig. 71. Sections of Positive Figures in Mixtures of Nitrogen, Oxygen, and Hydrogen.

nitrogen figure. In order to illustrate these points further, we have in Fig. 69 shown sections of figures in different mixtures of nitrogen and oxygen (and a sector of an argon air figure), but most of the details of the tops have unfortunately been lost in the reproduction. Some statistical data about figures in such mixtures have been collected in Table 12.

Mixtures of nitrogen and hydrogen. The effect of hydrogen is mainly to create a great number of short branches on the middle parts of the trunks while the influence on the top is much less pronounced. Sections of such figures are shown in Fig. 70.

Some examples of figures in mixtures of nitrogen, oxygen and hydrogen are shown in Fig. 71.

On the original photographs a number of other characteristic features are to be seen but in the reproductions in Fig. 69—71 most of these have been lost, and the further discussion of this problem must be deferred till a later paper.

Chapter VII.

Measurements of the Retardation Caused by Spark Gaps.

The velocity of the positive or negative discharge as determined by means of the arrangemnet shown in Fig. 43 may with a similar arrangement be used for the measurement of very short intervals of time. As an example hereof we shall quote some measurements made by this method of the retardation caused by spark gaps. A sketch of the arrangement is shown in Fig. 72. The spark gap g_2 is enclosed in a tube of insulating material, and the inside of this tube

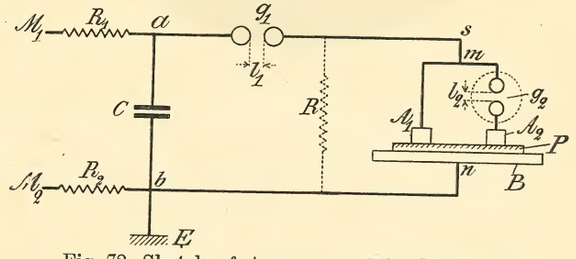

Fig. 72. Sketch of Arrangement for Measuring Spark Retardation.

may either be kept dark or the spark gap exposed to the light from a d. c. arc at a distance of 20 cm. from g_2. We call the two states of the gap respectively the normal and the ionized. The spark gap g_2 is inserted in a wire leading from the point m to the electrode A_2, another similar wire of equal length leading from m to the electrode A_1, equal to A_2. If there was no retardation in the gap g_2, the discharges from A_1 and A_2, caused by a spark in g_1, would start simultaneously and meet midway between A_1 and A_2. The retardation actually caused by g_2 can now be measured by determining the range r_0 of the discharge from A_1 at the moment the discharge from A_2 starts. The retardation T is then equal to

$$T = \frac{r_0}{v},$$

where v is the known velocity of the discharge from A_1.

Table 13 contains some results of a set of such measurements.

Table 13. Retardation Caused by Spark Gaps in Air at Atmospheric Pressure. Measured by Means of Negative Figures.
Velocity $v = 2.5 \times 10^7$ cm/sec.)

Spark Length l_1	Spark Length l_2	Spark Gap g_2	r_0	$T = \frac{r_0}{2.5 \times 10^7}$
mm.	mm.		mm.	sec.
6.0	1.0	normal	> 12.5	$> 5.0 \times 10^{-8}$
—	—	ionized	5.0	2.0×10^{-8}
—	—	ionized	5.5	2.2×10^{-8}
6.0	0.2	normal	6.5	2.6×10^{-8}
—	—	ionized	2.5	1.0×10^{-8}
6.0	0.1	normal	3.0	1.2×10^{-8}
—	—	ionized	0.5	0.2×10^{-8}

We have thus been able to measure the retardation caused by an ionized spark gap whose length is only about a hundredth part of the maximum spark length. By using positive

figures at a lower pressure it is possible to measure fairly accurately intervals down to or even below 1×10^{-9} second.

The influence of different physical conditions on the retardation of sparks is most easily studied by comparing two spark gaps, one placed between m and A_1, the other between m and A_2 (see Fig. 72).

I wish to express my indebtedness to Mr. O. Ellekilde for his assistance in some of these experiments and to Mr. J. P. Christensen for his valuable help in the whole investigation.

Royal Technical College of Copenhagen,
September 1918.

Meddelt paa Mødet d. 8. Marts 1918.
Færdig fra Trykkeriet d. 12. Februar 1919

Bibliography.

K. Antolik: 1. Über neue electrische Figuren und über das Gleiten electrischer Funken. Wied. Ann. 15 p. 475—491. 1882

W. G. Armstrong: 1. Electric Movement in Air and Water. First Ed. London 1897.

— 2. Second Ed. with a Supplement by Armstrong and H. Stroud London 1899.

W. v. Bezold: 1. Untersuchungen über elektrische Staubfiguren. Pogg. Ann. 140. p. 145—159. 1870.

— 2. Untersuchung über die electrische Entladung. Pogg. Ann. 140. p. 541—552. 1870.

— 3. Über die Zerlegung einer Entladung in Partialentladungen. Pogg. Ann. 140. p. 559—560. 1870.

— 4. Über das Bildungsgesetz der Lichtenbergschen Figuren Pogg. Ann. 144. p. 337—363, 526—550. 1871.

— 5. Über Lichtenberg'sche Figuren und elektrische Ventile. Wied. Ann. 11. p. 787—795. 1880.

— 6. Über die Untersuchung elektrischer Drahtwellen mit Hülfe von Staubfiguren. Wied. Ann. 63. p. 124—131. 1897.

E. W. Blake: 1. A Method of Producing, by the Electric Spark, Figures Similar to Those of Lichtenberg. Am. Journ. of Sc. and Arts. (2). 49. p. 289—294. 1870.

J. Brown: 1. On Figures Produced by Electric Action on Photographic Dry Plates. Phil. Mag. (5) 26. p. 502—505. 1888.

K. Bürker: 1. Über ein Dreipulvergemisch zur Darstellung elektrischer Staubfiguren. Ann. d. Phys. (4). 1. p. 474—482. 1900.

M. Esch: 1. Über den Vorprocess und die Verzögerung bei der Funkenentladung. Diss. 1908. 57. pp.

K. Hansen: 1. Photographie elektrischer Entladungen. E. T. Z. 37. p. 610—611. 1916.

W. Holtz: 1. Über die Lichtenbergschen Figuren und ihre Entstehung. Phys. Z. 6. p. 319—328. 1905.

— 2. Zur Darstellung Lichtenbergscher Figuren in Vorlesungen. Phys. Z. 7. p. 162—163. 1906.

G. C. Lichtenberg: 1. Nova methodo naturam ac motum fluidi electrici investigandi. Commentatio prior. Novi Commentarti Soc. Reg. Sc. Gottingensis. T. 8. p. 168—180. 1778.
— 2. Commentatio posterior. Commentationes Soc. Reg. Sc. Gott. Classis mathematicae T. 1. p. 65—79. 1779.
R. Mach und S. Doubrava: 1. Beobachtungen über die Unterschiede der beiden electrischen Zustände. Wied. Ann. 9. p. 61—76. 1880.
S. Mikola: 1. Untersuchungen über die Lichtenbergschen Figuren und über die Strahlung des Kondensators. Phys. z. 18. p. 158—168. 1917.
G. Quincke: 1. Über elektrischer Staubfiguren auf Isolatoren und durchgehende, reflektierte, sekundäre und rückläufige elektrische Strahlen. Ann. d. Phys. (4). 32. p. 91—147, 889—940. 1910.
E. Reitlinger: 1. Zur Erklärung der Lichtenbergschen Figuren. Sitzungsber. d. Wien. Akad. Math.-nat. Cl. 41. p. 358—376. 1860.
— 2. Vorläufige Note über Lichtenberg'sche Figuren in verschiedenen Gasen. Sitzungsber. d. Wien. Akad. Math.-nat. Cl. 43. p. 25—26. 1861.
P. T. Riess: 1. Über elektrische Figuren und Bilder. Abh. d. K. Akad. d. Wiss. Berlin. p. 1—50. 1846.
— 2. Reibungselektricität. Bd. 1—2. Berlin 1853.
S. P. Thompson: 1. On the Cause of the Difference in Lichtenberg's Dust-Figures. Preliminary Note. Proc. Roy. Soc. London. 58. p. 214—215. 1895.
M. Toepler: 1. Über den inneren Aufbau von Gleitbüscheln und die Gesetze ihrer Leuchtfäden. Ann. d. Phys. (4). 53. p. 217—234. 1917.
E. T. Trouvelot: 1. Sur la forme des décharges électriques sur les plaques photographiques. La lumiére élec. 30. p. 269—273. 1888.
A. v. Waltenhofen: 1. Über den Lullin'schen Versuch und die Lichtenberg'schen Figuren. Pogg. Ann. 128. p. 589—609. 1866.
K. Wesendonck: 1. Untersuchungen über Büschelentladungen. Wied. Ann. 30. p. 1—50. 1887.
G. Wiedemann: 1. Über das elektrische Verhalten krystallisirter Körper. Pogg. Ann. 76. p. 404—412. 1849.

Contents.

Det Kgl. Danske Videnskabernes Selskab.

Mathematisk-fysiske Meddelelser. **IV**, 7.

ON THE LICHTENBERG FIGURES

PART II.

1. THE DISTRIBUTION OF THE VELOCITY IN POSITIVE AND NEGATIVE FIGURES

2. THE USE OF LICHTENBERG FIGURES FOR THE MEASUREMENT OF VERY SHORT INTERVALS OF TIME

BY

P. O. PEDERSEN

WITH TWO PLATES

KØBENHAVN

HOVEDKOMMISSIONÆR: ANDR. FRED. HØST & SØN, KGL. HOF-BOGHANDEL

BIANCO LUNOS BOGTRYKKERI

1922

Det Kgl. Danske Videnskabernes Selskabs videnskabelige Meddelelser udkommer fra 1917 indtil videre i følgende Rækker:

Historisk-filologiske Meddelelser,
Filosofiske Meddelelser,
Mathematisk-fysiske Meddelelser,
Biologiske Meddelelser.

Prisen for de enkelte Hefter er 50 Øre pr. Ark med et Tillæg af 50 Øre for hver Tavle eller 75 Øre for hver Dobbelttavle.
Hele Bind sælges dog 25 pCt. billigere.
Selskabets Hovedkommissionær er *Andr. Fred. Høst & Søn* Kgl. Hof-Boghandel, København.

Det Kgl. Danske Videnskabernes Selskab.
Mathematisk-fysiske Meddelelser. **IV**, 7.

ON THE LICHTENBERG FIGURES

PART II.

1. THE DISTRIBUTION OF THE VELOCITY IN POSITIVE AND NEGATIVE FIGURES
2. THE USE OF LICHTENBERG FIGURES FOR THE MEASUREMENT OF VERY SHORT INTERVALS OF TIME

BY

P. O. PEDERSEN

WITH TWO PLATES

KØBENHAVN
HOVEDKOMMISSIONÆR: ANDR. FRED. HØST & SØN, KGL. HOF-BOGHANDEL
BIANCO LUNOS BOGTRYKKERI
1922

Introduction.

In Chapter IV of Lichtenberg Figures Part I[1] we have described a method for the measurement of the spreading-velocity of the positive and negative Lichtenberg figures, and the method was there used in determining the mean values of these velocities in the neighbourhood of the electrodes. In Chapter VII it was, furthermore, pointed out how a similar method may be used for the measurement of time-lag in electric sparks.

Since then we have carried out a rather lengthy investigation on this question, viz. time-lag in electric sparks, the results of which will be published elsewhere. In the course of this investigation it was found desirable to investigate how the spreading-velocity varies from the electrode, where the velocity is greatest, to the final boundary of the figure, where it is zero. It was also found necessary to make a closer study of the theory of these measurements and especially to investigate the possible errors introduced by sloping wave fronts. The results of our investigation of these two questions are presented in the present paper.

The main problem to be solved may be stated as follows: A Lichtenberg figure starts at a certain moment from

[1] P. O. Pedersen: On the Lichtenberg Figures Part I. Vidensk. Selsk. Math.-fysiske Medd. I, 11. Copenhagen 1919. In the following referred to as L. F. I.

an electrode and t seconds later its outer boundary has reached to a distance of r cm from the electrode. The described space r will then depend upon the time t, say

$$r = F(t). \qquad \text{(I)}$$

The function F depends upon the amplitude of the impulse, the nature and density of the gas, the thickness of the photographic plate (P in Fig. 1), and possibly other conditions. The problem is to determine the function F.

This function being known, the velocity U, is given by

$$U = \frac{dF(t)}{dt} = U(t), \qquad \text{(II)}$$

and the time-interval t corresponding to a known space r may be found by solving (I) with regard to t. We will write this solution in the form

$$t = f(r). \qquad \text{(III)}$$

On the other hand if (II) or (III) are known we may therefrom deduct the relation (I).

The final range R of the figure will be given by

$$R = F(\infty). \qquad \text{(IV)}$$

We have determined the relation (I) in two different ways:

a) By measurements of corresponding values of t and r by means of the method given in L. F. I. and briefly described in section 1. below.

b) By deducing the relation (II) mathematically from the shape of the separating line between two figures originating from straight electrodes. The details of this method are given in section 2. below.

In section 3. it is proved that the results obtained by means of a) and b) agree with each other.

Section 4. treats of the influence of sloping wave fronts, section 5. discusses some details with regard to the shape of the separating line, and section 6. contains some concluding remarks.

1. The Method used for the Measurement of Corresponding Values of the Time t and Space r in Relation (I).

The method used for these measurements is indicated in Fig. 1. E is a small influence machine, connected to the

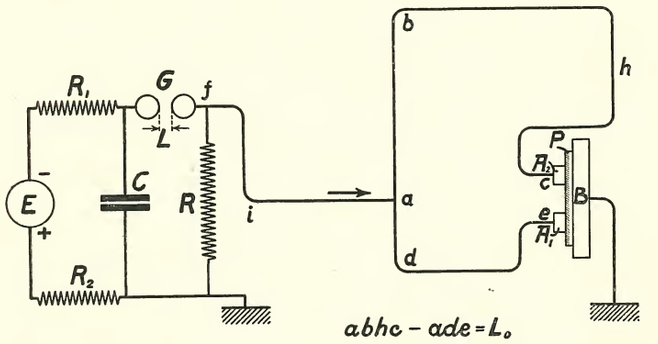

Fig. 1. Diagram of Circuit used for the Measurement of Corresponding Values of t and r in Formula (I).

condenser C through two large resistances R_1 and R_2, f. inst. two slate pencils. G is the primary spark gap, A_1 and A_2 two electrodes, the shape and relative position of which are shown in Fig. 2. A_1 and A_2 are placed on the sensitive film of a photographic plate P, resting on a metal plate B connected to earth. A wire $f\,i\,a$ connects the primary spark gap with the point a of the loop $e\,d\,a\,b\,h\,c$ connecting A_1 and A_2, and the length of the wire $a\,b\,h\,c$ is L_0 meters longer than $a\,d\,e$. One terminal of the condenser

C is connected directly to earth, the wire system and the electrodes A_1 and A_2 through the large resistance R.

In order to make a measurement the handle of the influence machine is slowly turned until a spark passes the spark gap G. An electric impulse or wave will then

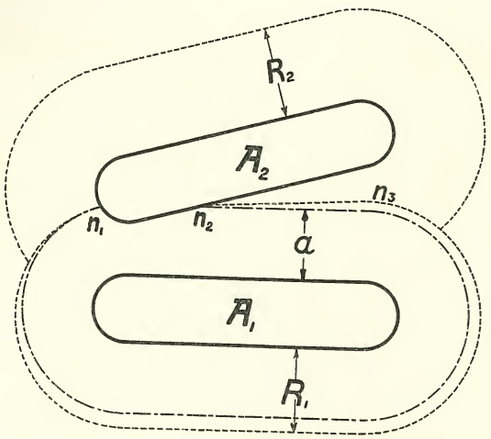

Fig. 2. Shape and Relative Position of the Lichtenberg Electrodes A_1 an A_2 in Fig. 1.

travel out along the wire fia, and at the point a this impulse is partly reflected and partly transmitted into the wires $a\,b$ and $a\,d$. The reflected wave is travelling back along the wire $a\,i\,f$, and the two transmitted waves travel respectively along the wires $a\,b\,h\,c$ and $a\,d\,e$. If the impulse impedances of the three wires meeting in the point a are equal, the amplitude of the reflected impulse will be $-\frac{1}{3}V_0$, while that of the transmitted impulses will be $\frac{2}{3}V_0$, the amplitude of the incident impulse being denoted by V_0.

Of the two transmitted impulses that one travelling along the wire $a\,d\,e$ will reach the electrode A_1 t_0 seconds

before the impulse travelling along $a\,b\,h\,c$ reaches the electrode A_2, where

$$t_0 = \frac{L_0}{v} = \frac{L_0}{3\times10^8}, \qquad \text{(a)}$$

the wire $a\,b\,h\,c$ being L_0 meters longer than $a\,d\,e$. It is supposed that the impulses travel with a velocity v equal to that of light. In reality the velocity will be a little smaller, and t_0 determined by means of (a) therefore comes out too small; but if the wires are not too close to other conductors this error will only be relatively unimportant.

The Lichtenberg figure originating from A_1 will therefore start t_0 seconds before a corresponding figure starts from A_2. The first figure has therefore spread over a space a (see Fig. 2) before a figure starts from A_2. The two figures will meet along a line n_2n_3, the separating line, of which it is proved later on, that that part which is situated between the straight edges of the electrodes A_1 and A_2 generally is also very nearly a straight line. This straight part of the separating line starts from the point n_2 on the edge of A_2, and the distance from n_2 to the edge of A_1 is equal to the distance a travelled by the figure from A_1 in t_0 seconds. In this way corresponding values of the two variables in formula (I) are determined.

2. Impulses with Extremely Steep Front, Shape and Position of Separating Line.

We shall now consider how the position and shape of the separating line depends upon the function U in formula (II). In order to simplify our consideration we suppose, for the present, that the fronts of the impulses arriving at the electrodes A_1 and A_2 are extremely steep. We may then

indicate the velocities of the figures spreading from A_1 and A_2 by means of the curves $U_1(t)$ and $U_2(t)$ shown in Fig. 3, I. The velocity U_1 starts at the time $t = 0$

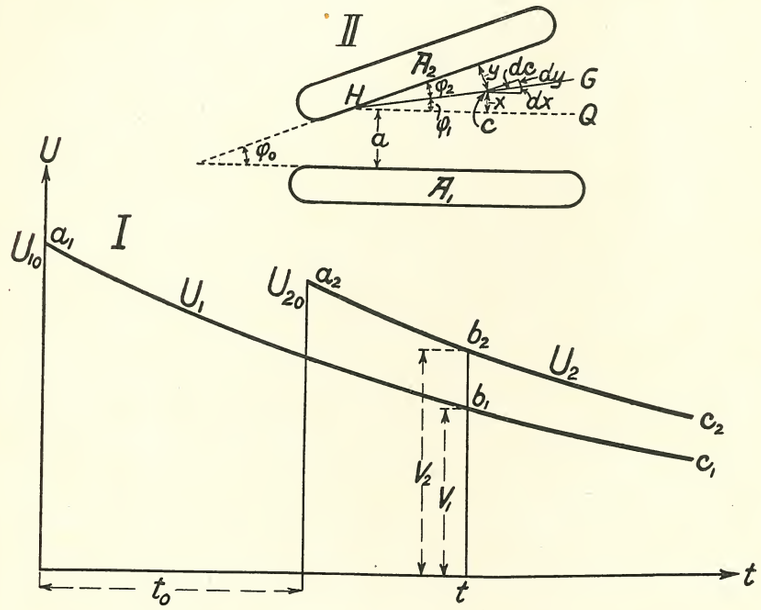

Fig. 3. Part I: Velocity Curves U_1 and U_2 for Figures spreading from respectively A_1 and A_2, the Figure from A_1 starting t_0 seconds before that from A_2.
Part II: Position of the Electrodes A_1 and A_2 and of the Straight Part HG of the Separating Line.

with the initial velocity U_{10}, and U_2 at the time $t = t_0$ with the velocity U_{20}.

At the moment the figure starts from A_2 the outer boundary of the figure from A_1 will be at a distance a from the edge of A_1, where

$$a = \int_0^{t_0} U_1 \cdot dt. \tag{1}$$

The separating line starts at the point H on the edge of

A_2 just reached by the figure from A_1 at the moment the figure from A_2 starts (see Fig. 3, II). The distance of H from the edge of A_1 is therefore equal to a.

Later on it will be proved that that part HG of the separating line which is lying between the straight edges of A_1 and A_2 is also a straight line for all values of the time interval t_0.

We shall now consider the mathematical consequences of this straightness of the separating line with regard to the possible forms of the velocity function U.

Let dc be an element of the straight separating line (see Fig. 3, II), we have then with the symbols used in the figure:

$$dx = dc \cdot \sin \varphi_1, \quad \text{and} \quad dy = dc \cdot \sin \varphi_2.$$

At the same time we have

$$dx = U_1 \cdot dt, \quad \text{and} \quad dy = U_2 \cdot dt,$$

dt being the time it takes to form the element dc of the separating line while U_1 and U_2 are the instantaneous values of the two velocities at the moment t.

We have accordingly

$$\frac{dy}{dx} = \frac{\sin \varphi_2}{\sin \varphi_1} = \frac{U_2}{U_1} = k, \tag{2}$$

were k is a constant.

Equation (2) may be written

$$U_2(t) = k \cdot U_1(t). \tag{3}$$

If, instead of the time interval t_0 we choose $t_0 + dt$, the separating line will also be straight, but the corresponding constant k will have a different value k' dependent upon dt but independent of t. We may therefore write

$$k' = k(1 + \alpha\, dt),$$

were α is a constant.

Instead of (3) we get

$$U_2(t-dt) = k' \cdot U_1(t). \qquad (4)$$

From (3) and (4) it is easily deduced that

$$\frac{dU_2}{U_2} = -\alpha \cdot dt,$$

or

$$U_2(t) = U_2' \cdot e^{-\alpha t} = U_{20} \cdot e^{-\alpha(t-t_0)}, \qquad (5_1)$$

and therefore

$$U_1(t) = U_{10} \cdot e^{-\alpha t}, \qquad (5_2)$$

the value of the constant k being

$$k = \frac{U_{20}}{U_{10}} \cdot e^{\alpha t_0}. \qquad (5')$$

When the separating line is straight, the velocity functions must necessarily be those given in (5_1) and (5_2) in which U_{10}, U_{20}, and α are constants. And vice versa with these velocity functions the part of the separating line under consideration will always be straight.

It follows from equation (5_2) that

$$r = F(t) = \int_0^t U_1 \cdot dt = \frac{1}{\alpha} \cdot U_{10} \cdot (1-e^{-\alpha t}), \qquad (6)$$

and the range

$$R_1 = \frac{1}{\alpha} U_{10}, \qquad (7)$$

or

$$U_{10} = \alpha R_1. \qquad (7')$$

Equations (6) and (5_2) may therefore be written:

$$r = F(t) = R_1(1-e^{-\alpha t}), \qquad (8)$$

and

$$U_1 = \alpha(R_1 - r) = U_{10} - \alpha r. \qquad (9)$$

The velocity decreases linearly with increasing distance from the edge of the electrode.

We shall next determine how the angle φ_2 between the separating line and the electrode A_2 depends upon the

ratio of the velocities and on the angle $\varphi_0 = \varphi_1 + \varphi_2$ between A_1 and A_2.

We evidently have (see Fig. 3, II):

$$\frac{\sin\varphi_2}{\sin\varphi_1} = \frac{U_2(t)}{U_1(t)} = \frac{U_{20}}{U_{10}} \cdot e^{\alpha t_0} = \frac{U_{20}}{U_{10}} \cdot \frac{R_1}{R_1 - a} = c \cdot \frac{R_1}{R_1 - a}, \qquad (10)$$

where $c = \frac{U_{20}}{U_{10}}$ is the ratio between the velocities just at the edges of the electrodes, and a is the distance travelled in t_0 seconds by the figure originating from A_1.

Supposing the angles φ_1 and φ_2 are so small that in formula (10), without any serious error, we may substitute φ_1 and φ_2 for respectively $\sin\varphi_1$ and $\sin\varphi_2$, this formula is then reduced to

$$\varphi_2 - \varphi_1 = \Delta\varphi = \varphi_0 \frac{a - (1-c)R_1}{(1+c)R_1 - a}. \qquad (10_1)$$

The angle φ_2 is then given by

$$\varphi_2 = \tfrac{1}{2}(\varphi_0 + \Delta\varphi). \qquad (11)$$

If $U_{10} = U_{20}$, $(c=1)$, equation (10_1) reduces to

$$\Delta\varphi = \varphi_0 \frac{a}{2R_1 - a}. \qquad (10_2)$$

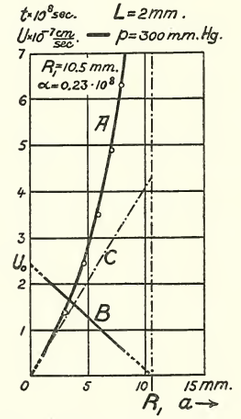

Fig. 4. Negative Figures. $L = 2$ mm; Pressure $p = 300$ mm Hg. $R_1 = 10.5$ mm; $\alpha = 0.23 \times 10^8$.

In the following the formulae (11) and (10_1) or (10_2) are used for the calculation of the angle between the separating line and A_2.

3. Experimental Proof by Means of the Method described in Sect. 1 of the Velocity Functions deduced in Sect. 2.

In Figs. 4—6 the points indicated by small circles represent corresponding values of a and t_0 determined by the method described in sect. 1, while the curves marked

A represent the theoretical relationship between a and t_0 according to equation (8), viz.:

$$a = R_1 (1 - e^{-\alpha t_0}).$$

The value of R_1 is measured directly on the photographic plate, while for α we have chosen such a value that the experimental points fall as closely as possible to the curve A.

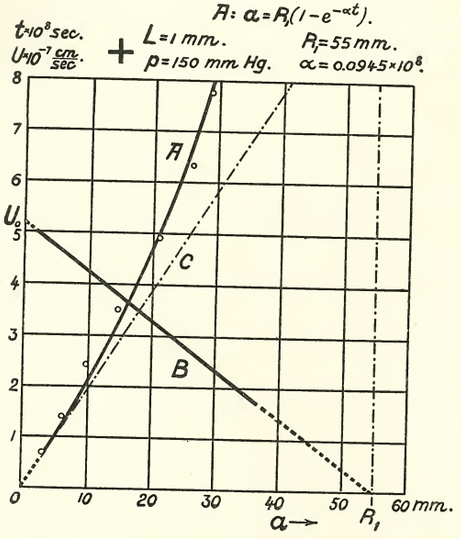

Fig. 5. Positive Figures: $L = 1$ mm; $p = 150$ mm. Hg.; $R_1 = 55$ mm; $\alpha = 0.0445 \times 10^8$.

Taking into account that there is only one arbitrary constant, namely α, the value of which can be chosen so as to accommodate the theoretical and the experimental values as much as possible, we may say that the results obtained by the two methods agree very well with each other.

In Figs. 4—6 the straight lines B represent the spreading-velocity of the figures at different distances from the electrodes according to formula (9). The equation of those lines is therefore

$$U_1 = \alpha (R_1 - a) = U_{10} - \alpha a. \qquad (9')$$

The broken lines C represent the tangents to the A-curves at the origin.

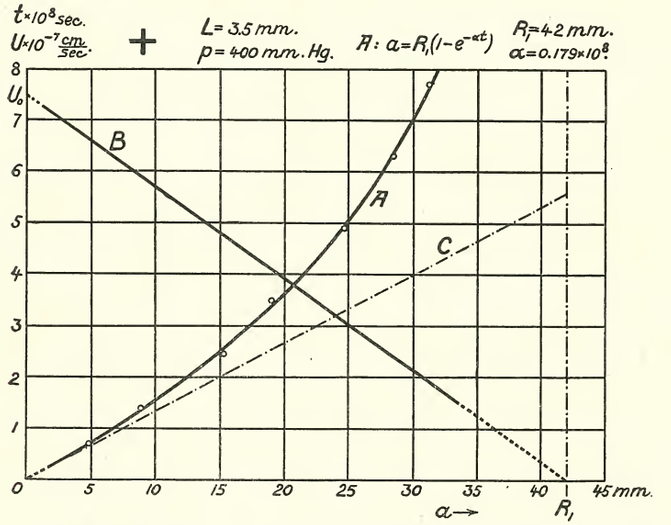

Fig. 6. Positive Figures. $L = 3.5$ mm; $p = 400$ mm Hg.; $R_1 = 42$ mm; $\alpha = 0.179 \times 10^8$.

In Fig. 7 the curve D represents the velocity function corresponding to the A-curve in Fig. 5.

The outermost parts of the velocity lines B in Figs. 4—6 and D in Fig. 7 are shown in broken lines and are only to be considered as theoretical extrapolations. It is hardly probable that the velocity goes down quite to zero, but the reduction in the range caused hereby is probably small.

Besides the experiments, of which the results are given in Fig. 4—6, we have made a number of other investigations aiming at the determination of the dependence of α upon spark length, gas pressure etc.

The results of these investigations are shown in Figs. 8 and 9 for positive and negative figures respectively. The values of α seem in both cases to be rather independent of the spark length but to increase linearly with increasing

pressure of the gas and much more rapidly for positive than for negative figures. In both cases the value of α seems to converge towards a definite value — about 0.075×10^8 for positive and 0.15×10^8 for negative figures — when $p \to 0$.

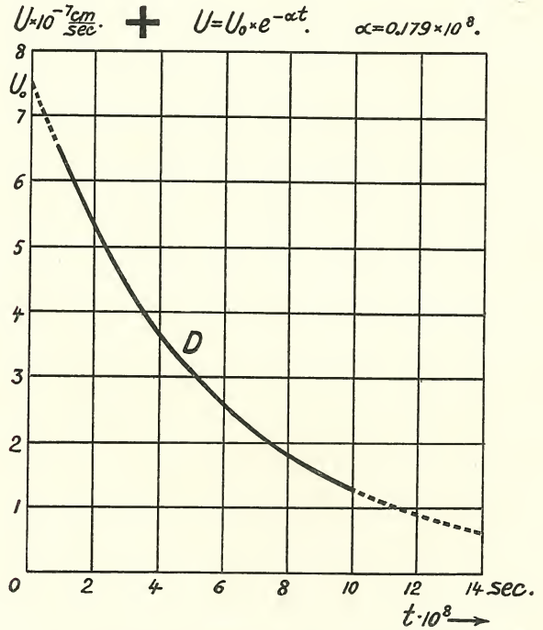

Fig. 7. Theoretical Velocity Curve corresponding to Curve *A* in Fig. 5.

In the upper parts of Figs. 8 and 9 are also shown the corresponding values of the range R and the initial velocity V_0. In most cases the ratio between gas pressure and spark length (both in mms.) has been equal to 100. Where this is not the case a number at the experimental point gives the value of that ratio. The curves marked R and U_0 give — for the said ratio equal to 100 — an approximate representation of the range and the velocity as depending upon the pressure of the gas.

According to the evidence given on the preceding pages

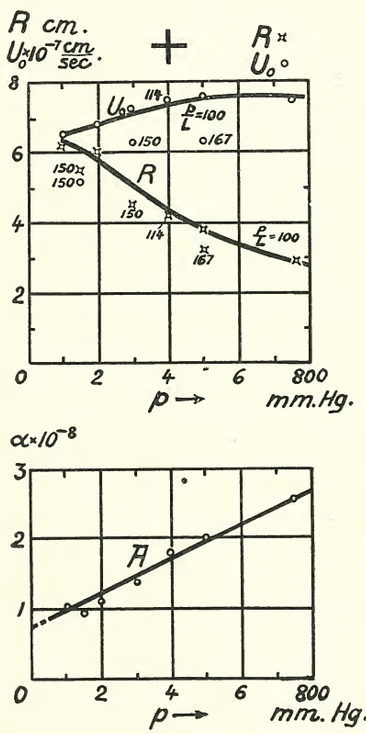

Fig. 8. Positive Figures. The values of the Coefficient α, the Range R and the initial Velocity V_0 as dependent upon the Pressure p and Spark Length L.

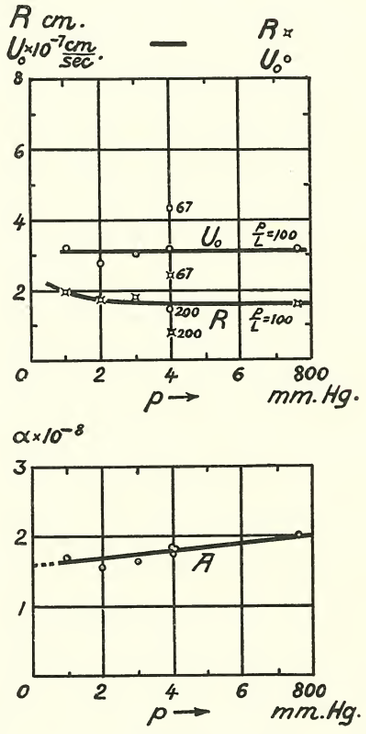

Fig. 9. Negative Figures. [In the lower parts of Figs. 8 and 9 the Ordinates are $\alpha \cdot 10^{-9}$ and not $\alpha \cdot 10^{-8}$ as indicated in the Figures.]

there can be but little doubt that our solution — represented by the equations (5_2), (8) and (9) — of the problem treated of is substantially correct.

In what follows we shall treat of some possible sources

of errors and their elimination, investigate in some detail the general shape of the separating line and last but not least furnish some experimental evidence of the straightness of the often mentioned part of this line.

Before closing this section it is necessary, however, to make a single remark. The spreading-velocity of the Lichtenberg figures, with which we are dealing here, are by no means the same as the velocities, by which the "sliding sparks" (Gleitfunken) studied by M. Toepler [1] extend themselves. It will be shown elsewhere that the two phenomenae, Lichtenberg figures and sliding sparks, differ very much from each other. Toepler found — by making use of the velocity of sound waves — that the velocity of a sliding spark is practically constant almost to the end of the spark, and there is hardly any reason to doubt the correctness hereof.

4. The Influence of Sloping Wave Fronts on the Shape of the Separating Line.

We have until now supposed that the wave fronts of the impulses were extremely steep in which case the initial velocity at the edge of the electrodes is also the maximum velocity. Generally, however, the wave fronts are more or less sloping, increasing gradually from zero to the maximum amplitude of the impulse. The velocity will then also increase gradually up to its maximum value U_0' (see Fig. 10 Part III). The duration of the sloping front is in Fig. 10 Part II—IV taken to be equal to τ_0. The amplitude of the impulse is taken as constant for all values of t greater than τ_0 (see Fig. 10 Part II) and for the same values of t the velocity is supposed to decrease exponentially with t.

[1] M. Toepler: Ann. d. Phys. (4) 21, p. 193—222, 1906.

We now extend this exponential velocity curve backwards to the point d_1, which is chosen in such a way that the two shaded areas, $o_1e_1b_1$ and $b_1d_1c_1$ are equal. The velocity corresponding to the point point d_1 is denoted by U_0 and

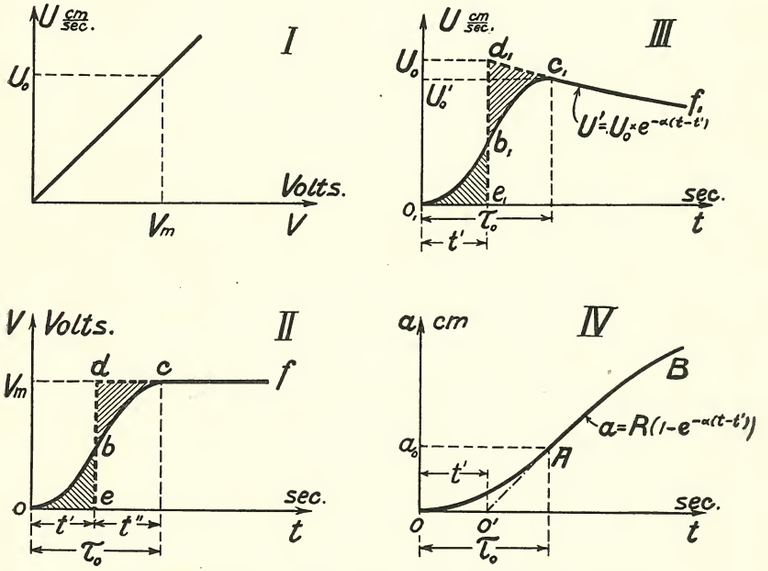

Fig. 10. The straight Line in Part I represents a Linear Relationship between the Velocity at the Edge of the Electrode and the Voltage of same.

In Part II the Line $o\,b\,c\,f$ represents the Front of an Impulse. The curve $o_1\,b_1\,c_1\,f_1$ in Parts III represents the Corresponding Velocities.

The curve OAB in Part IV represents the Distance travelled by the Outer boundary of the Figure in the Time t.

we call the curve $d_1c_1f_1$ the equivalent velocity curve, the equation of which is

$$U' = U_0 \cdot e^{-\alpha(t-t')} \quad [U' = 0 \text{ when } t < t']. \qquad \text{(b)}$$

The distance a which the outer boundary has reached in the time t is given by

$$a = \int_0^{t_0} U \cdot dt\,, \qquad \text{(c)}$$

and for all values of t_0 greater than τ_0 we may in this formula substitute the equivalent velocity U' for the actual velocity U.

In Fig. 11 we have shown two identical velocity curves U_1 and U_2 with a time interval of t_0 seconds and the corresponding distances r_1 and r_2 travelled by the figures from A_1 and A_2. It will presently be shown that what is measured on the photographic plate is the time interval

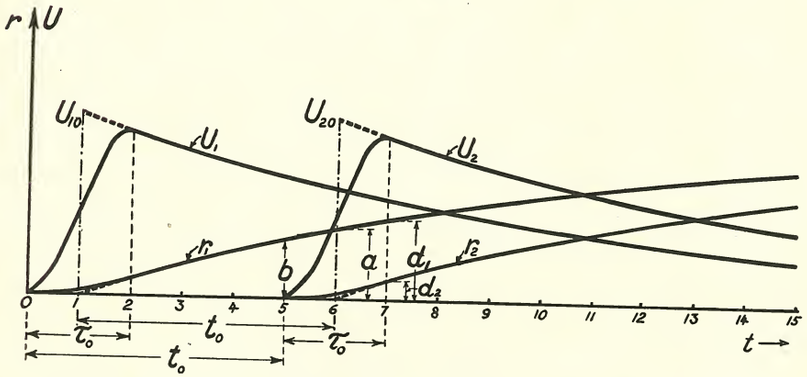

Fig. 11. Two identical Velocity Curves U_1 and U_2 with a Time Interval of t_0 and the Corresponding Distance Curves r_1 and r_2.

between the steep fronts of the equivalent velocity curves. What really is desired is to know the interval between the fronts of the two corresponding electrical impulses. In so far as the two impulses are identical in shape the time interval between the impulses will be exactly equal to the interval between the steep fronts of the equivalent velocity curves. If the two impulses have differently shaped fronts it is perhaps a little doubtful how to define the time interval between them. In this case the most natural way to define this time interval will presumably be the following: The front of the voltage

impulse $o\,b\,c\,f$ (see Fig. 10 Part II) is transformed to the "equivalent" voltage curve with vertical front, $e\,b\,d\,c\,f$, where the position of the vertical front $e\,d$ is chosen in such a way that the two areas $o\,e\,b$ and $b\,d\,c$ are equal. The time interval between the two voltage impulses is then taken as the interval between the vertical fronts of the two equivalent voltage impulses. If, as indicated in Fig. 10 Part I, the velocity U is proportional to the voltage V, the time interval between the vertical fronts of the equivalent velocity curves is very nearly equal to the time interval between the vertical fronts of the equivalent voltage impulses. Even in the cases where there is no proportionality between U and V the two time intervals will very nearly be equal. We may, therefore, without serious errors take the time interval between two voltage impulses as the time interval between the vertical fronts of the equivalent velocity curves, and this last interval is, as will be shown shortly, equal to the t_0 measured on the photographic plate. In all cases where the wave fronts of the two impulses are identical in form the error is zero.

In order to illustrate the influence of sloping wave fronts we have in Fig. 12 shown the separating line which would result from the two velocity curves shown in Fig. 11 and with a time interval of $t_0 = 5$. If the wave fronts were vertical the straight part $e\,d$ of the separating line would be continued to the point c at the edge of A_2. The sloping of the wave fronts causes the part $d\,c$ of the separating line to bend down to the position $d\,b_2$. The distance of the point b_2 from the edge of A_1 is equal to the distance b travelled by the figure from A_1 at the moment when the figure from A_2 just begins to start (see Fig. 11). The separating line again starts from the edge of A_2

at the point b_1 where the distance from A_1 again is equal to b. From the last point the separating line goes in a bent curve to the point g.

It is very easy by means of the r_1- and r_2-curves of Fig. 11 to draw the separating line in Fig. 12 and corresponding distances are marked in the same way in these

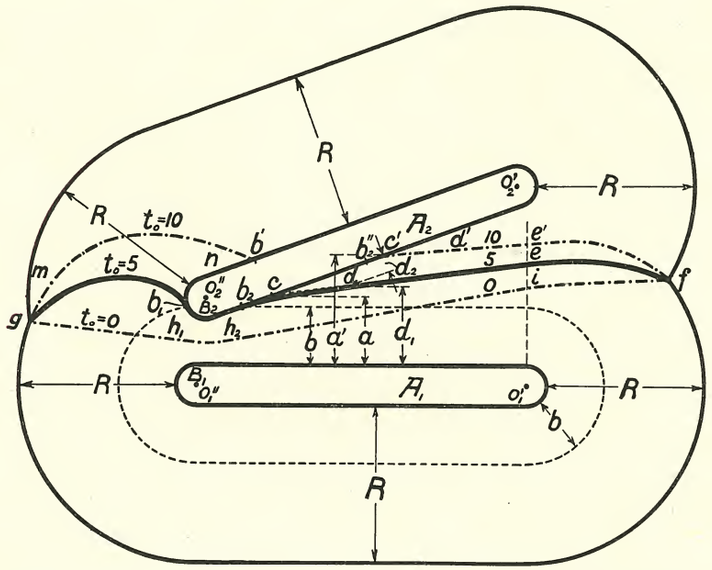

Fig. 12. Two Separating Lines corresponding to the Sloping Wave Fronts of Fig. 11. One for $t_0 = 5$ shown with a Heavy Line, the other, corresponding to $t_0 = 10$, in a broken Line. The final Range R is the same in both Figures.

two figures. Between the points d and e the separating line according to section 2., is a straight line, and, if extended beyond d, this straight line cuts the edge of A_2 in a point c. It is easily seen from Fig. 11 that the distance a of this point c from the edge of A_1 is equal to the distance travelled by the figure from A_1 at the moment,

the figure would start from A_2 if the velocity curve was the equivalent one with vertical front. The distance a is therefore equal to the distance travelled in the time t_0 by a figure spreading out according to the equivalent velocity curve. Such distances a it is which are plotted against the corresponding values of t_0 in Figs. 4—6.

5. The General Shape of the Separating Line. Experimental Proof of the Straightness of Part of this Line.

In Fig. 12 we have — besides the separating line already mentioned — in broken lines shown two other lines based on the velocity curves of Fig. 11 and corresponding to respectively $t_0 = 0$ and $t_0 = 10$. The common ends of all these separating lines will be at the points g and f. For $t_0 = 0$ the outer ends $g h_1$ and $i f$ of the separating line are straight lines passing vertically through the middle points of the two center lines $o_1' o_2'$ and $o_1'' o_2''$. The part $h_2 i$ of this separating line is also a straight line, namely the bisector of the angle between the edges of A_1 and A_2. For $t_0 = 10$ the straight part of the separating line is $e' d'$, while a' is the distance travelled by the outer boundary of the figure from A_1 in the time $t_0 = 10$.

In order to compare the theoretical with the actual separating line we have in Figs. 13, and 16—18 reproduced two positive and two negative velocity figures with the theoretical separating lines indicated by broken lines. We shall later on discuss the agreement between the actual and the theoretical separating lines. It is necessary to point out, however, that for such lines as the one shown in Fig. 12 corresponding to $t_0 = 10$ it is impossible for the figure from A_1 to reach the area in the neighbourhood of

n, and the figure from A_2 cannot turn round sufficiently to cover the area at m. The figures from A_2 will therefore cover the area n and the figure from A_1 the area m, as also appears from the Figs. 13, 16 and 18.

Fig. 13. Negative Velocity Figure. Broken Line shows Theoretical Form of Separating Line.

With negative figures it is impossible to obtain a separating line as that corresponding to $t_0 = 10$ in Fig. 13 without a spark passing between the points B_1 and B_2 on respectively A_1 and A_2. Such a spark may pass so early that it alters the position of the separating line. In velocity or time measurements by means of negative figures it is, therefore, always necessary to place the electrodes A_1 and A_2 at such a distance from each other that the point

where the separating line reaches the edge of A_2 is rather close to the point B_2. With positive figures, where the tendency to spark-over is much smaller, the position of A_1 and A_2 is not so critical.[1]

The two end points f and g of the separating line (see Fig. 12) deserve a little consideration. Supposing the ratio of the instantaneous velocities of the two figures is known it is easy to determine the direction of the separating line at these points. In Fig. 14 the line fp is vertical to fo'_1. At the time t the figure from A_1 has travelled the distance $R - \Delta r_1$ and the figure from A_2 the distance $R - \Delta r_2$, where R is the final range. The ratio $\frac{\Delta r_2}{\Delta r_1}$ must, according to the equations, (3) and (5_2), be equal to the constant ratio k of the velocities. It is easily shown that the angle ψ between the tangent to the separating line at f and the line fp is determined by

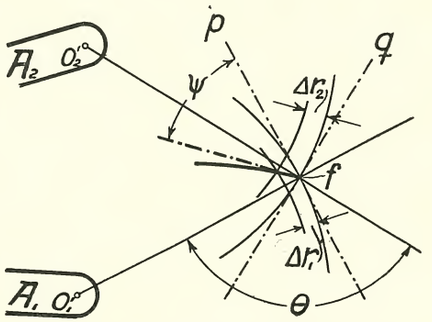

Fig. 14. Direction of the Tangent to the Separating Line in the End Point f.

$$\operatorname{tg} \psi = \frac{\sin \theta}{k + \cos \theta}, \tag{12}$$

where θ is the angle between the lines fo'_1 and $o'_2 f$.

If the angles ψ and θ are known, the ratio k is given by

$$k = \frac{\sin \theta}{\operatorname{tg} \psi} - \cos \theta. \tag{13}$$

From equation (12) it follows that

[1] This difference between positive and negative figures will be discussed elsewhere.

for $k = \infty, \quad 1, \quad 0$

we have $\psi = 0, \quad \frac{1}{2}\theta, \quad \theta.$

The correctness of these values is evident.

From equation (8) it follows, that

$$k = e^{\alpha t_0} = \frac{R}{R-a}. \tag{14}$$

That is, the value of the ratio k depends only on the values of R and a.

We have until now supposed that the final ranges R_1 and R_2 of the figures from A_1 and A_2 are equal. Generally that is not the case, R_2 for positive figures being somewhat smaller and for negative figures considerably greater than R_1. Further particulars about this question are to be found in L. F. I p. 32—33 and need not be discussed here. It is sufficient to point out that the position of the point c in Fig. 12 — and therefore the measured value of a — depends solely on the velocity (and range) of the figure from A_1. If, however, $R_1 \neq R_2$, the position of the points f and g are changed and the equations (12) and (13) do not hold good any longer.

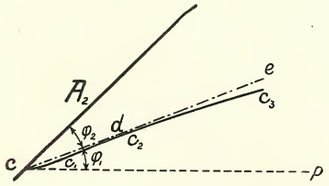

Fig. 15. $e\,c$ Theoretical Separating Line. $c\,c_1\,c_2\,c_3$ Actual Separating Line deformed by the Electric Field from the Charge on A_2 and its Figure.

Even if $R_1 = R_2$, the electrical fields due to the figures themselves will to a certain extent alter the theoretical forms of the separating lines. This deformation is, however, in most cases very small. We shall briefly consider these influences and suppose for the sake of simplicity that the front of the impulse is vertical. The figure from

A_1 (see Fig. 15) has just reached the line $c\,p$ at the moment the impulse reaches A_2. If then the ratio between the velocity of the two figures is constant, the separating line will be a straight line $c\,e$ through the point c. The electric field due to the charge on A_2 and on the figure spreading from A_2 will, however, cause some slight deformations of

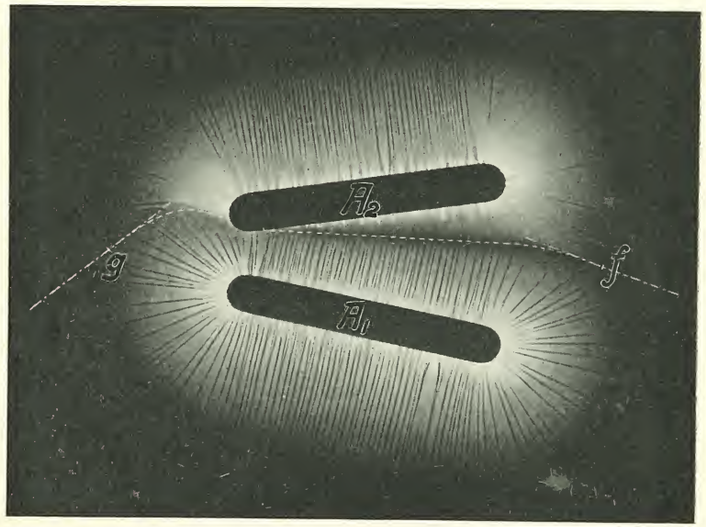

Fig. 16.

this line. The main effect of this field is that it retards the spreading of the figure from A_1 especially between the points c and d. Another, but generally very small effect, is the retardation of the spreading-velocity of the figure from A_1 between the points d and e resulting in a bending down of the separating line as shown in the curve $c_2\,c_3$. This effect is only perceptible if the point e is at a distance from A_1 very nearly equal to the final range of the figure

from A_1. In this case the electric density is much greater above than below the separating line and the figure from A_1 will therefore be retarded.

It is mainly in positive figures that the deformation at c_1 appears. This is no doubt, partly at least, due to the fact, that positive figures do not commence to spread be-

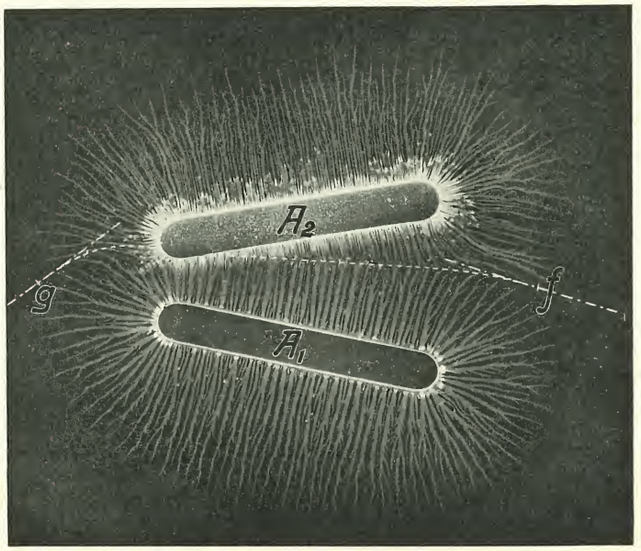

Fig. 17.

fore the tension has attained a certain value dependent upon the condition in the experiment, compare L. F. I p. 51 and 54, and the note on page 32 in the present paper.

Generally speaking the above mentioned deformations of the straight separating line are only very small and the position of the point c may therefore be determined with considerable accuracy. It is a great help in this that the

angle φ_2 which the theoretical straight separating line forms with A_2 may be calculated according to equation (10_2).

How closely the theoretical form of the separating line agrees with the actual one will be evident from an inspection of the negative velocity figure in Fig. 16 and the positive ones in Fig. 17 and 18. Furthermore we have on

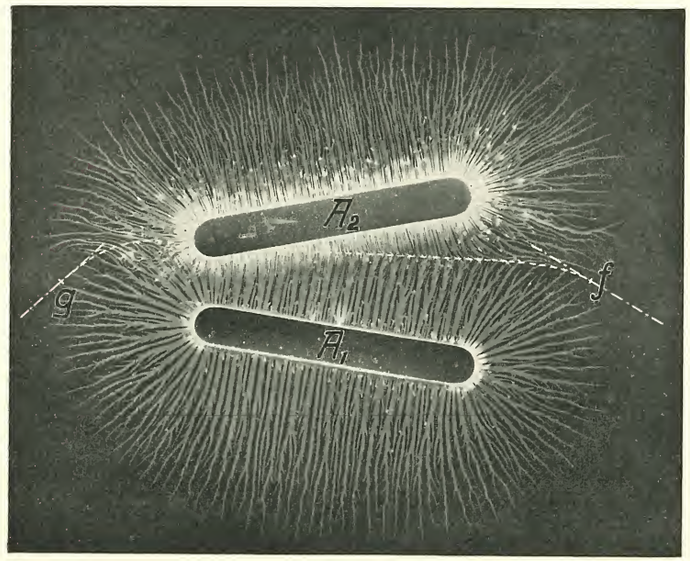

Fig. 18.

Plate 1 and 2 shown some magnifications of the straight part of the separating line from some positive — Plate 1 parts I-IV and Plate 2 Parts I-II — and negative — Plate 2 Parts III-IV — velocity figures. A closer inspection will show the remarkable "straightness" of these parts of the separating line. The bending down of this line close to A_2 in Parts II-IV on Plate 1 is due to a sloping wave front (see Fig. 12) and to the electric field from A_2, com-

pare Fig. 15. The bent part $a\,b$ in part II on Plate 2 is due to the end of A_1.

From an inspection of the figures on Plate 1 and 2 it is evident that the straight part of the separating line may — with the use of a magnifying glass — be drawn with great certainty. When the negative velocity figures in Figs. 13 and 16 give the impression that there is a rather great uncertainty with regard to the position of that line, this is only due to the circumstance that some of the details which serve to fix the exact position of the said line — and which are to be seen in parts III and IV of plate 2 — although very clear in the original plates have been lost in the copies.

As a further verification of the correctness of our results we may compare the angle φ_2 between the electrode A_2 and the straight part of the separating line measured on the plate with the value of that angle calculated according to the equations (10_2) and (11). A long series of measurements have shown that the observed and the calculated values of φ_2 agree fairly well, the differences being within the limits of possible errors. As an example we quote in Table 1 three such sets of measurements.

Table 1. Positive Velocity Figures.

Plate	R	a	φ_0	$\Delta\varphi$	φ_2 cal.	φ_2 obs.	φ_2 cal. — φ_2 obs.
M. 324	30 mm	8.6 mm	22°	3.7°	12.8°	12.5°	+ 0.3°
» 320	31 »	10.9 »	21°	4.5°	12.5°	12.6°	— 0.1°
» 327	34 »	13.0 »	19°	4.5°	11·8°	12.2°	— 0.4°

The two negative velocity figures Figs. 13 and 16 and a third one not reproduced here seem to form an exception to this agreement. The data for these three figures

Table 2. Negative Velocity Figures.

Plate	R	a	φ_0	$\Delta\varphi$	φ_2 cal.	φ_2 obs.	φ_2 cal. — φ_2 obs.
M. 319	32 mm	9.0 mm	21.2°	3.5°	12.3°	10.0°	+ 2.3°
» 320	25 »	9.5 »	19.2°	4.4°	11.8°	10.2°	+ 1.6°
» 321	32 »	12.0 »	20.0°	4.6°	12.3°	10.6°	+ 1.7°

are collected in Table 2, from which it appears that the calculated values are decidedly greater than those observed, and the differences are outside the limit of the possible errors. The cause of this discrepancy is the following:

As mentioned before the final range R_2 is — with relatively great values of t_0 — considerably greater than the range R_1. In order to investigate the correctness of the equations (12)—(14) for negative figures it was necessary to arrange matters in such a way that the two ranges become equal. In order to obtain this equality in range a shunt was inserted between the point c (see Fig. 1) and earth and the resistance of this shunt was given such a value that $R_1 = R_2$. Another effect of this shunt is, however, that the voltage at A_2 becomes somewhat less than the voltage at A_1, and consequently φ_2 obs. must be smaller than the value of φ_2 calculated by means of the equations (10_2) and (11).

In Figs. 13 and 16—18 we have shown the direction of the tangents to the separating line at the points f and g calculated by means of the equations (12)—(14). For the points f the calculated direction of the tangent agrees fairly well with the actual direction of the separating line at these points. For the points g there is no such agreement and the cause hereof is mentioned before and needs no further comment. Still it may be worth while to point out that the lines in the negative figures are straight from the

electrode A_1 and right to the theoretical separating line in the neighbourhood of the point g, and that they have a rather sudden bend where they pass over the said line, see especially Fig. 13.

The experiments have thus confirmed all the conclusions which we have drawn from the equations (5_2), (8) and (9).

6. The Measurement of Very Small Intervals of Time. Concluding Remarks.

We are now in such a position that we can use the spreading of the Lichtenberg figures for the determination of a very small interval of time t_0 which passes from the moment one electric impulse reaches the electrode A_1 to the moment when another impulse reaches A_2. In order to do this it is only necessary to determine the corresponding A-curve with a as abscissa and t_0 as ordinate, where a is the distance from the point c to the edge of the electrode A_1, c being the point where the straight part of the separating line cuts on the edge of A_2, see Figs. 3—6 and 12.

In practice there is no difficulty in fixing the position of the straight part of the separating line with sufficient accuracy. It is most easily done in the following way: A preliminary line is drawn and the corresponding value of a measured. With this value of a and the measured value of R_1 the angle φ_2 is calculated from the equations (10_2) and (11). A new straight line forming this angle with A_2 is then drawn in such a position, that it coincides as closely as possible with the actual separating line. In doing this a magnifying glass is of great help. If the new value of a corresponding to this separating line does

not differ considerably from the first, the new value of a may be taken as the correct one, if not, the procedure must be repeated once more. With a little experience this repetition will generally be found unnecessary. With the thus determined value of a we take from the A-curve the corresponding value of t_0.

This is, however, only true for those parts of the curves A in Figs. 4—6, which are drawn in full line. There is some uncertainty both for very small values of a and for such values which are but little smaller than the final range R. With regard to the first part there can be no doubt whatever that the wave front is not vertical, and the A- (and B-) curves must therefore necessarily have another form than that corresponding to equation (8) and (9). The first part of the A- and B-curves will, really, have a shape similar to that shown in dotted lines in Fig. 19. The A-curve will start from a point $-t'$ of the t-axis and the B-curve from the origin. The velocity curve will also, as shown in Fig. 20, start from the point $-t'$ of the t-axis. The duration of the sloping wave front is in both figures denoted by τ_0, and the symbols t' and t'' are the same as those used in Fig. 10.

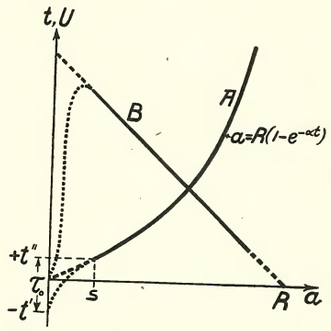

Fig. 19. Probable Form of the A- and B-Curves for Sloping Wave Front and for Very Small Values of a.

In the Figs. 4—7 t_0 is the time interval between the arrivals of the vertical fronts of the equivalent waves and, as shown before, the irregularities due to the sloping of

the wave fronts will not have any influence on the form or position of the A-curve for all such values of a which are greater than s, see Fig. 19, and these irregularities will have no influence whatever on the determination of the time interval t_0 between two impulses when $t_0 > t''$.

The duration, $\tau_0 = t' + t''$, of the sloping wave front is certainly very short. For the determination of the intervals below 5×10^{-9} seconds it would be desirable to know the exact form of the wave front. Some preliminary experiments with this object in view have been made, but the problem is rather difficult and no definite information can be given at present.

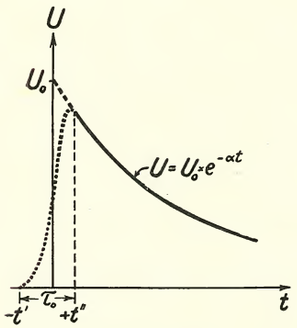

Fig. 20. Probable Form of the Velocity-Time Curve for Sloping Wave Front.

An inspection of the Figs. 4—6 and 8—9 will show that the method, as developed at present, is most convenient for the measurements of time intervals between 0.5×10^{-8} and 10×10^{-8} seconds. There is no doubt, however, that its useful domain can be extended down to or even below 1×10^{-9} seconds and up to say 2×10^{-7} seconds.

With regard to the other point of uncertainty, where the value of a approaches that of the range R, it is quite evident that such great values of a cannot be used for any exact measurements of t.

There still remains one question which ought to be mentioned: Do the figures start immediately when the voltage reaches the electrode or is there some delay? For the measurement of t_0 this question is, however, without any great importance — compare section 5. — and we shall therefore not enter into any detailed discussion of it at present, but this problem, which is closely connected with that of the formation of electric sparks, will be treated of elsewhere. A few words will, however, have to be said here with regard to some remarks by K. PRZIBRAM[1]. There is no doubt whatever that the formation of a positive figure does not begin before the voltage has reached a certain value dependent upon gas pressure and several other circumstances. This has already been pointed out in L. F. I, p. 52 and 54. We did not, however, mention this on p. 60 of that paper, where we said: "Supposing the two figures start simultaneously the ratio of the distances from the electrodes to the neutral discharge will be equal to the ratio of their velocities." The reason was that our main object then was to prove conclusively that the velocity of the positive is greater than that of the negative figures. A possible time-lag in the start of the positive figures would not invalidate our arguments, and we therefore did not think it necessary to enter into any further discussion of that point.

K. PRZIBRAM's interesting investigations seem to prove that there is a greater retardation in the start of the positive figures than could be explained by the existence of the above mentioned minimum voltage. Other circumstances point in the same direction. We do not, however, believe that this question, which is of considerable interest in several ways, can be considered as definitively settled.

[1] K. PRZIBRAM: (1). Phys. Zeitschrift 21, p. 480—484, 1920. (2). Wien. Ber. Math.-naturw. Kl. II a, 129, p. 151—160, 1920.

Résumé.

It has been shown that the three equations (I)—(III) on page 2 have the following forms:

$$r = R(1-e^{-\alpha t}), \qquad (I')$$

$$U = \alpha R e^{-\alpha t} = U_0 \cdot e^{-\alpha t}, \qquad (II')$$

and

$$t = \frac{1}{\alpha} \text{lognat} \frac{R}{R-a}. \qquad (III')$$

Some values of the constant α are given in Figs. 8 and 9.

The author desires to express his thanks to Mr. J. P. Christensen and Mr. A. G. Jensen for their valuable assistance during this investigation.

The author also desires to acknowledge his indebtedness to the Carlsberg Fund for its support of these investigations.

The Royal Technical College, Copenhagen,
Telegraph and Telephone Laboratory.

Bibliography II

containing some papers which were overlooked in the preparation of the first Bibliography or which have appeared since its publication.

Ragnar Arpi: Synthetische Studien über Dendritenstruktur, auf Metallographie und elektrische Entladungen angewendet. Arkiv f. mat., astr. och fysik. Bd. 8. Nr. 14. 1912.

B. Ell: Ny method att medels ljuskänsligt preparerade papper eller plåtar åskådliggöra kraftlinjernas riktning och relativa antal i ett elektrisk fält. Teknisk Tidskrift. Afd. Elektroteknik. 51. Årg. p. 49—55. 1921.

K. Przibram: 1. Beiträge zur Kenntniss des verschiedenen Verhaltens der Anode und Kathode bei der elektrischen Entladung. Wien. Ber. Math. naturw. Cl. Bd. C VIII. Abth. II a. p. 1161—1171. 1899.

— 2. Vorläufige Mitteilung über die photographische Aufnahme der elektrischen Entladung auf rotierenden Films. Ibid. Bd. C IX (II a). p. 902—904. 1900.

— 3. Photographische Studien über die elektrische Entladung. Ibid. Bd. C X (II a). p. 960—963. 1901.

— 4. Ueber das Leuchten verdünnter Gase im Teslafeld. Ibid. Bd. C XIII (II a). p. 439—468. 1904.

— 5. Ueber die Büschelentladung. Ibid. Bd. C XIII (II a). p. 1491—1507. 1904.

— 6. Büschel- und oszillierende Spitzenentladung in Helium, Argon und anderen Gasen. Ibid. Bd. C XVI (II a). p. 557—570. 1907.

— 7. Die Büschelentladung in Clor und die Beziehung zwischen Büschelentladung und Jonenbeweglichkeit. Ibid. Bd. CXXI (II a). p. 2163—2168. 1912.

— 8. Einpolige elektrische Figuren und Elektronenaffinität. Ibid. Bd. 127 (II a). p. 395—404. 1918.

— 9. Ueber die elektrischen Figuren. Phys. Zeitschr. 19. p. 299—303. 1918.

— 10. Form und Geschwindigkeit. Die Naturwissenschaften. Heft. 6. p. 103—107. 1920.

— 11. Ueber die Ladung der elektrischen Figuren. Wien. Ber. Math.-naturw. Kl. Abt. II a. 128 Bd. p. 1203—1221. 1919.

K. Przibram: 12. Ueber die elektrischen Figuren. II. Mitteilung. Phys. Zeitschr. 21. p. 480—484. 1920.
— 13. Der Vorsprung der negativen Entladung vor der positiven. Wien. Ber. Math. naturw. Kl. II a. Bd. 129. p. 151—160. 1920.
K. Przibram und E. Kara-Michailova: Orientierte Gleitbüsche auf Kristallflächen. Zeitschr. f. Physik. 2. p. 297—298. 1920.
J. Spiess: Ueber die auf Wasser gleitenden electrischen Funken. Wied. Ann. 31, p. 975—982. 1887.
A. A. Cambell Swinton: Electrical Discharges. The Electrical Review. Vol. XXXI. p. 273—275. 1892.
M. Toepler: Ueber die physikalischen Grundgesetze der in der Isolatorentechnik auftretenden elektrischen Gleiterscheinungen. Archiv für Elektrotechnik. X. p. 157—185. 1921.
Usaburo Yoshida: 1. Figures produced on Photographic Plates by Electric Discharges. Mem. Coll. Sc. Kyoto Imp. Univ. Vol. II. p. 105—116. 1917.
— 2. Further Investigations on the Figures produced on Photographic Plates by Electric Discharges. Ibid. p. 315—319.

Forelagt paa Mødet den 10. Februar 1922.
Færdig fra Trykkeriet den 20. Juni 1922.

I

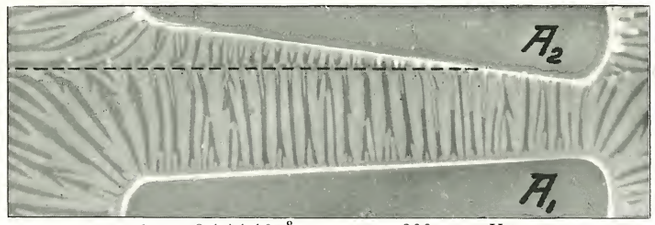

+

$t_0 = 2.1 \times 10^{-8}$ sec; $p = 300$ mm Hg.

II

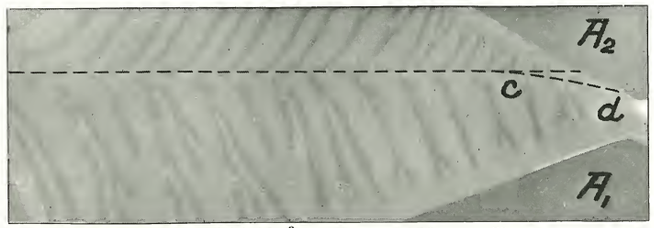

+

$t_0 = 2.45 \times 10^{-8}$ sec; $p = 150$ mm Hg.

III

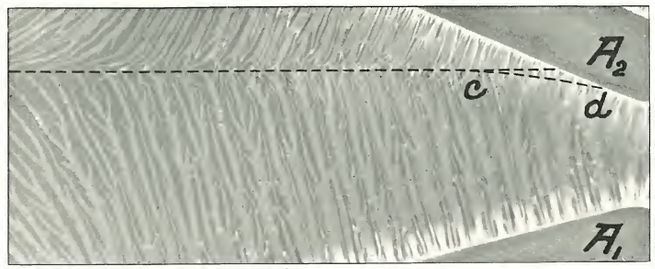

+

$t_0 = 3.5 \times 10^{-8}$ sec; $p = 500$ mm Hg.

IV

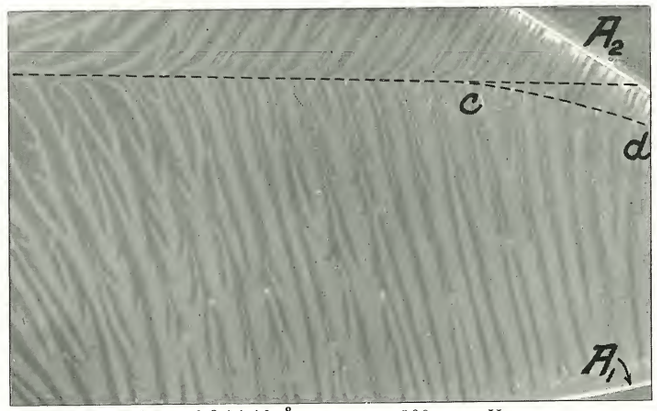

+

$t_0 = 6.3 \times 10^{-8}$ sec; $p = 300$ mm Hg.

I

+

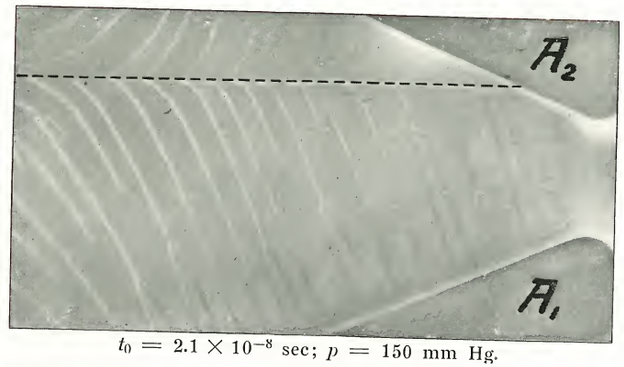

$t_0 = 2.1 \times 10^{-8}$ sec; $p = 150$ mm Hg.

II

+

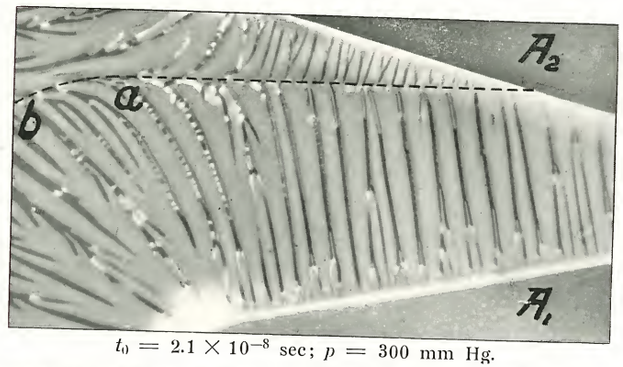

$t_0 = 2.1 \times 10^{-8}$ sec; $p = 300$ mm Hg.

III

—

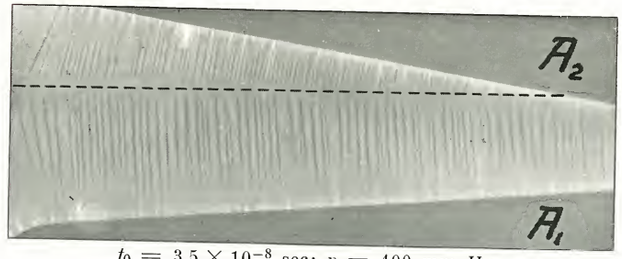

$t_0 = 3.5 \times 10^{-8}$ sec; $p = 400$ mm Hg.

IV

—

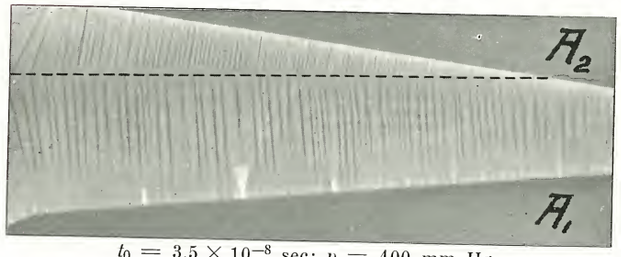

$t_0 = 3.5 \times 10^{-8}$ sec; $p = 400$ mm Hg.

MATHEMATISK-FYSISKE MEDDELELSER

UDGIVNE AF

DET KGL. DANSKE VIDENSKABERNES SELSKAB

3. BIND (Kr. 13,75):

9. BIND (under Pressen):

Det Kgl. Danske Videnskabernes Selskab.

Mathematisk-fysiske Meddelelser. **VIII,** 10.

ON THE LICHTENBERG FIGURES

PART III. THE POSITIVE FIGURES

BY

P. O. PEDERSEN

WITH 28 PLATES

KØBENHAVN

HOVEDKOMMISSIONÆR: ANDR. FRED. HØST & SØN, KGL. HOF-BOGHANDEL

BIANCO LUNOS BOGTRYKKERI

1929

Det Kgl. Danske Videnskabernes Selskabs videnskabelige Meddelelser udkommer fra 1917 indtil videre i følgende Rækker:

Historisk-filologiske Meddelelser,
Filosofiske Meddelelser,
Mathematisk-fysiske Meddelelser,
Biologiske Meddelelser.

Hele Bind af disse Rækker sælges 25 pCt. billigere end Summen af Bogladepriserne for de enkelte Hefter.

Selskabets Hovedkommissionær er *Andr. Fred. Høst & Søn*, Kgl. Hof-Boghandel, København.

Det Kgl. Danske Videnskabernes Selskab.
Mathematisk-fysiske Meddelelser. **VIII**, 10.

ON THE LICHTENBERG FIGURES

PART III. THE POSITIVE FIGURES

BY

P. O. PEDERSEN

WITH 28 PLATES

KØBENHAVN
HOVEDKOMMISSIONÆR: ANDR. FRED. HØST & SØN, KGL. HOF-BOGHANDEL
BIANCO LUNOS BOGTRYKKERI
1929

CHAPTER I

Introduction.

The determination of the spreading-out-velocity of the LICHTENBERG Figures has been discussed in some previous publications which have also touched upon the problem of the formation of these figures[1].

In the meantime the photographic LICHTENBERG Figures have been successfully applied to the study of surges on high tension lines, especially the kind of surges due to lightning[2]. They have also been used for the measurement

[1] P. O. PEDERSEN: "On the Lichtenberg Figures": Part I. Vidensk. Selsk. Math.-fys. Medd. Vol. I, No. 11. Copenhagen (February 1919); Part II. Vol. IV, No. 7, Copenhagen 1922; referred to as L. F. I and L. F. II respectively. — "Die Ausbreitungsgeschwindigkeit der Lichtenbergschen Figuren und ihre Verwendung zur Messung sehr kurzer Zeiten". Ann. d. Physik (IV) Bd. 69, p. 205—230, 1922.

[2] J. F. PETERS: "The Klydonograph" "El. World" Vol. 83, p. 769—773, 1924. — J. H. Cox and J. W. LEGG: "Trans. A. I. E. E." p. 857—870, 1925. — K. B. MCEACHRON: "Trans. A. I. E. E.", p. 712—717, 1926. — J. H. COX, P. H. MCAULEY and L. GALE HUGGINS: l. c. p. 315—329, 1927. — J. H. COX: l. c. p. 330—338, 1927. — R. J. C. WOOD: "Trans. A. I. E. E." p. 961—968, 1925. — EVERETT S. LEE and C. M. FOUST: "Trans. A. I. E. E." p. 339—348, 1927 and "Gen. Elec. Review" Vol. 30, p. 135—145, 1927. — W. W. LEWIS: "Trans. A. I. E. E." p. 1111—1121, 1928. — E. W. DILLARD: l. c., p. 1122—1124, 1928. — J. G. HEMSTREET and J. R. EATON: l. c., p. 1125—1131, 1928. — PHILIP SPORN: l. c., p. 1132—1139, 1928. — N. N. SMELOFF: l. c., p. 1140—1147, 1928. — H. MÜLLER: Mitteil. d. Hermsdorf Schomburg Isolatoren G. m. b. H., Heft 27, p. 813—829, 1926. — P. O. PEDERSEN: "Ingeniøren", p. 201—209, 1928. "Danmarks Naturvidenskabelige Samfunds Skrifter", A. No. 18, Copenhagen 1928. — MÜLLER-HILLEBRAND: "Siemens Zeitschr." 7, p. 547—551, 605—612, 1927. — E. BECK: "The Electric Journal", p. 591—595, 1928; p. 50—53, 1929.

of very short intervals of time, down to 10^{-10} sec. and even less[1]. Such measurements have been used extensively by the writer[2], by M. Iwatake[3] and others for the determination of time lag in electric sparks. The problem of spark lag and spark formation will, however, be treated of elsewhere.

Fig. 1 shows a sketch of the diagram of connections used for obtaining photographic *L. F.*, compare L. F. I, Fig. 10.

In L. F. I the previous theories of the formation of the L. F. have been mentioned and it is hardly necessary to

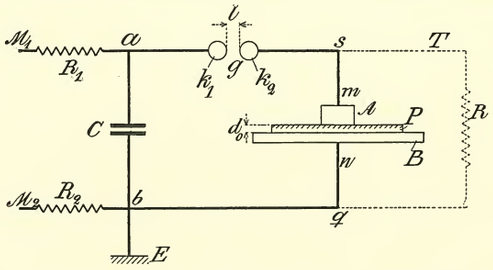

Fig. 1. Diagram of connections for obtaining photographic L. F. M_1 and M_2 are leads from the high tension source. R_1, R_2 and R_3 high resistances (slate pencils or the like). P a photographic plate, B a metal plate connected to earth E.

renew this discussion, especially because no sound theory could be worked out before the velocity of the figures was known.

[1] P. Heymans and N. H. Franck: "Phys. Review" (II). Vol. 25, p. 865—869, 1925.

[2] P. O. Pedersen: (a): Vidensk. Selsk. Math.-fys. Medd. Vol. IV, No. 10, Copenhagen 1922. — (b): l. c. Vol. VI, No. 4, Copenhagen 1924. — (c): "Teknisk Tidskrift (Elektroteknik)", p. 174—184, Stockholm 1923. — (d): Ann. d. Physik (IV). Bd. 71, p. 317—376, 1923. — (e): l. c., Bd. 75, p. 827—847, 1924.

[3] M. Iwataka: "Technology Reports Tôhoku Imp. University" Vol. 7, Nr. 1, p. 57—86, 1927. This paper contains an extensive bibliography on the time lag of electric sparks.

There are, however, one or two exceptions to be mentioned below.

U. Yoshida[1] has given a theory of the formation of the negative figures and of the characteristic dark radii in these figures which is in the main satisfactory. His theory is, with one important exception to be mentioned later, identical with that given by the writer in L. F. I[2]. According to Yoshida the negative figures are due to negative ions which the electric field drives away from the electrode and which cause ionization by collision along their paths. Yoshida does not state the nature of these ions and he does not point out that they must necessarily be electrons, as shown in L. F. I. But this necessity did not exist at the time when Yoshida worked out his theory because the great velocity of the spreading out of the L. F. was not known then.

K. Przibram, who has contributed a long series of important papers[3] on the L. F. has accepted the same view of the formation of the negative figures[4], while M. Toepler[5,6] has been led to a somewhat different interpretation of the negative figures in his important and long continued investigations of gliding discharges.

All circumstances considered, the main points of the

[1] U. Yoshida: (a): Mem. Kyoto Imp. University, Vol. II, p. 105—116. 1917. — (b): l. c., p. 315—319. 1917.

[2] The writer did not know of the two mentioned papers of Yoshida at the time he wrote L. F. I, which paper was presented to the Royal Danish Soc. of Science on March 8, 1917.

[3] See bibliography in "L. F. II", p. 35.

[4] K. Przibram: (a): Phys. Zeitschr. Bd. 20, p. 299—303. July 1919. — (b): Die elektrischen Figuren in Handb. d. Physik Bd. XIV, p. 391—404, 1927.

[5] M. Toepler: (a): Phys. Zeitschr. Bd. 21, p. 706—711, 1920. — (b): Arch. f. Elektrotechnik Bd. 10, p. 157—185, 1921.

[6] K. Przibram: l. c., (b): p. 403—404.

above mentioned theory of the formation of the negative figures are so well founded that it is hardly necessary to discuss this problem further. In what follows we therefore only treat of the negative figures in so far as it is necessary in order to throw light on the formation of the positive figures.

The theory of the secondary and tertiary figures given in L. F. I has lately been fully corroborated in some interesting experiments of U. YOSHIDA[1] who has also given experimental proof of some further consequences of that theory. M. TOEPLER[2] has also investigated these secondary and tertiary figures and his results agree fairly well with those obtained in L. F. I and by YOSHIDA. We therefore need not further discuss the theory of these figures.

The only outstanding problem is therefore the formation of the positive figures, but this question is, no doubt, the most important and also the most difficult of all the problems connected with the theory of the L. F. In the course of the last 10 years we have made many experiments aiming at the elucidation of the nature of the positive figures. Most of the experimental material — containing among other things some 2500 photographic L. F. — was collected in the years 1918—20. But it was only about a year ago that the writer succeeded in putting forth a hypothesis which made it possible to establish a coherent theory of the formation of the positive figures explaining all their peculiarities in a satisfactory manner.

Before entering upon the detailed discussion of the experimental results and their theoretical explanation, it

[1] U. YOSHIDA and G. TANAKA: Mem. Kyoto Imp. University. Vol. V, No. 2, 145—152, 1921.

[2] M. TOEPLER: Phys. Zeitschr. Bd. 22, p. 78—80, 1921.

will be convenient to dwell a little on some preliminary questions, namely concerning the nature of the photographic impressions of L. F. in various gases.

With regard to the terminology adopted in the following we have to lay stress on the fact, that LICHTENBERG figures and discharges only refer to the well known, regular figures

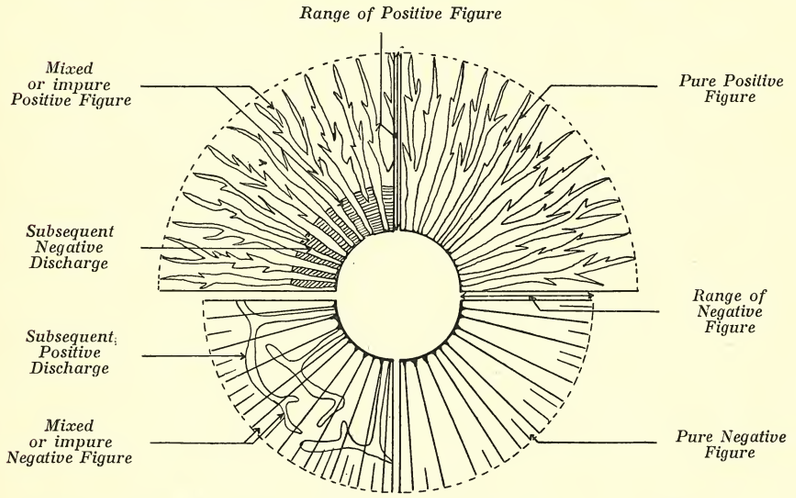

Fig. 2. Regular or simple Lichtenberg Figures. Upper part Positive and lower part Negative Figures. Right hand part pure, left hand part impure or mixed Figures.

showing the characteristic differences between positive and negative discharges and of relatively feeble luminosity but not to the bright sparks or spark tracks which occur if the *p. d.* is sufficiently high and of sufficient duration. Photographs of such spark tracks are to be seen on plate 1, parts VI—VII, and one single track on part III, plates 3 I, 7 II, and 11 I and IV.

The Lichtenberg discharges and figures may start either directly from the electrodes or from the above named

bright spark tracks. In the following we will call the first kind regular the latter kind irregular figures and discharges. Samples of the first kind are shown in L. F. I figs. 2, 3, 6, 7, 8, 9, 12, 13, 19, 26, 27, 28 and in this paper on plate 1, parts I and V, plate 2, parts I—III and

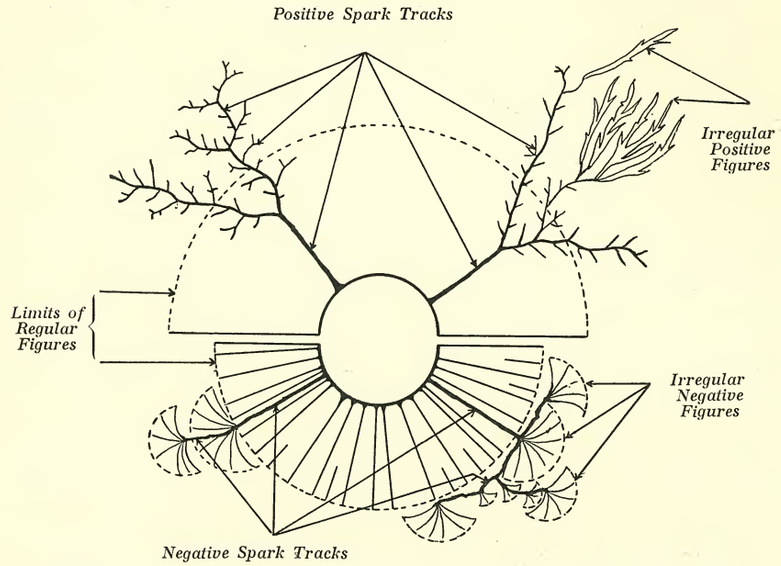

Fig. 3. Composite Lichtenberg Figures.

plate 3, parts I—III. Samples of the latter kind are seen in L. F. I figs. 4 and 5 and in this paper plate 1, parts III, VI and VII and plate 3 part I.

The regular figures will normally always be formed by a potential flash of very short duration. If the *p. d.* is not of very short duration, bright spark tracks will be formed, and from these will again start irregular figures which — especially in case of positive ones — will cover and obscure the regular figure.

A figure consisting of only a regular Lichtenberg figure is often called a simple figure. Such a simple figure is said to be pure if only one single discharge — positive or negative — has taken place; see f. inst. plate 1, parts IV and V, plate 2, part III, plate 3, parts II and III, plate 14, part II and plate 25, part III. If the first discharge has been followed by a second one — generally somewhat weaker — of opposite sign, the figure is said to be a mixed or impure one; see f. inst. plate 1, part II, plate 2, parts I and II, plate 14, part I, plate 15, parts I and II, plate 18, part II and plate 25, part I.

The schematical figures 2 and 3 illustrate this terminology.

CHAPTER II

1. Photographic or "Electrographic" Action?

Are the L. F. due to the photographic effect of the luminosity of the discharge, or to some more direct action of the discharge on the sensitive film — to what may be called an "electrographic" action?

J. Brown[1] considered the luminosity of the discharge to be too feeble to cause the photographic images in the ordinary way and he quoted some experiments in support of this view. It has been proved, however, by U. Yoshida[2] that Brown's experiments are not conclusive.

A. A. Campbell Swinton[3] tried to settle the question by placing discs of non-actinic ruby glass and clear glass on the sensitive film, the small electrode resting on these discs. The ruby glass stopped all action, the clear glass allowed the action to take place all over the plate, though on account of the thickness of the glass, and the consequent intervening distance between the discharge and the film, the details of the figure produced were somewhat blurred and indistinct. Subsequently, using very thin glass, this indistinctness was almost entirely eliminated.

From these results Campbell Swinton draws the conclusion that "the action is due to the ordinary photochemical effect of the light produced by the spark, which though feeble in intensity to the eye, is blue, and must be remarkably actinic".

[1] J. Brown: Phil. Mag. (5) Vol. 26, p. 503—505, 1888.

[2] U. Yoshida: Mem. Coll. Sc. Kyoto Imp. University Vol. II, No. 2, p. 105—116, 1917.

[3] A. A. Campbell Swinton: "The Electrical Review" Vol. 31, p. 273—275, 1892.

Even if it is ultimately proved that Campbell Swinton's opinion is right we cannot consider his experiments conclusive. There is thus no doubt whatever that the light emitted from the spark tracks is strong enough to give the ordinary photographic image, and it is also evident that this light will be cut off by the inactinic ruby glass disc. And with the high potential differences used by Brown and Campbell Swinton such spark tracks will occur in every case. The question here discussed only concerns the Lichtenberg figures proper, and in this case it is much more difficult to attain a decision. With this aim in view we have made a number of experiments of which we shall quote some in the following.

Ebonite discs 0.3 mm thick cut off completely. This is in agreement with Campbell Swinton's Experiments.

The following experiment will show, however, that the conditions are completely altered with very thin plates. In the figure plate 7, part I the electrode was placed on a mica plate 0.05 mm thick, and the mica covered the photographic film below the line marked *mn*. The mica plate was covered by a dry layer of inactinic red ink. The photographic image shows clearly the Lichtenberg discharges, while the strong light from the spark tracks — as f. inst. *bc*, *de—f—g—h and hij* — is completely cut off. These spark tracks were certainly on the upper side of the mica plate and the Lichtenberg discharges are seen to start from these tracks. (At a few points, f. inst. that marked *g*, the red ink coating has been defective and an

image of a short portion of the spark track is to be seen).

As the strong light from the spark tracks in this case has been unable to penetrate the inactinic coating of the mica plate, it is altogether impossible that the feeble luminosity of the Lichtenberg discharges on the upper side of the mica plate can be the cause of the photographic L. F. below this plate.

The photographic L. F. may in this case be due to: (a) the influence of the strong electric field on the photographic film; or (b) the ordinary photographic effect of the light emitted from points where there is a strong ionization by collision, such ionization taking place on the lower side of the mica plate directly below the Lichtenberg Figures which are formed on the upper side of the mica plate; or (c) possibly a combination of (a) and (b), the sensibility of the photographic film being increased by the strong electric field.

The proposition (a) cannot be true because an electric field does not in itself give any photographic image, but without further evidence it is not possible to choose between (b) and (c). This point is illustrated by plate 7, part I. From an inspection of this figure it appears that the Lichtenberg figures cross the boundary *mn* without any discontinuity[1]. It is also evident that the Lichtenberg discharges in the mica-covered part of the figure have started from certain spark tracks along the upper surface of the mica plate. The photographic L. F. cannot be due to an ordinary discharge between the mica plate and the photographic film, since if this were the case, the spark

[1] This fact is quite evident in the original photographs, somewhat less so in the reproduction.

tracks *abc*, *de—f—g—h* and *hij* would have been very bright in the image, and actually they do not show at all. The photographic L. F. below the mica plate must therefore be due to one of the effects (b) or (c).

Plate 7, part II shows the result of another experiment. The parts *VP 1* and *VP 2* of the photographic film were covered respectively with one and two layers of thin (0.02 mm) violet transparent paper, and other parts, *BP 1* and *BP 2*, respectively with one and two layers of 0.04 mm thick opaque, black paper.

The paper strips were soaked in clear vaseline and pressed against the photographic film, no air being left between the strips and the film. All superfluous vaseline was removed before exposing the film to the discharge, and all strips and vaseline removed before developing the photographic plate. The resulting figure is seen in plate 7, part II.

Below the violet paper both the L. F. and the spark tracks are to be seen, clearest of course with only one layer of the paper. Below the black paper strips, on the contrary, there is no image of either L. F. or spark tracks. (In the case of one layer there are some faint spots of light beneath the spark which has passed over the upper surface of the strip, these spots being no doubt due to small holes in the papers).

This experiment proves that a strong electric field does not give any image in the case where there is no air, and therefore no ionization by collisions at the surface of the photographic film. But the experiment does not absolutely prove that the image of the L. F. is due solely to the light emitted by the Lichtenberg discharge, because the photographic film is subjected to a strong electric field simultane-

ously with the exposure to the light from the discharge. This question can be settled, however, by means of the experiments illustrated in Fig. 4. Upon the film of the ordinary photographic plate P were placed some small pieces of photographic plates with the film downward, either as at P', with a small distance δ between the films, or as at a, b, c, with the two films in direct contact. Even in this case the films only touch each other in a number of points since the films of small broken pieces a, b, c have somewhat projecting edges. In all these cases the Lichtenberg discharges have taken place in the space between the two films. Plate 8, part I shows the result of such an experiment with three pieces: a, b, c, the main plate P and the three pieces of plate being developed in exactly the same manner. It appears that there is very little difference between the photographic intensity of the image on the main plate and on the small plates. Even in cases such as P' in Fig. 4, where there is a considerable distance between the two films, the intensity of the image on the upper film may be almost as great as on the main film, see plate 7, part III. Up to $\delta = 1$ to 1.5 mm the image on P' is quite distinct; for greater distances it becomes blurred.

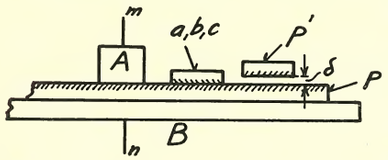

Fig. 4. Ordinary arrangement for obtaining photographic L. F., compare Fig. 1. P' and a, b, c are small pieces of photographic plates with the film downwards.

Since the intensity of the electric field at the film of the pieces P', a, b, c, is very small in comparison with the field at the film of the plate P, and since the photographic intensity is almost the same in the two cases, it

is proved that the photographic L. F. are due to the ordinary photographic effect of the light emitted by the discharge. But the light may come from discharges in a very thin layer of air between the photographic film and the covering plate, these discharges being either ordinary Lichtenberg discharges —, as in plate 7, part III and plate 8, parts I—II, — or in cases where the covering plates are very thin, very intense ionizations due to very strong fields at right angles to the film, as in plate 7, part I.

This point of view is in accordance with all the previously known facts and with a number of further experiments and observations of which only a few will be mentioned in the following.

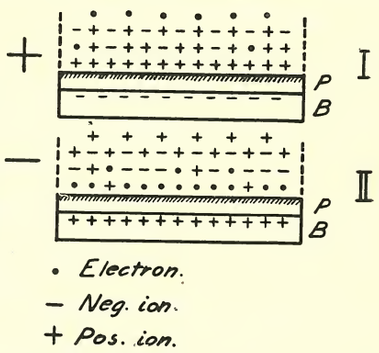

Fig. 5. Schematic representation of the distribution of electrons and positive and negative ions over the cross-section of positive and negative streamers.

With regard to the distribution of the photographic intensity it is to be remembered that the emission of light is mostly caused by the recombination of positive ions with either electrons or negative ions. Fig. 5 gives a schematical sketch of the distribution of electrons and positive and negative ions over the cross-section of positive and negative streamers. But the question of intensity-distribution will be taken up later on in Chap. IV 1 (d).

2. Lichtenberg Figures in Various Gases.

Air, nitrogen and argon give strong photographic L. F. both positive and negative, the last being by far the strongest. In oxygen the luminosity of the Lichtenberg discharges — both the visual and the photographic — is very small. It has not been possible to get positive photographic figures in almost pure oxygen — containing about one per cent of hydrogen —. In oxygen containing small amounts of atmospheric air or nitrogen very feeble positive photographic figures have been obtained, as for inst. plate 1, part II[1]. Part III is the corresponding negative figure.

It may be supposed that the positive discharge in oxygen is very feeble or even that there is no discharge at all in this gas, thus explaining the failure to obtain positive figures. But this supposition would be wrong, for there are strong positive discharges even in the purest oxygen, as may be proved by means of the dust method, using an electrically clean plate of ebonite instead of the photographic plate *P*. A photograph of such a dust figure is shown in plate 1, part I.

The photographic negative figure in oxygen is similar to the negative figure in air, but fainter, see plate 1, part IV. Owing to the faintness there is some difficulty in determining the range of the figures in oxygen. Table 1 contains some approximate values of such ranges in air and in oxygen[2].

[1] This positive figure is impure. The strong light in the neighbourhood of the electrode is due to a negative discharge taking place after the formation of the positive figure, see Chap. III 1 (d) and Chap. IV 1 (d).

[2] K. Przibram. (Wien. Ber. (II a) (a) Bd. 127, p. 395—404, 1918 and (b) Bd. 129, p. 151—160. 1920; (c) Phys. Zeitsch. Bd. 20, p. 299—303. 1919) found that the ratio $\frac{R+}{R-}$ was smaller in oxygen than in air (l. c.) (a) p. 402, (b) p. 151—2) while the writer previously came to the opposite result (L. F. I, p. 35 and 42). The new investigations have fully confirmed our previous results. The difference between Przibram's and our results is perhaps due to the circumstance that our measurements refer to simple, regular Lichtenberg figures both in air and in oxygen — compare plate 1, part IV — while the oxygen figures in Przibram's papers (l. c. (a) Figs. 4 and 5; (c) Figs. 5 and 6) are complicated figures with strong spark tracks similar to the figures in plate 1, parts VI and VII. On the other hand Przibram's positive nitrogen figure (l. c. (a) Fig. 3) is a regular simple L. F.

Table 1. $p = 350$ mm Hg.; $l = 3$ mm; $d_0 = 1.5$ mm.

Air.....	$R+ = 34$ mm[1]	$R- = 17$ mm	$\frac{R+}{R-} = 2.0$
Oxygen ($98\ O_2 + 2\ H_2$).	$R+ = 35$ mm[1]	$R- = 13$ mm	$\frac{R+}{R-} = 2.7$

The photographic positive figures are also very faint in hydrogen, see f. inst. plate 2, parts I and II. But large and finely branched dust figures may be obtained in this gas. The photographic negative figures are also fainter in hydrogen than in air or nitrogen, see plate 2, part III.

All these circumstances agree well with our previous result, namely that the photographic L. F. are caused by the light emitted by the discharge, the visual luminosity in hydrogen being considerably less than in air but greater than in oxygen.

For general information, some figures in other gases have been included. Thus plate 3, parts II and III show regular positive and negative figures in CO_2[2] while part I shows some positive spark tracks in the same gas[3].

[1] Other experiments also indicate that the range $R+$ is almost the same in air and oxygen.

[2] S. Mikola (Phys. Zeitsch. Bd. 18, p. 161, 1917) says: "In den anderen untersuchten Gasen (*O*, *H*, CO_2 und Leuchtgas) entwickeln sich die Strahlungsfiguren kaum sichtbar". This is strictly speaking only true of the positive figures in oxygen.

[3] The positive figure by Przibram (Wien. Ber. (II. a). Bd. 108, 1161—1171, 1899) indicates the presence of some air or nitrogen besides the gas CO_2.

We have not succeeded in obtaining photographic L. F. in pure helium. Plate I, part V shows a figure taken in a mixture of air and helium and plate 4, part II a figure from a mixture of air and argon.

The above remarks concerning the intensity of the luminosity refer only to the regular, pure L. F. The light from the spark tracks is very strong in all gases[1].

Plates 4—6 show parts of a number of positive figures in mixtures of N_2, O_2 and H_2 in various ratios. These figures will, however, be discussed later (Chap. IV. 3 (b)).

[1] Compare also Przibram l. c. (a) p. 399.

CHAPTER III

The Properties of the Positive Figures.

1. Differences of Form and other Features between Positive and Negative Figures.

With regard to the main points of these differences we may refer to the L. F. I and for ease of reference we repeat here figs. 6 and 7, which show respectively a positive and a negative photographic L. F. obtained by means of the experimental arrangement shown in Fig. 1.

Besides the very obvious differences between the two kinds of figures, which need no further comment, we shall in the following give some particulars about some specific points.

(a) Width of the Positive and Negative Spreaders.

The width of the negative spreaders varies greatly, the broadest ones having often ten times the width of the narrowest ones, compare f. inst. plate 25, part I and L. F. I Table 3, p. 28.

The positive spreaders on the contrary have in all cases almost the same width at the same distance from the tip, and the width is very nearly inversely proportional to the pressure of the gas if measured at distances from the tip which are also inversely proportional to the pressure. This relation is illustrated by plate 6, part I and by the figures in the following table.

The width of the positive spreaders measured at a certain distance from the tip depends very little upon the voltage or upon the thickness of the insulating plate.

Table 2. Effect of Gas Pressure on the Width of the Positive Spreaders.

Pressure p in mm Hg	Width of Spreaders t in mm	Distance from Tip to Test Point in mm	$p \cdot t$
5×760	0.027	0.10	103
3×760	0.043	0.17	99
2×760	0.07	0.25	108
760[1]	0.12	0.5	91
300[1]	0.29	1.3	87
150[1]	0.59	2.6	89
75[1]	1.42	5.2	106
34[1]	3.60	11.0	119
30	3.60	13.0	108
17	7.0	22	119
		Mean value	103

[1] From Table 7 in L. F. I p. 36.

(b) The Ramification of Positive and Negative Figures.

The negative spreaders show no ramification at all[1]. The positive spreaders ramify extensively and the number of branches per unit length of spreader is very nearly proportional to gas pressure, see Table 6, L. F. I p. 35.

This number of branches is greatest in H_2 and decreases in the following order: A, N_2, Air, CO_2 and O_2,

[1] In very broad negative spreaders the end is often divided by dark radii, see f. inst. plates 21 II, 25 II—III and 27 VI. These dark lines are quite similar to those issuing from the electrode, and the explanation of them offers no further difficulty. U. Yoshida (Mem. Coll. Sc. Kyoto Imp. Univ. Vol. II, No. 2, p. 114—15, 1917) has treated this question in a very thorough and convincing manner.

compare plates 1—6. The number of small branches about the middle of the spreaders is comparatively great in mixtures of H_2 and N_2, see plate 5, XI—XVI. An addition of some O_2 to such mixtures reduces the number of branches very considerably, see f. inst. plate 4 I and 5 I—V and XVII—XVIII.

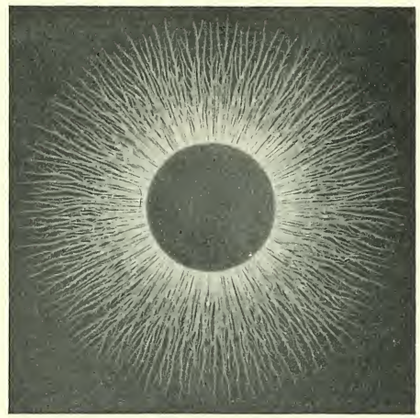

Fig. 6. Impure Positive Figure in Air.

(c) Boundary of the Positive and Negative Spreaders.

The photographic intensity of the negative figures falls off gradually at all points of the boundary but especially so at the outer edge. For the positive figures, on the contrary, the intensity drops down very abruptly to zero all along the boundary line. These properties of the positive and negative figures are illustrated by part II on plate 25.

(d) Distribution of the Photographic Intensity over the Area of the Positive and Negative Spreaders.

The photographic intensity of the negative spreaders has its greatest value at the electrode and on passing outwards it decreases gradually, becoming almost zero at the outer edge, see f. inst. plates I, parts III—IV, 2 III, 3 III, 12 I—IV, 25 I—IV, 26 I—IV, and 27 I—VI.

For pure positive spreaders, however, the photographic

intensity has very nearly the same value over the whole area of the spreaders, see f. inst. plates 1 V, 4 I—II, 5 I—XVIII, 6 I, III, 10 I—IV, 12 V—VII, 13 II, 14 I—II, 21 I, 22, 23 and 25 II.

This intensity of the positive spreaders is much less than the maximum intensity of the corresponding negative spreaders.

The innermost parts of the positive spreaders very often, however, show a comparatively very strong intensity which at some distance from the electrode drops down rather abruptly to the normal positive intensity, see plates 2 I—II, 6 II, 12 VIII, 14 I, 15 I—II, 18 I (lowest part), 20 I, III, and 21 I and III. This high intensity is due to a subsequent negative discharge caused by electrical oscillations in the discharge circuit. Such oscillations may also cause a subsequent positive discharge in a previously formed negative figure, see f. inst. plate 18 II (the right hand part) and plate 25 I.

Fig. 7. Pure Negative Figure in Air.

In a positive figure, a subsequent negative discharge will evidently take place mainly out along the positive spreaders, and the resulting high intensity will therefore, be confined mainly to the area of these spreaders. By increasing the damping of the discharge circuit and by making the conditions unfavourable for the formation of negative figures, these subsequent negative discharges may be partly or completely eliminated. In the last case pure positive

spreaders and figures are obtained. The damping is increased by reducing the leak resistance R, see Fig. 1, or by increasing the area of the positive figure, f. inst. by reducing the air pressure or by increasing — up to a certain point — the thickness of the insulating plate, compare L. F. I Fig. 34, p. 30. The range of the negative figure is, on the contrary reduced by increasing this thickness, as also appears from Fig. 34 in L. F. I.

It thus appears that pure positive figures are most easily obtained at reduced pressures and with great thickness of the insulating plate. These conclusions are in complete agreement with the experimental results.

With regard to the formation of subsequent positive discharges in previously formed negative figures the conditions are quite otherwise. We shall see later that negative discharges can start even with very low voltages — and from sharp points or edges probably down to almost zero voltage — while positive discharges do not start before the voltage has reached a certain minimum value, which decreases with decreasing pressure. The fact that impure negative figures generally only appear at low pressures is in complete agreement with this idea, for only at low pressures will the succeeding positive voltage be high enough to start a discharge.

U. Yoshida[1] considers the innermost bright part of the positive spreaders as due to an ionization caused by positive ions, while the outermost faint part is due to an ionization caused by negative ions, both these ionizations being essential to the formation of the positive discharge. We have seen, however, that the bright part is not a ne-

[1] U. Yoshida: Mem. Coll. Sc. Kyoto Imp. Univ. Vol. II, No. 2, p. 113, 1917.

cessary feature of the positive spreaders but may be eliminated altogether, and we think there can be no doubt that the bright part of the positive spreader here considered is due to a subsequent negative discharge.

On the other hand, if the voltage across the Lichtenberg gap is kept on long enough, both the positive and the negative ions will cause ionization, but the corresponding discharges and their images differ considerably from the Lichtenberg discharges and figures. We shall return to this question later on.

We thus come to the conclusion that the normal simple positive figure is pure and has almost the same photographic intensity over the whole area of the spreaders.

2. Range and Spreading-out-Velocity of the Positive and Negative Figures.

(a) Velocity of Positive and Negative Discharges.

The spreading-out-velocity is considerably greater for the positive than for the negative figures, f. inst. 2 to 4 times as great, see L. F. I p. 60.

(b) Relation between Air Pressure and Velocity.

The velocity, U, increases with decreasing pressure, p, for both positive and negative figures, but the manner in which U depends upon p is otherwise very different for the two kinds of figures, see fig. 8. At low pressures the velocity of the negative figures increases rapidly with decreasing pressure and this rapid increase continues down to a pressure of about 20 mm, which is about the lowest possible pressure at which the velocity can be measured

in this manner[1]. For high pressures the velocity of the negative figures decreases slowly with increasing pressure.

The velocity of the positive figures, on the other hand, approaches a certain maximum value U_m with decreasing

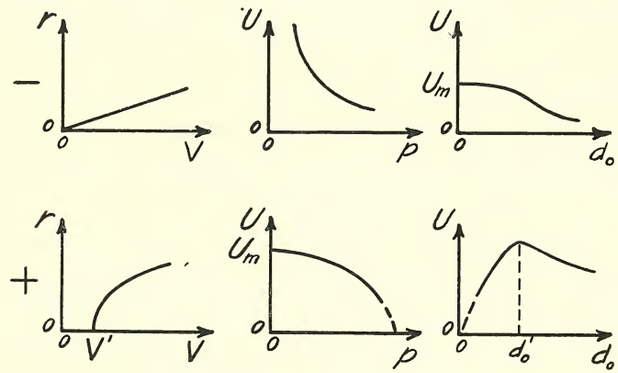

Fig. 8. Schematic representation of (1) the Range r against the Voltage V; (2) the Velocity U against the Pressure p; (3) the Velocity U against the total Thickness d_0 of the insulating Plate.

pressure and drops down to zero if the pressure is increased above a certain critical value, depending mainly on the voltage.

(c) Relation between Thickness of the Insulating Plate and Velocity.

For negative figures the velocity decreases with increasing thickness of the insulating plate; having its greatest value U_m for $d_0 = 0$. For positive figures the velocity seems to be zero for $d_0 = 0$, and for small values of d_0 the velocity increases rapidly with increasing values of d_0. At a certain thickness the velocity attains its highest value and decreases with further increase of d_0.

[1] See figure 24, p. 53.

(d) Relation between Voltage and Range of the Figures.

For negative figures the range, r, seems to go down to zero together with the voltage. In the case of positive figures there is a certain minimum voltage below which there is no discharge, and below which the range is accordingly equal to zero.

3. The Starting of the Positive and of the Negative Figures.

(a) Starting of the Negative Discharges.

From a finely pointed electrode placed directly on the photographic plate, even the smallest negative potential seems to start a figure at least if the potential is above some two hundred volts but the figures are very small at low potentials where the radius of the figure is proportional to the applied potential. This is shown in plate 21, part II to which again corresponds the straight line marked (—) in fig. 9.

(b) Starting of the Positive Discharges.

Under similar conditions, positive figures are only started if the potential is above a certain limit, the value of which increases with increasing air pressure. On the other hand, if a positive figure starts at all, it has always a finite and not inconsiderable range. For small potentials there is thus no proportionality between size of figure and potential. This is shown in plate 21, part I which again corresponds to curve (+) fig. 9.

This question is of such importance for the understanding of the formation of the positive figures that a closer consideration was necessary.

The production of a positive discharge — a positive figure — through the influence of a transitory potential depends not only upon potential and the air pressure, but also upon a series of other conditions, although the two first named factors are the most influential. We shall therefore first consider the influence of these two.

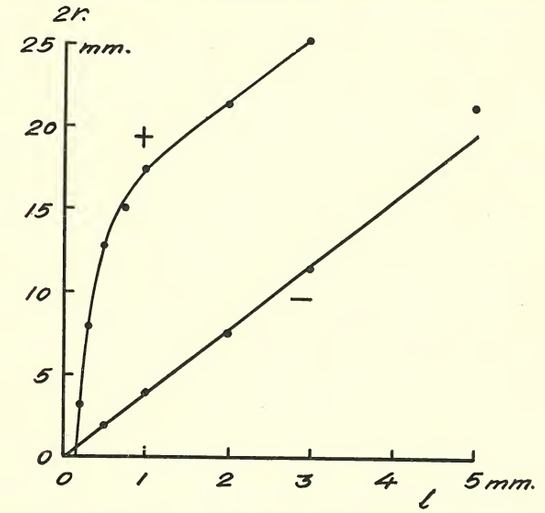

Fig. 9. Range r of positive (+) and negative (—) Figures against the spark length l.

Plate 21, part I shows how the size of the positive figures depends upon the potential at atmospheric pressure, but the conditions near the limit where figures may or may not appear are more favourably elucidated at lower pressures.

For general information plate 22 shows a number of figures produced at constant pressure (p = 100 mm Hg) but applying different potentials.

Where potentials here and in what follows are stated in volts, they are generated by a high-voltage D. C. dynamo,

and the spark gap g in fig. 1 is replaced by a discharge key, the design of which we shall come back to later. The potential stated is the voltage across the discharge key before this is closed. Different forms of electrodes have been used; the figures reproduced on plate 22 and 23 were taken with a sharp-edged 3 mm cylindrical brass rod resting directly on the photographic plate.

At 100 mm pressure figures only appeared at potentials above 1160 volts. $V = 1366$ produces a pronounced figure having a radius of about 15 mm, as is also the case with the voltages 1382, 1400, 1410, 1430, 1446, 1478, 1536, 1541, 1581 and 1593 volts. At 1556 volts no discharge appeared at all, while all potentials above 1600 volts produced a figure. An inspection of the pictures on plate 22 shows that all the branches are of nearly equal length at potentials from 1366 to 1593 volts, and that the number of branches increases, although somewhat irregularly, with increasing potential. At 1556 volts the number of branches dropped to zero, no discharge appearing. This indicates a certain irregularity in regard to number of branches, whereas their range is nearly independent of the potential value within the critical interval.

The figures on plate 23 correspond to the constant potential 1190 volts, while the air pressure is varied from 40 to 101 mm Hg. At $p < 80$ mm the discharge appears as a uniform disc near the electrode with a number of teeth or branches stretching outward from the disc edge. At $p > 80$ the branches start directly from the electrode and they are of practically equal length at pressures from 80 to 99 mm, while their number decreases, though somewhat irregularly, with increasing pressure. At $p > 100$ the number of branches is zero, i. e. no discharge occurs at all.

Those series of figures presented on plates 22 and 23 are not especially selected or arranged but include all records taken in these particular series, which series again have been selected arbitrarily from a greater number.

To elucidate these conditions further we have in figs. 10—12 presented graphically the range r and the number of branches n as functions of either potential or air pressure. These curves also confirm the fact that the discharge — i. e. formation of the image — does not fail to appear because the length of the branches decreases toward zero but, on the contrary, because their number becomes zero. They also confirm the above mentioned irregularity in the dependency of n on pressure or potential.

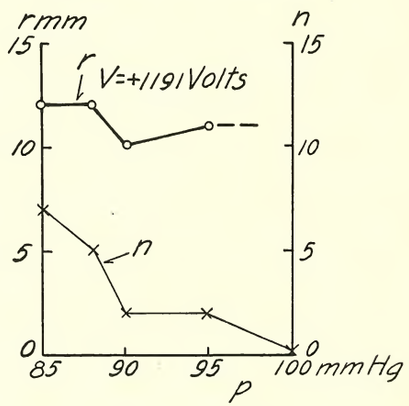

Fig. 10. Range r and number of spreaders n against the pressure p. ($V = +1191$ Volts).

The electrode used in the tests recorded in figs. 10—12 was a 3 mm round brass-rod the end of which was a plane surface, but nothing was especially done in order to keep the electrode sharp-edged. On the other hand a series of investigations have been carried out in order to ascertain how the shape and the state of the electrode may influence the formation of figures within the critical interval. The results of some of these investigations are shown in figs. 13—16. Four different forms of electrodes have mainly been tried: a 6 mm brass ball has been used for some of the tests in all of the figures; a rounded 3 mm brass rod is used in some of the

tests in fig. 13; a sharp-edged electrode was used in some of the tests in figs. 13—15[1]; an electrode consisting of a

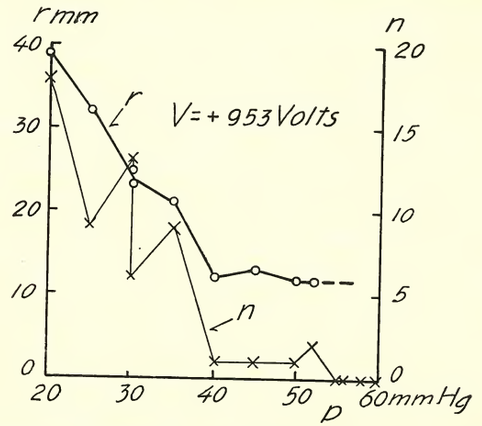

Fig. 11. Range r and number of spreaders n against the pressure p. ($V = +933$ Volts).

brass tube with very thin walls — 0.15 mm thick — which was kept very sharp edged by grinding, was used in some of the tests in fig. 16; finally we have for some tests in

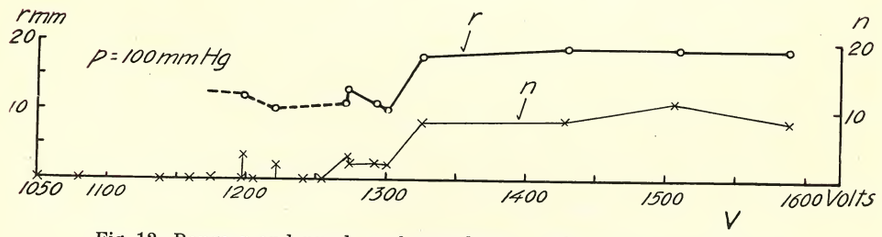

Fig. 12. Range r and number of spreaders n as functions of the $p.d.$ V. ($p = 100$ mm Hg).

fig. 16 used a pointed electrode kept carefully pointed by repeated grinding. If nothing is stated to the contrary all

[1] This shape of electrode will gradually lose its sharp edge by the repeated cleaning process. For this reason we adopted the next electrode shape, a thin-walled tube.

the electrodes were kept "clean" by rubbing with carborundum[1]. The shape of the electrodes is stated in each figure. In some of them is indicated, in the same manner as in fig. 13, whether the figures consist of a uniform disc near the electrode. Finally in fig. 15, for some cases, the number of spreaders is indicated by figures. In fig. 16 we have only stated the number of spreaders n but not their length r, the values of which are given in figs. 13—15.

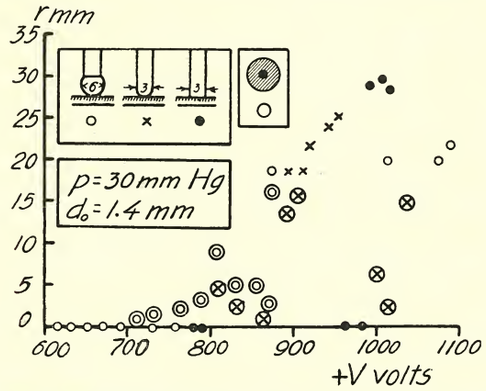

Fig. 13. Range r as function of the $p.d.$ V for three different shapes of the electrode. The large circles indicate that the figure has a continuous disc surrounding the electrode. ($p = 30$ mm Hg; $d_0 = 1.4$ mm).

Fig. 13, which refers to the conditions at 30 mm pressure, indicates that a figure is formed somewhat more easily from a spherical electrode than from a rounded or a sharp-edged rod, although the difference between the two first mentioned is not very pronounced. These tests also prove that with sharp-edged electrodes there are formed either spreaders of considerable length or no spreaders at all. With the spherical electrode and with the rounded rod the conditions change more gradually, since with these elec-

[1] See P. O. Pedersen: l. c., (a) p. 25, (d) p. 336.

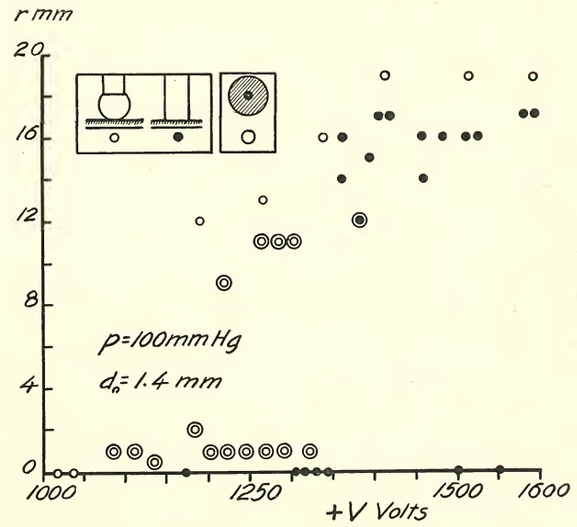

Fig. 14. Relation between Range r and Voltage V.

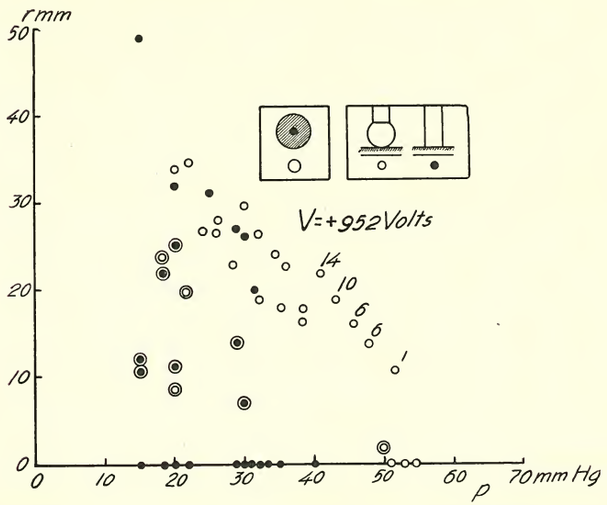

Fig. 15. Range r as function of the pressure p. ($V = +952$ volts). The figures at some of the representative points indicate the number of spreaders.

trodes figures of small range may be obtained within the critical interval. We will come back to this question later on.

Fig. 14, referring to tests at 100 mm pressure applying different potentials, and fig. 15, where the potential is kept constant at 952 volts but the air pressure is varied, show exactly similar relations with regard to the spherical elec-

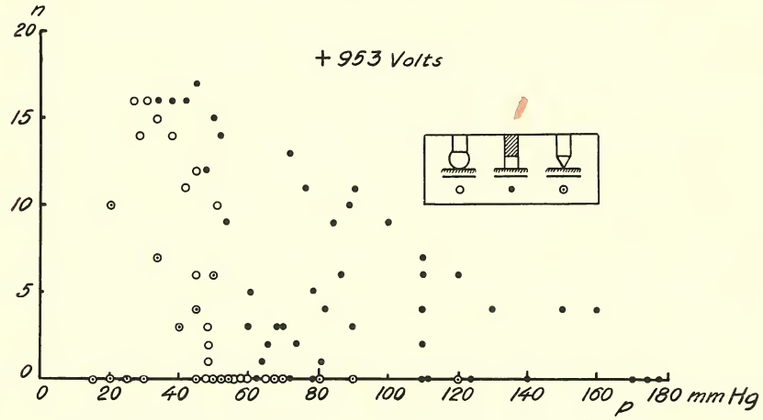

Fig. 16. Number of spreaders n as function of the pressure p. ($V = +953$ volts).

trode and the sharp-edged rod. Finally, in fig. 16 is shown the number of spreaders (n) formed with spherical, tubular and pointed electrodes, for $V = 953$ volts and varying air pressures. It appears from this figure that figures are most easily formed from the tube electrode, less easily from the spherical one and least easily from the pointed electrode. For negative figures the reverse is the case; they are formed by far more easily from a pointed than from a spherical electrode.

The small range sometimes attained by the figures within the critical interval with the spherical electrode and

with the rounded rod may possibly be due to the vertical electric field which forces the discharges, started beneath these electrodes, down towards the film of the photographic plate, thus preventing them from spreading out in the normal way. The considerable decrease in range of the positive figures when the plate thickness d_0 tends to zero

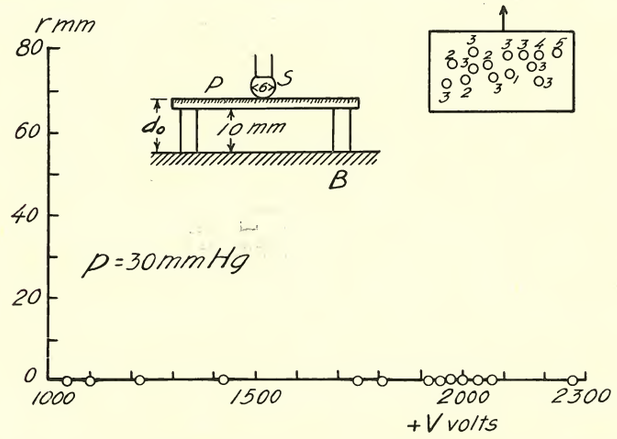

Fig. 17. Range r of positive figures from a spherical electrode. Thickness d_0 of insulating medium 11.4 mm. Experimental points marked by small circles. The figures at the experimental points denote the number of spreaders.

(see L. F. I fig. 34) suggests such an explanation. To elucidate this behaviour we have among others made the test shown in fig. 17.

The spherical electrode rests as usual directly on the film of the photographic plate P which, however, does not rest directly on the earthed plate B, but is raised 10 mm by means of the ebonite blocks shown. In this case the vertical field beneath the electrode will not be very strong, and, as expected, we find that under these conditions the spherical electrode gives either no discharge at all or

forms comparatively very long spreaders as with the sharp-edged electrodes[1].

We have also investigated whether the design of the discharge key may influence the starting of the figures. Among others we have tried ordinary discharge keys and also mercury vacuum keys which in other respects show very special behaviour[2]. We have, however, not been able to ascertain any difference in the effect of the various keys.

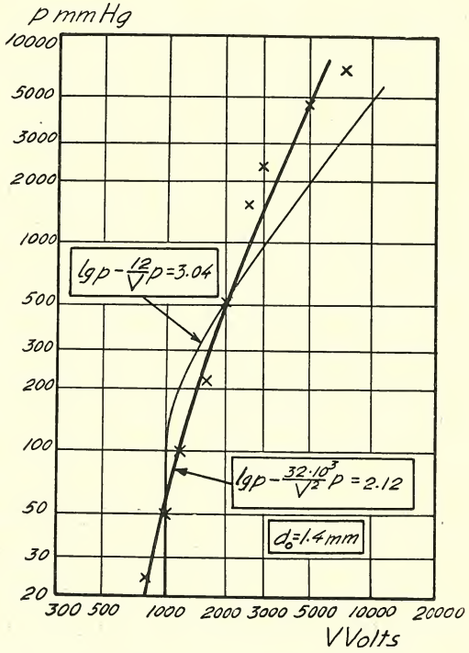

Fig. 18. Corresponding critical values of pressures p and $p.d.$ $V.$

From the foregoing it appears that it is not possible to state with any great certainty the maximum air pressure at which a given potential may start a discharge, or conversely, at what minimum potential a discharge may be started at a given air pressure. The uncertain or fortuitous nature of the formation of figures

[1] The ranges represented by the points in the square frame are really greater than stated but the full range could not be determined as the figures — when discharges were started at all — passed beyond the edges of the photographic plates.

[2] P. O. Pedersen: Videnskabernes Selskabs Math.-fys. Medd. IV, Nr. 5, 1922. — Proc. Inst. Radio Eng. Vol. 13, p. 215—243, 1925.

within the critical interval prevents a true determination of a (p, V)-curve for this critical transitory interval. It is possible, however, on account of the large amount of experimental material available, to fix fairly correct corresponding values of p and V within the critical interval. Such sets of values are marked with crosses in fig. 18 for values of p from 22 to 7000 mm and of V from 700 to 7000 volts. We shall subsequently take up a discussion of this figure.

So far we have only considered "clean" electrodes but we have found that within the critical interval the formation of positive figures is independent of whether the electrodes are clean or slightly greased (unclean). Corresponding tests with negative figures show that these are formed much more easily from "clean" than from unclean (slightly greased) electrodes.

4. The Conductivity and the Spreading-out-Conditions of the Positive and Negative Figures.

There is a very pronounced difference in the manner in which the positive and the negative spreaders conduct electricity and in their ability to promote and initiate spark formation.

To elucidate this behaviour we have made the experiments described in the following.

(a) Conductivity of Positive and Negative Spreaders.

As soon as the edge of a negative figure reaches an outer electrode, a spark will pass between the two electrodes even where the outer electrode comes only very

slightly inside the final range of the figure; see for example plate 26, parts I—IV. The spark discharge brings the two electrodes to a nearly equal potential.

In the case of positive figures, spark formation occurs only when the outer electrode comes far inside the range of the figure; see for instance plates 14 II and 15 I—II and also "L. F. I" figs. 45—50, L. F. II fig. 18 and "A. d. Ph." fig. 18. These relations were previously observed by U. Yoshida[1] and are also mentioned in "L. F. II" p. 22 and "A. d. Ph." p. 220.

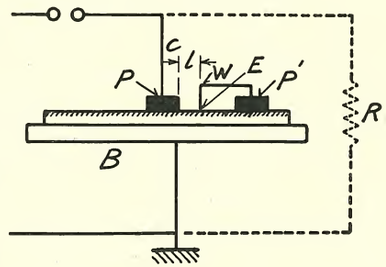

Fig. 19. Diagramatical representation of the electrical connections used in the experiments referred to in fig. 20 and in plate 12, parts I—VII.

For the further investigation of these relations, we have made among others the following experiments: Besides the usual electrode P, see fig. 19, a free electrode P' was placed on the film of the photographic plate. From P' a metal wire W is run to a point E of the film distant l from P. An account of the experimental results is given in fig. 20, parts III—V, and here are also shown the shapes of the electrodes employed, parts I—II. In part III the abscissa shows the ratio $\frac{l}{R}$, where l is the distance from the end E of the wire W to the electrode P, and R is the length of the spreaders from this electrode. The ordinate shows the ratio $\frac{R'}{R}$ of the spreaders from P and P' and for the positive figures also the ratio $\frac{n'}{n}$ of the number of spreaders from P' and P respectively.

[1] U. Yoshida: Mem. Coll. Sc. Kyoto Imp. Univ. Vol. II, No. 2, p. 115—116. 1917.

From parts III—V it appears that the conditions are essentially different for positive and negative figures with

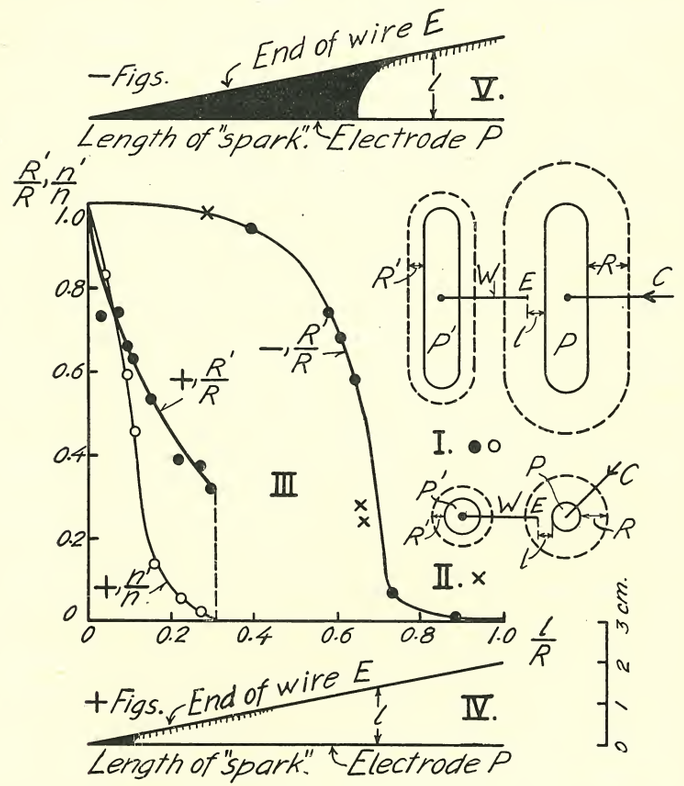

Fig. 20. Conductivity and sparking within positive and negative figures. In parts IV and V the black portions indicate that sparking has taken place. Air; $p = 760$ mm. Hg.

regard to conductivity and spark formation. With negative figures, pronounced spark formation occurs between the end E of the wire W and the electrode P when $\frac{l}{R} < 0.65$, and the ratio $\frac{R'}{R} > 0.9$ as long as $\frac{l}{R} < 0.5$. Not until

$\frac{l}{R} > 0.7$ does R' attain very small values and still at $\frac{l}{R} = 0.8$ to 0.9, R' has not decreased quite to zero. For positive figures conditions are entirely different. Here the formation of figures from P' stops completely when $\frac{l}{R} \cong 0.3$, and sparks are only formed when $\frac{l}{R} < 0.12$. Further the value of $\frac{R'}{R}$ decreases quite rapidly with increasing values of $\frac{l}{R}$ so that $\frac{R'}{R}$ has gone down to about 0.3 at $\frac{l}{R} = 0.3$ while for negative figures $\frac{R'}{R}$ remains nearly constant ($\cong 1$) up to $\frac{l}{R} = 0.4$.

In plate 12, parts I—VII, are reproduced some figures taken with the electrode arrangement shown in fig. 20, part I, though they only show the conditions existing near the end E of the wire W. (In these pictures the electrode P is placed to the left of E). From these pictures it appears that the spark formation is started at E, see for example plate 12, parts I and V, and 13 II. This relation is indicated schematically in fig. 20, parts IV and V.

From fig. 20, part III, it thus appears that "negative" sparks formed in this manner have a comparatively high conductivity, since the subsidiary figure starting from P' has nearly the same range as the one from P, as long as $\frac{l}{R} < 0.5$. Contrary to this the conductivity of the "positive" sparks is comparatively small, since both the length and the number of spreaders decreases very rapidly with increasing values of $\frac{l}{R}$ even at very small values of this quantity. A comparison of parts III and IV, fig. 20, on the other hand, shows that positive spreaders may allow a certain passage of electricity without the formation of a spark, since under these particular circumstances positive

sparks are only formed when $\frac{l}{R} < 0.12$ while the subsidiary figure does not fail to appear until $\frac{l}{R} > 0.3$.

Fig. 20 at all events shows that both conductivity as well as tendency to spark formation is much smaller for positive than for negative figures.

(b) Influence of the Duration of the Pulse upon the Positive and the Negative Spreaders.

A corresponding difference of very pronounced character is found in another connection, namely the manner in

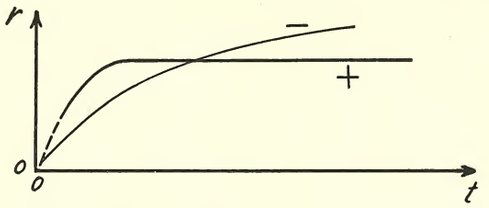

Fig. 21. Schematical representation of the range r of positive and negative figures as functions of the duration t of the *p. d.*

which the positive and the negative figures behave when exposed to potentials of comparatively long duration. This may be varied f. inst. by varying the length L_0 of the lead to the electrode from which the figure starts, L_0 being reckoned from the condenser C fig. 1. The longer L_0 is, the longer will the electrode be subjected to the potential. This point has already been investigated in "L. F. I" p. 32 (figs. 36 and 37). It is found that the radius of the negative figures increases with increasing length of the wire L_0 — at all events for lengths of wire up to about 25 m — as shown in fig. 21. This ability of the negative figures to grow larger is also illustrated in plate 28, part II. The needle-shaped Lichtenberg electrode in the diagram (part III)

denoted by K, is first exposed to the potential corresponding to the spark length L of the spark gap shown. A surge travels out along the open line 8 m long and the *p. d.* is nearly doubled by reflection at the end. The Lichtenberg gap K is consequently exposed to a *p. d.* corresponding to the spark length L during $\frac{16}{3 \cdot 10^8} = 5.3 \cdot 10^{-8}$ sec. after which the *p. d.* momentarily increases to about the double value. In the negative figure, the growth of which had

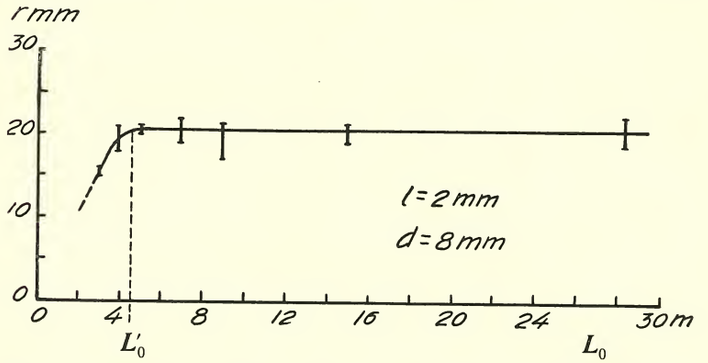

Fig. 22. Range r of positive figures as a function of the length L_0 of the connecting wire. (All experimental determinations of r fall within the heavy vertical lines shown).

practically ceased after the lapse of $5.3 \cdot 10^{-8}$ seconds at the lower *p. d.*, this is evinced by a continued growth under the influence of the higher *p. d.* A darker ring in the figure marks clearly the boundary between the original and the subsequently formed part of the figure. It is clearly seen that the increased growth occurs exclusively as a continuation of the original spreaders.

We shall see later that positive figures formed under similar conditions behave entirely differently; they have already attained their full range at $L_0' = 4.5$ m, as appears

from fig. 22, which shows the results of experiments carried out recently.

If we assume the *p. d.* in the wave front to increase gradually from zero to its maximum value V_0 over the length L' of the wave front, then the time τ during which the Lichtenberg gap is exposed to the maximum *p. d.* $2V_0$ will be determined by

$$\tau = \frac{2L_0' - L'}{3 \cdot 10^{10}} \text{ sec.,} \qquad (1)$$

L_0' and L' being measured in cm and assuming the capacity of the Lichtenberg gap to be negligible.

If we assume the range of the positive figures to depend only on the value of the maximum *p. d.* and to be entirely independent of its duration then, according to (1), the length of the wave front must be determined by $L' = 2L_0' = 9$ m.

If, on the contrary, the wave front were perfectly steep i. e. $L' = 0$, then a value of $\tau = 3 \cdot 10^{-8}$ sec. would correspond to $L_0' = 4.5$ m.

Actually L' must have a finite length and the duration τ_0 of the maximum *p. d.* necessary for the positive figures to attain their full range must thus have its value between

$$0 < \tau_0 < 3 \cdot 10^{-8} \text{ sec.} \qquad (2)$$

If the value of L' is known, then τ_0 may be determined by means of (1), but this question we will return to elsewhere.

(c) Irregular Figures caused by Pulses of long Duration.

Beside the regular, simple figures mentioned, there will, however, be formed other peculiar figures if the *p. d.* is maintained for a sufficiently long time. In this respect too positive and negative figures show great differences.

In the negative figures the discharge tracks formed when the *p. d.* is maintained long enough will follow the already formed negative spreaders. In no case have we observed such discharge tracks in the spaces between the original spreaders. Plate 27 shows some enlarged reproductions of negative discharge tracks; they mainly follow the centre line of the spreader concerned, but many show some smaller irregular bends. In some cases they may jump from one spreader to another. Such a case is seen in part VI. Here the spreader in which the discharge track starts is very short and separated from its neighbours by narrow and little ionized spaces. If the discharge track followed this spreader, it would find areas having little pre-ionization, and it is therefore found easier to jump to one of the neighbouring spreaders and then to continue along this. It is such jumps which form the sharp bends in the negative spark tracks, see f. inst. plate 26, part I and L. F. I fig. 5.

These discharge tracks will develop into sparks if the *p. d.* is maintained somewhat longer, but if a spark has been formed, the light from it will generally blur the figure and make it impossible to discern the details of the L. F. which existed before the formation of the spark.

From plate 27 it appears that the negative discharge tracks are very narrow.

With positive figures the conditions are entirely different. If the positive *p. d.* is maintained for some time, a new figure is often formed with its spreaders — trunks as well as branches — fitting themselves in proper order into the spaces between the trunks and branches of the first figure.

The new figure, figure no. 2, may, according to circumstances, pass beyond the boundary of figure 1, but it may also stop earlier.

An example is shown in plate 28, part I. This figure is taken under conditions quite analogous to those obtaining for the formerly mentioned negative figure shown in part II. Under the influence of the *d. p.* corresponding to the spark length L the figure has reached its full range (corresponding to this *p. d.*), within the $5.3 \cdot 10^{-8}$ sec. during which this potential was maintained. The outer boundary of the corresponding regular figure is marked by the drawn circle. The maintaining of the *p. d.* during the time mentioned, and its further increase for a short space of time has caused both some special discharges around and near the electrode, and also the starting of a number of new spreaders, which have had to "squeeze" themselves out between the original spreaders as is clearly recognised in the figure. Many of these subsequently formed spreaders have a greater range than those first formed.

The particular discharge phenomena which take place directly at the electrode will be treated of later.

At low pressures figure number 1 will often cover practically the whole surface, particularly after it has passed a little away from the electrode. In that case figure number 2 is not easily formed. Under especially favourable conditions, figure number 2 may be formed even down to a pressure as low as 150 mm. An example is shown in plate 6, part III. This figure shows clearly 2 sets of spreaders: a set of shorter ones which was formed first and a set of longer ones formed afterwards. That the order of formation is as stated may be inferred with certainty from the form of the spreaders, since the trunks and the branches of

figure no. 2 "squeeze" themselves into the spaces between the trunks and branches of figure no. 1.

From the tracks followed by the trunks and branches of figure no. 2, it appears clearly that the trunks and branches of figure no. 1 were present with a sharply localized positive charge at the moment when figure no. 2 was formed. On the other hand, the spreaders of figure no. 1 cannot have possessed ability to conduct to any greater extent at the moment in question, since, if they had, they would simply have continued to grow in length because the field would then be strongest at their tips. The new spreaders start directly from the electrode in the spaces between the former ones, although the electrical conditions here are very unfavourable for a start because the existing charge on the first spreaders reduces the field at the starting points.

At atmospheric pressure this phenomenon is produced very easily and examples of such are given in plate 10, part III, plates 16 and 17. In these figures a, b, c ... mark spreaders of figure no. 1 while a', b', c' ... refer to figure no. 2, a'', b'', c'' to figure no. 3 and so on. On plate 17 4 successive discharges are clearly seen.

Beside this number of successive Lichtenberg discharges, another kind of positive discharge, essentially different from the Lichtenberg ones, will occur if the positive potential is maintained for a sufficient length of time. For instance, it has not their regular and sharply defined forms but is of a blurred character, while it has a higher brilliancy and has no well defined range, but spreads out further the longer the potential is maintained. Such discharges are seen near the electrode on plate 9, part I

(especially at the electrode A_2), plate 16, parts II and IV, plate 17, plate 18, part II, and plate 20 II.

This positive discharge, (which is of a kind quite different to the Lichtenberg discharges, and will be treated of elsewhere in connexion with the question of spark formation) develops into highly luminous positive spark tracks if the *p. d.* is maintained long enough, and such sparks are shown schematically fig. 3 and examples of actual figures are shown plate 3, part I, plate 7, plate 11 I and IV and L. F. I fig. 4.

This discharge form must not be confounded with the previously mentioned flow of negative electricity from the electrode out along the positive spreaders, which often occurs when the discharge is so slightly damped that oscillations take place in the discharge circuit; see above under 1 (d).

Comparison shows that the character of this subsequent negative discharge is entirely different from the irregular positive discharge just mentioned: The negative flow occurs only out along the already positively charged spreaders, while the spaces between them remain untouched. This is not so in the case of the positive discharge. The boundary of the subsequent negative discharge is fairly sharp; this, also, is not the case with the positive one. The irregular positive discharge is often the starting base for the Lichtenberg discharges no. 2, 3 ....

Very often subsequent negative discharges and irregular positive discharges appear in the same figure, giving the innermost part of the figure a highly luminous and irregular appearance; see plate 9, part I (especially electrode A_2), plate 16 IV and 20 II.

It is of importance in this connexion again to emphasize that neither the subsequent negative nor the irregular positive discharges are necessary parts of the positive Lichtenberg figures; they are only complications which have nothing to do with the regular L. F., and which may easily be avoided by suitable arrangements, see thus plate 1, part V, plates 4, 5, 14 II, 22 and 23.

U. Yoshida[1] seems to consider both the subsequent negative discharge and the irregular and comparatively slow positive discharge as a normal and essential part of the positive Lichtenberg figures, in that he assumes the manner of formation to be somewhat different for the inner and for the outer part of the figure. Thus he says in his paper (b) p. 315: "In the anode figures (Fig. 3 and 13 of the former paper) we notice that every branch consists of two parts; namely a more intense portion near the electrode, and a weaker portion more removed. When a celluloid film is used instead of a common photographic plate, these two portions are more clearly distinguishable as seen in fig. 18 of the former paper, and fig. 1 of this paper, the ends of the intense portions of the branches terminating with a continuous outline".

That the subsequent negative discharge should in the latter case be predominant over the positive one is fully in agreement with the explanation we have given of the phenomenon in section 1 (d) above.

It is emphasized above that we cannot agree with U. Yoshida on this point.

(d) Resumé.

The results set forth above may be briefly summarized as follows:

[1] U. Yoshida: (a) Mem. Coll. Sc. Kyoto Imp. Univ. Vol. II, No. 2, p. 115—116, 1917. — (b) l. c. No. 6, p. 315—319, 1917.

For negative figures the range increases with increasing duration of the *p. d.* and, when the *p. d.* is maintained for a sufficient length of time, spark tracks will be formed along and inside the original spreaders — but never in the spaces between them. These spark tracks begin as fine threads with a somewhat irregular course.

For the positive figures the range of the first formed figure is independent of the duration of the *p. d.* — at all events when its value exceeds $3 \cdot 10^{-8}$ sec. If the *p. d.* is maintained long enough, there may be formed a new positive figure having a range greater or smaller than that of the first one, and in which the spreaders of the new figure fit themselve into the spaces between the spreaders of the first figure.

If the *p. d.* is maintained still longer, irregular positive spreaders, of a kind entirely different to Lichtenberg ones, may be formed. From these irregular positive spreaders there may be started new Lichtenberg spreaders which then fit themselves into the spaces between those already present.

5. Various Questions relating to the Formation of the Lichtenberg Figures, especially the Positive ones.

(a) Influence of Initial Ionization.

In order to solve the question of how positive figures are formed, it is most essential to know what influence an ionization within the area to be covered by the figure may have upon the formation and appearance of the figure. To show the importance of this question we may cite the

following extract from U. YOSHIDA[1]: "If the potential of the anode is increased sufficiently, the negative ions, which were present just before the formation of the photographic impression by the ionisation commences, will be pushed toward the portions of the electrode where the electric force is strong, and will ionise the gas molecules with which they collide. The negative ions thus produced will also do the same thing; and many positive and negative ions will be produced. The group of positive ions, which will be left behind as negative ions are pushed toward the anode, will now act as a portion of the anode; and, repeating the same process as before, further branching and elongation of the anode branch will take place. With this explanation, the properties of the anode branches (that they are irregular in their branchings and elongations, and that their branches end in sharp points) will be immediately understood; because the formation of these branches is due to the presence of negative ions which would be distributed irregularly".

We have therefore made this question the subject of a fairly thorough investigation, the result of which was that in no case were we able to ascertain any influence of an existing ionization on the formation of the regular positive (or negative) figures — setting aside such unimportant cases in which the conductivity became so large that the electric fields, determining the course of formation, were liable to considerable distortion.

In the following we shall describe some of these investigations. Plate 16, I shows the result of such a test. Immediately prior to (10^{-6} sec. before) the formation of

[1] U. YOSHIDA: l. c. (a), p. 113.

the positive figure shown, the spot S was illuminated by a strong spark. By this means a strong ionization is caused photo-electrically within the area of the spot, which ionization cannot have vanished entirely before the figure was formed, and consequently the ionization within the spot must have been very much stronger than outside. In spite of this no influence of the ionization on the course or the appearance of the spreaders is to be observed.

Against the validity of this test it may possibly be said — although in our opinion unjustly — that the ionization is located at a place in the middle of the positive spreaders where the spreading out of these is going on with great strength and speed while the influence of such an ionization may be expected to be particularly obvious at the ends of the positive spreaders. Plate 10 III therefore shows the result of another test where the ionized spot A is located at the tips of the spreaders e' and f', but the presence of the ionized spot had also in this case no influence upon the form and course of the spreaders.

We have further investigated the formation of figures over an area where a strong ionization takes place simultaneously with formation of the figure. The results of a couple of these tests are shown in plate 10 I and II. Here the ionization was effected by means of a powerful Radium preparation resting a few millimeters above the photographic plate during the formation of the figure. The action of the radio-active rays was in the main confined to a limited area by means of shielding. The pictures show the ionized portions to be rather intensely luminous but it is also clearly seen that there is no difference in the formation of the positive figure inside and outside the ionized part of the plate.

An ionization by collision of the character mentioned by U. Yoshida, but in which the active negative ions are no doubt mainly electrons, may be brought about in various ways of which a few will be mentioned in the following.

With the arrangement shown in fig. 23 a series of pictures has been taken the general character of which appears from plate 6 II. The distance between the electrodes A_1 and A_2 is chosen so that the positive and the negative spreaders only just meet one another. Plate 13 I shows an example of this. As the positive and the negative discharge here take place exactly simultaneously plenty of free electrons will be present at the outer ends of those positive spreaders which reach over — or nearly over — to the outer ends of the negative spreaders. An ionization by collision will then occur at this place, as the positively charged tips of the positive spreaders will attract the free electrons with great strength. But the pictures show clearly that the discharge tracks thereby formed have a character altogether different to that of the positive spreaders[1].

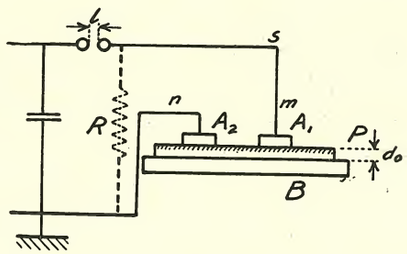

Fig. 23. Arrangement for simultaneous registration of positive and negative figures on one photographic plate. The metal plate B is insulated.

These discharge tracks go partly directly from the ends of the positive to the ends of the negative spreaders, and partly they connect the ends of neighbouring positive spreaders. The outer ends of a few of the positive spreaders have

[1] This feature is already mentioned in L. F. I, figs. 62 and 63.

apparently been bent by the electric field towards the nearest part of the negative figure.

Plate 24 I—IV shows enlarged portions of similar figures taken at atmospheric pressure. We see also here that the presence of a strong ionization, (in which, no doubt, there are a great number of free electrons), may be the cause of discharge tracks starting from the ends of the positive spreaders, but also that these discharges are not similar to regular positive spreaders. We will come back later to the formation and appearance of these discharge tracks; see appendix 3.

Similar conditions are found in the pictures shown in plate 18 I—II. In part I the positive spreaders go far into the area of the negative figure but in spite of this they fully preserve their character. In part II a positive discharge is subsequently started from the negative electrode and the course of this discharge is determined mainly by the electric force from the electric charge in the negative figure. (The same applies to the subsequent positive discharge in the negative figure shown plate 25 I. In these cases also the positive spreaders preserve their typical character.

In very many cases ionization by collision occurs by mutual action between the positive spreaders. This is thus the case in plate 18 I at the points marked 1—9. See also plate 14 I and II which are taken with the apparatus disposed as in fig. 24 — the same as fig. 43 in L. F. I.

In plate 14 I this ionization by collision occurs especially in such places where, after the formation of the positive spreaders, a strong electric field arises at right angles to their direction of propagation. In part II these discharges occur especially at the meeting line of the two figures.

The same applies to the ionization by collision in the neighbourhood of the meeting line of the positive figures on plate 15 I and II.

In all cases where such ionization occurs, the discharge has a character essentially different

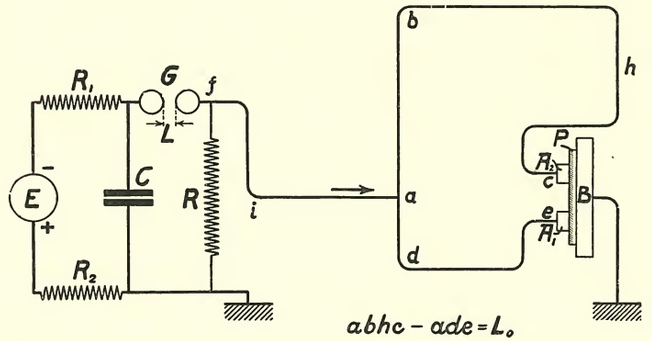

Fig. 24. Arrangement for determining the spreading-out-velocity of the Positive Figures.

to that typical of the positive Lichtenberg spreaders — to mistake the one for the other is impossible.

(b) Influence of Strong Simultaneous Ionization.

If a great number of electrons are set free at the same time and place as that at which spreaders are formed, then a very peculiar phenomenon occurs which we will examine a little more closely. Such a release of electrons may be effected by illumination of the photographic plate by an intense electric spark, preferably of short duration, since the plate will be blackened too much if the spark lasts too long. The number of electrons released will also only increase with the duration of illumination during a very short time interval, as the released electrons are for

the greater part captured within 10^{-6} sec. by oxygen or water molecules, or the like, thus being[1] transformed into heavier, less active, ions, whose number will further decrease very rapidly owing to recombination between positive and negative ions.

The most simple experimental method is to apply a spark potential so high that a spark will pass from electrode A to the metal plate B below, see fig. 1. Another equally simple method is to let a spark pass between the electrodes A_1 and A_2 in fig. 23. In plate 11, I and IV show a few examples produced by the first method, II and III by the second. We will first examine the second. In that part of the photographic plate which is exposed to light from the spark, the positive spreaders are surrounded by a "soft", comparatively intensely luminous "veil" or rim, while those parts which are in the shadow have the normal appearance. The results are exactly similar in the first named case where the spark passed between the electrode A and the metal plate below. Part I shows such a picture taken in atmospheric air; part of the positive spreaders have here become strongly distinguished by the very strong rim-formation. Part IV shows a similar discharge in oxygen and is even more significant, since in this case the positive Lichtenberg discharges themselves are so faintly luminous that they cannot be photographed, see p. 16 above. But here they appear very distinctly owing to the strong rim-formation although the latter is weaker than in atmospheric air. This smaller intensity is caused by the fact that negative figures which are formed by ionization by collision are also less luminous in oxygen

[1] P. O. Pedersen: "Propagation of Radio Waves". Copenhagen 1927 (Fig. IV 7, p. 46).

than in atmospheric air. With negative figures — see parts II and III — a luminous ring appears a little outside the photographic boundary of the figure.

The luminous edges around the positive spreaders are caused by ionization by collision, which takes place in the strong fields immediately outside their boundary owing to the presence of numerous free electrons which may instantaneously start such ionization. We shall see later that there is reason to assume that the positive charge is of about equal intensity over the entire cross-section of positive spreaders. The electric field is therefore strongest at the very edge. The fact that the light intensity is greatest here is in good agreement with this.

In case of negative figures the outer boundary is not quite sharp, for, as stated before, the photographic intensity decreases gradually towards zero. We shall show later that there is reason to assume that the negative "electric" figure, a very short time after its formation, is slightly larger than the photographic figure, and that the charge-gradient is steepest at the edge of the "electric" figure. Consequently the strongest field and the most luminous rim is also found here.

It is thus possible fully to explain the source of these luminous rims. The foregoing discussion further shows that the figure formation — positive as well as negative — proceeds in the normal manner in spite of the presence of a great number of electrons and ions, while the luminous rims are caused by ionization by collision analogous to that which U. Yoshida and others assume to be the cause of the formation of the positive spreaders. But the discharge caused by this ionization by collision

has, as appears from the positive pictures, a character entirely different to that of the positive spreaders.

U. Yoshida[1] has also treated this rim effect but has only tried to find an explanation in accordance with the one given for "dark sparks" ("dunkle Funken") i. e. founded on the Clayden effect[2], but he comes to the conclusion: "that the phenomenae observed are not photographic reversals of any kind ever known" (p. 319), which result is at all events not in contradiction to the one arrived at by us.

Some of the features touched upon in the preceding part are also treated rather more thoroughly in Appendix 3.

(c) Influence of Various Irregularities in the Photographic Film.

We have also investigated the effect of various irregularities prepared in or on the surface of the photographic film over which the positive figure spreads out. For example, plate 10 IV shows a case in which thick, electrically non-conducting ink lines were drawn over the film. They do not appear to affect the spreading-out of the figure. Plate 9 II shows the effect of some pencil lines over the film. It is clearly seen from the appearance of the figure at line 2 that this line is a fairly good conductor. On the other hand the positive points ending near line 1 are perfectly normal, proving that a considerable conductivity produced in this way has no effect on the formation of the positive spreaders, as long as these do not come into contact with the conducting lines.

[1] U. Yoshida: l. c. (b).

[2] With reference to the formation of these "dark sparks" see P. Metzner (Verh. d. D. phys. Ges. Bd. 13, p. 612—616, 1911). Extraordinary beautiful samples of such dark sparks are found in Lord Armstrong: "Electric Movement in Air and Water", plates nos. 18 and 34 (London 1899). With regard to an explanation of these dark sparks on the basis of the Clayden effect we may refer to R. W. Wood (Phil. Mag. vol. 6, p. 577—590, 1903), K. Schaum (Verh. d. D. phys. Ges. Bd. 13, p. 676—679, 1911) and to M. Volmer und K. Schaum (Zeitschr. f. wiss. Phot. Bd. 14, p. 1—14, 1914).

(d) Ionization and Negative Discharges.

In the preceding paragraphs we have mainly treated only the spreading-out-conditions of the positive figures. The formation of negative figures is also, however, within very wide limits, independent of an existing ionization. Our reason for not entering much into this question is that we consider the formation of the negative figures as already fully explained in L. F. I.

As the main result of the investigations described and referred to in this section, we may set forth the conclusion that the formation of regular Lichtenberg figures is independent within very wide limits of the intensity of an existing ionization.

CHAPTER IV

The Formation of the Positive Figures.

A. Preliminary Discussion of various Hypotheses.

At the outset various possibilities can be assumed for the process of formation of positive figures, and several hypotheses to this effect have already been set forth[1]. However, in our opinion at least, none of the hypotheses already advanced can be brought into agreement with the experimental results. In this section we will give a brief account of the reasons which have led us to this view; in section *B* we will then give an account of the hypotheses we have arrived at through our investigations, and we shall here have occasion to give further reasons why we cannot accept the older hypotheses.

1. Formation of Positive Figures as due to Positive Ions moving away from the Electrode.

The process of formation of positive figures may be assumed to proceed analogously to the formation of the

[1] With regard to the various hypotheses for the formation of Lichtenberg figures see L. F. I chapt. I—II and K. Przibram: "Die ionentheoretische Deutung der elektrischen Figuren", Handb. d. Physik. Bd. 14, p. 402 ff. 1927.

negative ones, except that here positive ions, and not electrons, are moving outwards from the electrode, and by ionization by collision produce the necessary number of new positive and negative ions and electrons, the positive charge of the figure being mainly due to the movement of the latter towards the electrode.

The active positive ions may be either ordinary atomic or molecular ions, corresponding to the particular gas in which the discharge takes place[1], or they may be H^+-particles (Protons).

If positive figures were formed in this manner, then (α) their appearance should in the main features agree with that of the negative ones[2], (β) the relation between the spreading-out-velocity and the thickness d_0 of the plate should in the main be the same for positive and for negative figures, and finally (γ) the spreading-out-velocity should be considerably smaller for positive than for negative figures.

In chap. III it is, however, shown that none of these consequences are in agreement with the facts, in fact the spreading-out-velocity is even considerably greater for positive than for negative figures. In section *B* of the following it will further be shown that the spreading-out-velocity of the positive discharges is so great that the figure formation cannot take place in the manner here considered.

[1] Also S. Mikola (Phys. Zeitschr. Bd. 18, p. 161. a. f. 1917) seems mainly to have this view, though he considers both "Die korpuskulare Strahlung des Kondensators" and further "Die impulsive Strahlung des Kondensators" as active in the formation of figures and the second of these rays he considers to have electro-magnetic character.

[2] We have been unable to feel convinced by the reasons given by K. Przibram (l. c., p. 403) for the great difference in appearance between the positive and the negative figures on the basis of this hypothesis.

2. Formation of Positive Figures due to Negative Ions (Electrons) moving Inwards to the Electrode.

The formation of positive figures could also be assumed to proceed in the following manner: Negative ions from the outer edge of the figure are drawn inward towards the electrode, the necessary number of negative ions being produced by ionization by collision at the outermost ends of the spreaders. The positive charge on the figure is also in this case in the main due to the negative ions moving toward the electrode.

Here again there are several possibilities, in that the ionization by collision may be initiated either (α) by means of the (natural) ionization present in the air directly in front of the outer edge of the figure while this is being formed, or (β) by means of ionization by collision initiated by some positive particles driven out of the tips of the positive spreaders by the electric field.

(α). U. Yoshida is — as mentioned in chap. III 5 (a) — a follower of the first one of the here named theories. But since the experiments discussed in chap. III 5 (a) and (b) show that the circumstances of formation and the appearance of positive figures are independent within very wide limits of an initial ionization either previous to or simultaneous with, the formation of the figure, we cannot suppose the figures to be formed in the manner set forth under (α).

But even setting aside the said experiments — which we indeed consider as conclusive — the hypothesis set forth under (α) would meet with a number of difficulties. It would thus be difficult to give a satisfactory explanation

of the very marked difference in appearance of the positive and the negative figures, of the difference in their spreading-out-velocity and initial conditions and of the dependency of the range on the plate thickness. Further, it would be difficult to explain the sharp boundary lines found, and the fact that the width of the positive spreaders is inversely proportional, and their number directly proportional, to the applied air pressure.

Completely decisive for the dismissal of this hypothesis are also the examples given in chap. III 5 (a) and (b), which show that even though such suction or drawing in of negative ions (or electrons) may occur under particular conditions, the discharge-tracks thereby formed have a character entirely different from that of the positive spreaders.

By this means we have, in our opinion, proved the untenability of the hypothesis in question.

(β). There remains now only the hypothesis mentioned under (β), which we shall subject to a more thorough discussion.

B. Theory of the Positive Figure according to the Hypothesis 2 (β).

0. Further Specification of this Hypothesis.

The foremost positive particle p^+, see fig. 25, is assumed to travel with the velocity U in the front of the positive spreader Q_+. The foremost particle has a sufficiently high velocity to act in a strongly ionizing manner, and releases a considerable number of electrons, indicated by dots in fig. 25. These electrons are pulled toward the tip of the spreader by the very strong field existing here, and on

their way they release by collision a further large number of electrons, which are then pulled towards the electrode by the field along the spreader.

In this manner the strong electric field will automatically follow the foremost particle. The field strength at the

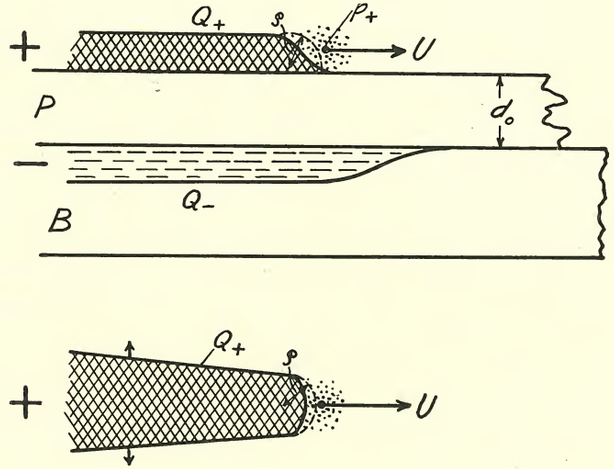

Fig. 25. Schematical Representation of the conditions at the Tip of a Positive Spreader. *P* is the photographic Plate, *B* the earthed metal Plate, see fig. 1.

tip of the spreader cannot be directly measured, but its approximate value may be estimated by the following considerations.

Assuming the *p. d.* between the positive electrode and the grounded plate *B* to be 15 000 volts, this will correspond to a spark length of about 2 mm. A drop in potential will, however, occur out along the positive spreader, and the potential at the tip of the spreader at the moment in question is assumed to be 9 000 volts. It is further assumed that the outermost tip has a spherical shape with a radius ϱ cm. The foremost particle p^+ at a distance $(\varrho + \Delta\varrho)$

from the centre of the spherical spreader tip will then be exposed to an electric field $E_{\varrho+\Delta\varrho}$ which may with approximation be put equal to

$$E_{\varrho+\Delta\varrho} = \frac{\varrho}{(\varrho+\Delta\varrho)^2} \cdot V_0, \tag{1}$$

which for $\Delta\varrho = 0$ reduces to

$$E_\varrho = \frac{1}{\varrho} \cdot V_0. \tag{2}$$

If the front particle is inside the spherical part and the charge density is assumed to be constant, then the field at a distance $(\varrho - \Delta\varrho)$ from the centre will be determined by

$$E_{\varrho-\Delta\varrho} = \frac{\varrho-\Delta\varrho}{\varrho^2} \cdot V_0. \tag{3}$$

If, on the other hand, the total charge is located on the surface of the sphere, we have

$$E_{\varrho-\Delta\varrho} = 0. \tag{4}$$

$E_{\varrho-\Delta\varrho}$ will in general have a value somewhere between those determined by (3) and (4).

$E_\varrho = \frac{V_0}{\varrho}$ is thus the highest value attainable for the field intensity.

If $E_{\varrho+\Delta\varrho}$ at a given moment is greater than the field value E_U, necessary to maintain the velocity U of the front particle, then this velocity will increase. The distance $(\varrho+\Delta\varrho)$ will thereby become greater, but this is again — according to (1) — followed by a decrease in the field intensity.

If, on the contrary, $E_{\varrho+\Delta\varrho} < E_U$ the velocity of the particle will decrease but the distance $\varrho+\Delta\varrho$ will thereby also be decreased and $E_{\varrho+\Delta\varrho}$ will consequently increase. From this it appears that the particle will adjust itself to

a distance where the field intensity and the velocity have corresponding values.

This, however, assumes that

$$E_\varrho = \frac{V_0}{\varrho} > E_{U_0}, \tag{5}$$

where U_0 is the smallest velocity at which the front particle can be controlled in the manner referred to.

The positive front particle will in fact almost, or possibly completely, lose its ionizing ability if its velocity decreases below a certain value, see App. 1, sections 6 and 7. At this limit the strong ionization at the tip will cease and the intensity of the electric field in which the front particle is located will become much weaker. The particle will then lose its velocity within a very short distance. This process will actually already have set in at a velocity at which the particle still possesses some ionizing ability, and the critical value of U_0 will therefore be so high that considerable ionization still takes place. The actual value of U_0 cannot, however, be calculated beforehand, though such a limiting value no doubt exists.

The front particle may, however, be brought to a standstill by another cause. It will not always contain a positive charge but will sometimes be positive and sometimes neutral, as is well known from investigations of positive rays and other high-speed positive particles, see App. 1. If we call the distance travelled by the particles in a charged state l_1, and the distance travelled in a neutral state l_2, then we know from experience that the ratio $\frac{l_1}{l_2}$ decreases with decreasing velocity. This ratio seems, however, especially in cases where the positive particle is a proton, to approach a limiting value which does not

further decrease with decreasing velocity, see for example fig. 2 in App. 1. These relations are, however, not quite certain, compare App. 1, section 6.

The deduced values for the ratio $\frac{l_1}{l_2}$ are at all events only valid for the average values of these distances, and the actual distances may show very considerable differences. If the particle travels 10^{-4} cm without charge, then it will decrease considerably in velocity. If it has been retarded so much that it has come inside the strongly charged spherical front, then the field intensity drops so considerably that the particle, even if it becomes positively charged again, has only very little chance of regaining the necessary velocity; if it does not, it will be drawn back and more into the charged sphere, and completely lose its velocity.

In both of the above described cases the front-ionization ceases and the growth of the positive spreader stops. The strong electric field at the tip decreases simultaneously because the positive charge is spreading out, although comparatively slowly, by which means V_0 decreases and the radius ϱ increases. The drop in V_0 is due to the spreading out of the positive electricity available over a larger area, and as no perceptible ionization now occurs at the tip, no negative electricity is carried away toward the electrode. V_0 must therefore decrease.

We shall now proceed to give a more detailed explanation of the characteristics of the positive figures mentioned in chap. III, but we may remark here that in part 2 of the following we are led to the assumption that the positive front-particles are protons.

1. Differences in Shape of Positive and Negative Figures.

(a) Width of Positive Spreaders.

The width of the positive spreaders is, as was shown in chapter III 1 (a), inversely proportional to the air pressure p[1].

Immediately after the passage of the front-particle the spreader will be very thin and this the more so the smaller is the velocity of the particle. This primary ionization channel is strongly positively charged, because part of the electrons set free through the ionization by collision in the tip of the channel are drawn toward the electrode. The value of the positive charge is mainly determined by the capacity of the channel and by the fact that the potential in the channel is smaller than the potential of the electrode by an amount corresponding to the ohmic drop of potential along the spreader. We will return to this point later. The ionization along the spreader is so intense that the electrons pulled toward the electrode only represent a fraction of the total number set free by the ionization by collision.

Repulsion between the resulting positive charges in the spreader will cause an increase in thickness of the spreader, and this increase will occur with a rapidity inversely proportional to the air pressure, as is more thoroughly shown in App. 2. The thickness — or width — of the spreader a given time after the passage of the front-particle will therefore — ceteris paribus — also be inversely proportional to the air pressure.

As we shall see later the luminous effect must be

[1] Parts of the following accounts apply also to discharges in the free atmosphere — as is easily seen.

assumed to arise a certain time after the original ionization, and the intensity of the photographic picture of the spreader must therefore also as a whole be inversely proportional to the air pressure.

The rate of increase of the thickness of the spreader must also — ceteris paribus — be proportional to the resulting charge per unit length of the spreader, and this charge must have a value increasing with increasing potential across the Lichtenberg spark gap[1]. The *p. d.* between the spreaders and the earthed plate B decreases, as said before, from the electrode towards the edge of the figure, and the drop in potential is the greater the higher the air pressure. But as the width t of the spreaders is measured at a distance from the tip inversely proportional to the air pressure, it may be assumed that the spark potential will have no appreciable influence on the value of t thus measured.

The preceding further shows that the width must increase fairly regularly from the tip towards the electrode. This regular increase in width is only found, however, at such distances from the electrode where the spreaders are so wide apart that they do not interfere with each other's lateral spreading. For Lichtenberg figures, the discharge takes place over the surface of an insulating plate. Here the plate surface will form a geometric boundary to the figure and further the induced charge Q_- on the metal plate B, see fig. 25, will, in proportion to the thickness of the insulating plate, exert a greater or smaller influence upon the electric field immediately in the neighbourhood of the spreader Q_+. In the following we shall consider the

[1] In the neighbourhood of the electrode the field from neighbouring spreaders will hinder a free lateral development of the spreader.

influence which the air pressure and other factors exert upon the formation of the spreader.

We will first, on the basis of the schematic representation in fig. 26, look at the conditions at very low pressures.

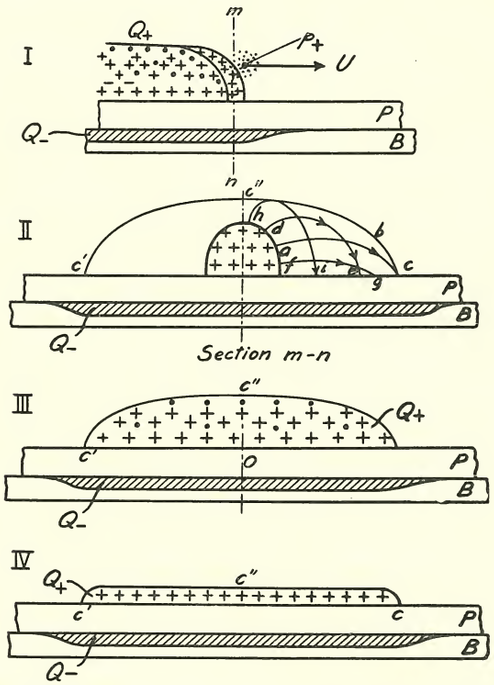

Fig. 26. Schematical Representation of the manner of formation of Positive Spreaders at low Pressures.

Part I represents the tip of a positive spreader. Immediately around the front-particle p_+ will be found some electrons and a corresponding number of positive ions. The number, however, is comparatively small because the air pressure is low. Both electrons and positive ions are indicated by dots in the figure. Immediately behind the front-particle will exist, within a limited layer, a very dense

positive space charge, due to the very strong ionization by collision occurring in the very strong field at the tip of the spreader, combined with the great mobility of the electrons which allows their quick removal by the field toward the left — in the direction of the electrode — while the comparatively heavy positive ions may be considered as nearly stationary within the very short intervals of time here in question.

Due to mutual repulsion the positive ions will during the time following move outward — f. inst. a in part II along the path a-c — and the attraction from the induced charge Q_- will finally force the ion down against the surface of the plate P. The smaller the air pressure, and the greater the velocity of the ion, the fewer collisions will it undergo on its way.

Even if the front travels so rapidly that no considerable number of free electrons get time to recombine with positive ions to form neutral molecules, or with neutral molecules to form heavy negative ions, nevertheless, at such low pressures a sufficient number of electrons may easily be carried away toward the electrode, thus enabling the capacitive positive charge on the spreader — and the corresponding induced negative charge Q_- — to increase in accordance with the width of the spreader. The charge density per unit length of the spreader will therefore increase very rapidly. By this means also the forces tending to drive the positive ions outward will become great. Since the ions have at the same time a high mobility, owing to the low pressure, the width of the spreaders must also become great.

In part II it is assumed that the ion a travels the farthest before it impinges upon the plate P at c. Ions

which start from higher points such as d and h or from lower points such as f will then impinge upon P at shorter distances from the centre of the spreader.

The positive ions which hit the surface of the plate will be pulled down against it by the electric field and will then be retained by the electric forces between the ion and the molecules in the surface of the solid plate. These positive ions will thus almost completely lose their mobility.

After a short time the state of charge will pass through the state III and approach the state IV, where the density per unit area σ of Q_+ and Q_- (which have the same numerical value) is very nearly constant over the entire width of the spreader in that

$$\sigma = \frac{\varepsilon}{4\pi d_0} \cdot V,$$

where ε is the dielectric constant of the plate and V the $p.\ d.$ between the point of the spreader considered and the plate B.

Those positive ions which are not retained in this way will recombine with a corresponding number of negative ions or electrons and this recombination will in the main occur evenly distributed over the cross section $cc''c'$ — see part II — since the above mentioned scattering of the positive ions occurs with such great velocity[1], and the density of these ions is so great, that the air particles within this cross section are set in such violent motion that effective mixing takes place.

The spreading out occurs in an analogous manner at higher air pressures, but the scattering velocity of the

[1] See also later.

positive ions is smaller and the dispersal of the electrons is slower so that the width of the spreader becomes smaller. Another contributory cause is that the original ionization channel, formed by the front-particle, has a smaller cross-section and accordingly also a smaller charge density. The width of the spreader must therefore decrease with increasing air pressure.

Fig. 27 shows schematically various states of the formation of a positive spreader.

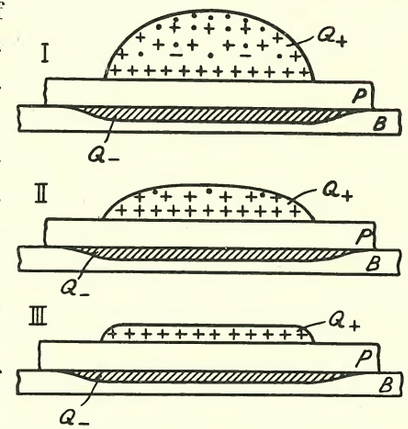

Fig. 27. Schematical Representation of various States of a Cross-Section of a Positive Spreader at Atmospheric Pressure.

With regard to the influence of the spark length on the width of the spreaders, we have already mentioned that the width at a distance from the tip inversely proportional to the air pressure is practically independent of the potential value on the electrode.

Generally speaking, the width will increase with increasing spark length, but to a smaller degree, because the induced charge Q_- increases at the same rate as Q_+, so that the direction of the field will be independent of the value of the two charges. Added to this, we here have near the electrode the above mentioned additional factor that neighbouring spreaders prevent the free spreading out of the single spreader.

The dependency of the width on the thickness d_0 of the insulating plate is evidently partly due to the fact that

the induced charge Q_- at thin plates comes up near Q_+, so that the electric field at the edge of Q_+ has a powerful component perpendicular to the surface of the plate, and partly to the fact that Q_+ and Q_- at a given voltage will increase rapidly with decreasing values of d_0. The positive ions will therefore move with great velocity, but owing to the geometrical form of the field they will nevertheless impinge on the plate at a comparatively short distance from the centre of the spreader. It is not easy to say off-hand which of these two causes has the greatest influence. The value of d_0 has actually very little influence upon the width as long as d_0 is not too small. For very small values of d_0, however, the width of the spreaders will decrease with decreasing d_0 but as the original ionization channel has a finite thickness the width will not become quite zero as $d_0 \to 0$.

In the foregoing we have first discussed the ionization by collision at the tip and thereupon the increase in width of the spreaders. These processes actually occur simultaneously and the total ionization will be almost proportional to the final width of the spreaders.

We shall see later — under section (d) — that the photographic width must be very nearly the same as the width cc' of the charge; see fig. 26 and 27.

The hypothesis set forth thus fully explains the fact that the width of the positive spreaders increases with decreasing pressure, with increasing potential and with increasing plate thickness. An exact quantitative calculation cannot be carried out, but the simple considerations set forth indicate that the width must be inversely proportional to the air pressure. All the results mentioned in

chap. III 1 (a) with regard to the dependency of the width on the various parameters are thus explained in a satisfactory manner by the hypothesis set forth.

(b) Number of Branches.

The number of branches per unit of length of a spreader must, ceteris paribus, be proportional to the air pressure. The number of suitable particles at those points where the field is strongest — i. e. at the edges of the spreaders — must in fact be proportional to the number of such particles per unit volume, i. e. to the air pressure.

The number of branches will also depend on the nature of the gas, but this we will return to later.

(c) Boundary-line of the Positive Spreaders.

The limits of the photographic image of the positive spreaders are determined by the limits to which the positive ions have spread at the moment when emission of light occurs. According to the foregoing, the spreading out of the positive ions is coterminous with the resulting positive charge; compare sect. (a) and figs. 26 and 27.

It appears from Appendix 2 that the outer boundary of a charge which spreads out owing to mutual repulsion will have a decided inclination to become sharp. The various conditions mentioned above under sect. (a) regarding the sidewards spreading out of the spreaders also contribute to the same effect.

These circumstances, combined with what will be set forth under the following sect. (d), offers a satisfactory explanation of the comparatively sharp boundary lines of the positive spreaders.

(d) Photographic Intensity.

The difference in luminosity of positive and negative figures is due to the fact that in the case of negative discharges, some of the positive ions set free by ionization by collision travel towards the electrode, while the main part of the negative charge is formed by electrons moving outward from the electrode or its immediate vicinity. This — as we shall see later — results in an exceedingly strong ionization at and near the electrode.

The light is produced in the main by recombination between the positive ions and the electrons and to a much smaller degree by recombination between positive ions and negative ions produced by neutral molecules combining with electrons. Where no positive ions are present no light appears. To this circumstance may be ascribed the fact that the luminosity at the outer boundary of the negative figures decreases gradually towards zero, since here the ionizing intensity, and consequently also the density of positive ions, decreases gradually.

Even when the field at the outer boundary has become so weak that ionization by collision has ceased, the electrons will be driven further out by the field but will in the mean time have combined with neutral molecules to form negative ions. But since no ionization occurs, no positive ions are produced, and therefore no light appears. We shall show later, under sect. 5 (a), that we are able to confirm by other means the fact that the charge has spread beyond the luminous part of the figure.

Corresponding conditions exist with regard to the dark lines of the negative figures. In this case also electrons and negative ions will pass in from the neighbouring parts of the spreader after the ionization by collision has ceased,

but no, or at least extremely few, positive ions. The photographic luminosity will therefore also be extremely small.

For positive figures the conditions are entirely different. Here the highly mobile electrons set free by ionization by collision will be driven up from the photographic plate to the surface of the spreader by the field — compare fig. 27 I—II — and the field will then set them moving toward the electrode. The number of electrons absorbed by the electrode will be just sufficient to give the spreader a charge corresponding to the *p. d.* between the spreader and the plate *B*. Part of the rest of the electrons combine with positive ions, while others combine with neutral molecules to give negative ions, which again later combine with positive ones. The light is mainly produced by combination of positive ions with electrons or with negative ions.

The ionizing intensity is much smaller near the electrode than in the case of negative figures. The photographic intensity is therefore also comparatively small but will, on the other hand, be nearly uniform over the entire length of the spreader. The ionization will in fact, as said before, be very nearly proportional to the width of the spreader and will not be influenced by the electrons carrying negative charge from the spreader tip toward the electrode. The voltage drop along the positive spreaders is in fact so small that these electrons will cause no appreciable ionization by collision.

In single cases, the outermost tips or branches may be less luminous than the rest of the spreaders, see plates 4 I, 5 and 6 I which are taken at low pressures. At atmospheric pressure the corresponding branches are comparatively shorter. Possibly here the velocity of the front

particles has become so small that the initial ionization which they cause is insignificant.

In this way we have accounted for the very peculiar difference between positive and negative figures with regard to light distribution. But it may still be asked: Can the spreaders really increase noticeably in thickness in the very short time elapsing before the positive and negative ions have recombined and before the light resulting therefrom is emitted?

The greater part of the recombination no doubt occurs within 1 to $2 \cdot 10^{-7}$ seconds. The emission of light probably occurs within a similar time interval after the recombination[1].

If, for example, the *p. d.* between the point in question of the spreader and plate *B* is 9 000 volts, and the thickness of the photographic plate about 1 mm, then the intensity of the electric field at the edge of the spreader will be of the order of 100 000 volt cm^{-1}. If we put the mobility of the ions at atmospheric pressure equal to 1.8 cm sec^{-1} per volt cm^{-1}, then the velocity of the edge will be $1.8 \cdot 10^{-5}$ cm sec^{-1}. The edge of the spreaders will then in the course of $1 \cdot 10^{-7}$ seconds move a distance of 0.18 mm. The increase in width of the spreader may thus attain the necessary velocity, and this velocity, moreover, is so high that the ionization at the tip may be assumed to be proportional to the width *t*.

This great velocity, combined with the great density of ions will, as said above, cause very vigorous movements inside the air volume occupied by the spreaders. By this means a very effective mixing occurs through the

[1] J. Franch u. P. Jordan: Anregung von Quantensprünge durch Stösse, p. 201, 1926.

entire cross section of the spreader whereby the density of the positive ions as such and negative ions as such will be practically the same over a cross section. The luminosity will therefore also very nearly be the same over the whole width of the spreader.

The occurrence of this vigorous motion further offers an explanation of various phenomena of a mechanical nature in connection with the formation of the figures. We may just mention the formation of dust figures or the depressions produced in the surface by the spreaders when the figure is formed over water or other liquids. Of a different nature are the permanent indentations made by Lichtenberg figures in the surface of melting pitch, which were noticed by E. W. Blake[1], and which are no doubt due to the electric forces between the charges of the spreaders and of the plate *B*.

2. Range and Velocity of the Positive Figures.

(a) Relation between Range and Velocity and the *p. d.*

According to L. F. II formulae (I)—(II) we have that:

$$x = R(1 - e^{-\alpha t}), \tag{I}$$

and

$$U = \alpha R e^{-\alpha t} = U_0 \cdot e^{-\alpha t}, \quad U_0 = \alpha R \tag{II}$$

where R is the range of the figures and x the length of the spreaders at time t.

From (I) and (II) we have that

$$U = U_0 \cdot \frac{R - x}{R}. \tag{III}$$

[1] E. W. Blake: Am. Journ. Sc. and Arts (2) Vol. 49, p. 289—94, 1870.

According to App. 1, formula (7) the maintenance of a velocity U requires an electric force X determined by:

$$X = k\sqrt{U} \qquad \text{(IV)}$$

where k is a constant dependent upon the nature and the pressure of the gas and also on the nature of the particle.

From (III) and (IV) we have that

$$X = k\sqrt{U_0} \cdot \sqrt{\frac{R-x}{R}}. \qquad (1)$$

From this we find the corresponding *p. d.* distribution by putting, according to formula (2) p. 63.

$$X = \frac{1}{\varrho} V, \qquad (2)$$

where ϱ is the radius of the strongly charged tip of the spreader. The length of this radius cannot be determined beforehand but it is reasonable to assume ϱ to be proportional to the range of the front particle at the velocity in question. This range, according to App. 1 formula (2), is proportional to $U^{\frac{3}{2}}$ so that the above formula may be written

$$X = \frac{aV}{U^{\frac{3}{2}}}, \qquad (2')$$

where a is the constant from formula (2) in App. 1.

From the above formulae we have that

$$V = \frac{k}{a} U_0^{\frac{1}{2}} U^{\frac{3}{2}} \sqrt{\frac{R-x}{R}} = \frac{k}{a} \cdot U_0^{\frac{2}{2}} \left(\frac{R-x}{R}\right)^{\frac{3}{2}}. \qquad (3)$$

When $x \to 0$ then $V \to V_0$ and $U \to U_0$ and we therefore get

$$U_0 = \sqrt{\frac{a}{k} \cdot V_0}. \qquad (4)$$

This expression agrees in the main with the experimental results; compare L. F. I p. 50, fig. 52.

According to (II) we have

$$R = \frac{U_0}{\alpha},$$

and since according to Ann. d. Ph. Bd. 69, p. 214 α is very nearly independent of the *p. d.* V_0, it then follows from the above formulae that

$$R \cong c\sqrt{V_0}, \qquad (5)$$

which also on the whole agrees with experiment; compare L. F. I p. 39.

Formula (3) determines the dependency of the *p. d.* on the distance from the electrode at the instant when the front particle is passing the point in question. We will then proceed to investigate how the resistance of the spreaders must depend upon the time elapsed since the start of the ionization, in order that by application of Ohm's law we may come to the said expression for the *p. d.* We may here emphasize, however, that these calculations are only rough estimates. The conditions in the discharge tracks are so complicated and so little known, that a theory satisfactory in all details cannot be developed at present.

For the sake of simplicity we will therefore assume that the initial ionization following the tip of the spreader has the same value all along the discharge track. For a length element dx of the spreader the resistance may be $r \cdot dx$. We further assume that after a lapse of time t' reckoned from the commencement of the ionization the resistance has increased to $e^{\beta t'} \cdot r \cdot dx$.

The resistance M_y of the length y of the spreader at

the moment when this has the range y is consequently determined by

$$M_y = r\int_0^y e^{\beta t'} \cdot dx = r\int_0^y e^{\beta (t_1 - t_2)} \cdot dx\,,$$

where t_1 is the time from the start of the discharge until when it has reached the distance y, while t_2 is the time at which the spreader has attained the length x.

From (I) we have that

$$e^t = \left(\frac{R}{R-x}\right)^{\frac{1}{\alpha}}, \tag{6}$$

where t and x are corresponding values of time and spreader length.

Consequently we have

$$M_y = r\int_0^y \left(\frac{R-x}{R-y}\right)^{\frac{\beta}{\alpha}} \cdot dx = \frac{r}{\frac{\beta}{\alpha}+1}\left(\frac{R^{\frac{\beta+1}{\alpha}+1}}{(R-y)^{\frac{\beta}{\alpha}}} - (R-y)\right). \tag{7}$$

For the current i we have the following expressions

$$i = \frac{V_0 - V_y}{M_y} \quad \text{and} \quad i = h\,V_y\,U\,, \tag{8}$$

where h is proportional to the capacity of the spreader per unit of length and therefore also approximately proportional to the width t of the spreader.

If we put the two quantities in (8) equal we get

$$V_y = V_0 \cdot \frac{\left(\frac{R-y}{R}\right)^n}{\left(\frac{R-y}{R}\right)^n + K_0 R\left(1 - \left(\frac{R-y}{R}\right)^{n+2}\right)}, \tag{9}$$

where

$$K_0 = \frac{hr}{\frac{\beta}{\alpha}+1} \quad \text{and} \quad n = \frac{\beta}{\alpha} - 1\,. \tag{10}$$

Consequently, for $y = 0$, $V_y = V_0$, and for $y = R$, $V_y = 0$.

As h is very nearly proportional, and r inversely proportional, to the width of the spreader, then K_0 is very nearly independent of this width.

From (9) we have

$$\frac{dV_y}{dy} = -V_0 \cdot \left(\frac{R-y}{R}\right)^{n-1} \cdot \frac{K_0\left(n+2\left(\frac{R-y}{R}\right)^{n+2}\right)}{\left[\left(\frac{R-y}{R}\right)^n + K_0 R\left(1-\left(\frac{R-y}{R}\right)^{n+2}\right)\right]^2}. \tag{11}$$

For

$$K_0 R\,(n+2) = n \tag{12}$$

we have for $y \to 0$ and $y \to R$

$$\left(\frac{dV_y}{dy}\right)_{y\to 0} = \left(\frac{dV_y}{dy}\right)_{y\to R} = -V_0 \cdot \frac{n}{R} \cdot \left(\frac{R-y}{R}\right)^{n-1}. \tag{13}$$

If we further put $n = \frac{3}{2}$ then we see not only that V_y at $y = 0$ and $y = R$ has values equal to those determined for V by (3) but also that $\left(\frac{dV}{dy}\right)$ at the points considered has the same value in the two cases since, according to (4), we have

$$V_0 \cdot \frac{n}{R} = \frac{3}{2} \cdot \frac{R}{a} \cdot U_0^2\,.$$

With regard to the various assumptions on which the above results are deduced, we must still add a few remarks.

The assumption that the original resistance per unit of length is constant along the entire spreader is not correct. There is reason to assume the resistance to be inversely proportional to the width, but the quantity of electricity consumed by charging of the spreader is at the same time nearly directly proportional to the width. It will, however, in the main be the product of resistance and capacity of

the spreader which is the deciding factor, and this product will, as mentioned, be very little dependent on the width. It is, however, to be assumed that the capacity decreases somewhat more slowly than the conductivity with decreasing width, and the product $(r \cdot h)$ will therefore increase a little under these conditions. The error caused by the slightly tapered form of the spreaders will, all things considered, hardly have any considerable value, but for the thinner spreaders there will be a tendency to a smaller velocity and a smaller range than for the wide ones, a result which is confirmed by plate 4 I.

We will now discuss the assumption that the conductivity decreases at the rate $e^{-\beta t}$. The conductivity is mainly due to the free electrons the number of which per cm^3 we will call N. We therefore simply write the conductivity of the spreader as

$$\frac{1}{r} = \lambda = \frac{c}{A} \cdot N, \tag{14}$$

where A is the cross-sectional area of the spreader and c is a constant.

The free electrons may be lost by recombination with positive ions or by forming negative ions with neutral molecules.

In the cases where the ionization is not extremely strong and where no strong outer field is found, we shall have in the first case

$$\frac{dN}{dt} = -\alpha N^2 \quad \text{or} \quad N = \frac{N_0}{1 + \alpha t N_0}, \tag{15}$$

where, at atmospheric pressure, $\alpha \cong 1 \cdot 6 \cdot 10^{-6}$.

In the second case we have

$$\frac{dN}{dt} = -bN \quad \text{or} \quad N = N_0 \cdot e^{-bt}, \tag{16}$$

where b is a constant which is proportional to the air pressure but also to a large extent depends upon the nature of the gas. For hydrogen and nitrogen b will thus be very nearly equal to zero, while for oxygen b will be of the the order of 10^6 at a pressure of 760 mm Hg.

A rough calculation of the maximum resistance shown by the spreaders and the number of ions per cm^2 of a cross section of the spreader — in both cases on the assumption that the thickness of the spreaders (perpendicular to the plate) is about $^1/_4$ mm — leads, however, to the result that the density must be 10^{12} to 10^{13} electrons per cm^3. We have, however, further assumed that we can apply a value of the conductivity calculated on the basis of the kinetic gas-theory. But at such intense ionization and such strong fields as are here considered, neither formula (15) nor (16) can be applied; nor will the general kinetic theory lead to results of even approximately the right order. The conditions in highly conductive air spaces are as a whole very little known; compare f. inst. the efforts to establish a plausible theory for the conductivity of the electric arc[1]. We shall therefore not enter further into this question here but shall merely remark that, considering the agreement found with experiment, when assuming the conductivity to decrease at the rate $e^{-\beta t}$, there is reason to believe that the conductivity of strongly ionized spaces in the main decreases in the said manner, the value of β being about $5 \cdot 10^{-7}$. Presumably this result cannot be dismissed at the outset as unreasonable.

A few more remarks may be made with regard to the decrease of the conductivity as a function of time. First, the conductivity will maintain a considerable value as long as

[1] H. Hagenbach: Handb. d. Phys. Bd. 14, p. 346 1927.

a great number of electrons are set free at the tip of the spreader. We will come back later to this question under 4 (a). Secondly, even when all of the free electrons have disappeared, the discharge track will retain some conductivity owing to the heavy ions still present. But this conductivity is so inconsiderable, at least at higher pressures, that it is of no significance for the passage of the comparatively strong currents existing in the spreaders during their formation.

At comparatively low pressures the conductivity due to the ions may be of such value that it may have some influence upon the formation of the spreaders. The conductivity due to the ions will decrease at a slower rate than the conductivity due to the electrons, and the following conditions may then occur: the growth of the spreader stops completely, or very nearly completely, because the ohmic voltage-drop becomes too high, after which the part of the spreader already formed will be charged comparatively slowly to a higher potential owing to conductivity due to the ions. Especially at the tip the potential may increase considerably. The result of this is that a new spreader starts from the tip of the old one, or that the tip of the latter gains renewed speed. Examples of such cases are quite frequent; see thus plate 21 IV and 23 (p = 50 mm Hg.). In some few cases this process may be repeated several times; see plate 12 IX.

The conductivity due to ions at all events plays an important rôle for the continued growth of the spreaders if the potential on the electrode is maintained for a comparatively long time, but this question will be treated later. The leading away of the charge from the figure through the shunt R — see fig. 1 — also mainly depends on the conductivity due to ions.

Although it has not been possible to work out an explicit theory for the conditions in the strongly conductive spreaders, the considerations set forth above show that the formation of the spreaders, as known from experience, may be explained in a reasonable manner by means of the hypothesis set forth about the manner of formation of the positive spreaders.

As for the negative figures there exists in the main no doubt with regard to their mode of formation, and a detailed analysis of the above treated questions is therefore of less interest for these figures. We shall therefore make only a few remarks concerning their mode of formation.

Since their conductivity is mainly due to free electrons, the amount of electricity neccessary to charge the negative figure must for the most part originate in electrons travelling outward from the electrode. A strong ionization must therefore occur at, and in the neighbourhood of, the electrode, with intensity decreasing outwards. A minor part of the charge is due to positive ions moving toward the electrode. On their way outward the electrons will cause ionization and this will be the stronger the stronger is the field. Since the latter increases towards the electrode, this will also be the case for the ionization by collision. The outer edge of the figure is determined by the condition that the field becomes too weak here to maintain ionization by collision.

(b) Relation between Range and Velocity and the Thickness d_0 of the Insulating Plate.

With decreasing thickness d_0 of the insulating plate, the electric field at the tip of the positive spreaders will increase, but its direction will at the same time be bent

down towards the plate; the track of the front particle will therefore also have a downward direction as indicated by the arrow U in fig. 28.

When the front particle hits the plate it will be stopped. The tendency to impinge on the plate will increase with decreasing thickness of the plate and consequently the range of the figure will go toward zero simultaneously

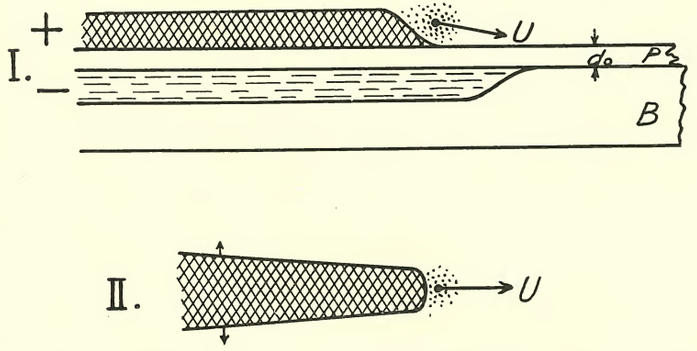

Fig. 28. Schematical Representation of the Conditions at the Tip of a Positive Spreader for small Thicknesses of the Insulating Plate.

with the plate-thickness. For very great values of d_0 the electric field, and therefore also the velocity, will become comparatively small. The velocity consequently attains a maximum value at an intermediate value of d_0. This is in complete agreement with the experimentally determined relation between velocity and plate-thickness; see fig. 8 in this paper and L. F. I, p. 56, fig. 59.

The range of the positive figures as a function of d_0 — if, as is to be expected, α remains constant — must be governed by a similar relation, and this is also in agreement with the experimental results set forth in L. F. I, p. 30, fig. 34.

In the case of negative figures the electrons at the end

of the spreader will also be drawn down towards the plate, and the thinner the plate, the stronger will be the field. The front-ionization will therefore also be the stronger, the thinner the plate. This strong ionization will very rapidly set free electrons in sufficient number to supply the proper negative charge to the negative spreader. When this is effected, the surplus of electrons coming from the electrode and its vicinity will not be pulled down toward the plate, but can move freely in the air under the influence of the field. Since the field at the edge increases with decreasing thickness of the plate, the velocity, and simultaneously the range, will approach a maximum when the plate thickness decreases toward zero. This result, also, is in agreement with experience; compare L. F. I, p. 30, fig. 34 and fig. 8 in this paper.

(c) Relation between Range and Velocity and the Pressure. Nature of the Positive Front Particle.

It appears from equation (IV) in section (a) above and equations (2), (6), and (7) in App. 1 that

$$k = k_0 \cdot p, \tag{1}$$

where p is the air pressure and k_0 a constant.

From equation (2) in App. 1 we find that

$$a = \frac{a_0}{p}. \tag{2}$$

Equation (4) in section (a) will consequently give

$$U_0 = \sqrt{\frac{a}{k} \cdot V_0} = \frac{1}{p}\sqrt{\frac{a_0}{k_0} \cdot V_0}, \tag{3}$$

so that according to the theory the velocity of the positive spreaders should be inversely proportional to the air pressure.

Their range is accordingly determined by

$$R = \frac{U_0}{\alpha} = \frac{1}{\alpha p} \cdot \sqrt{\frac{a_0}{k_0} \cdot V_0}. \qquad (4)$$

Since α decreases somewhat with decreasing pressure, the range will, according to equation (4), increase somewhat more rapidly with decreasing pressure than it would if R were proportional to $\frac{1}{p}$. This is in good agreement with the formulae given by v. Bezold and S. Mikola[1] and our experimental determination of the dependency of the range on the air pressure, at not too low pressures is also fully in agreement with this.[2]

But from fig. 42 L. F. I it further appears that at very low pressures R increases more slowly with decreasing pressure than it should according to equation (4). Fig. 58 in L. F. I further shows that the velocity approaches a finite limiting value — U_m in fig. 8 above — when the pressure approaches zero.

It is also easily seen that at extremely low pressures the manner of formation must be different from that assumed here. If we f. inst. assume that in the limit the pressure becomes zero, then the front particle will nevertheless by unable to attain a velocity greater than that corresponding to a free fall through the entire *p. d.* V_0. We consequently have

$$U_{p \to 0} < 1.38 \cdot 10^6 \sqrt{\frac{z}{M} \cdot V_0}, \qquad (5)$$

where M is the mass of the particle with the hydrogen atom as unity, and $(z \cdot e)$ its charge.

The value given by the right hand term in (5) is not attained before the particle has travelled through the total

[1] L. F. I, p. 41. [2] l. c., Fig. 42.

p. d. V_0. Right at the electrode the velocity will be zero. On the other hand the method used in these investigations for measuring the velocity, (see L. F. I), determines particularly the velocity near the electrode. Applying this method to the case of freely moving particles will consequently lead to values of U considerably lower than those given by the right hand term of equation (5). Finally, the spreading-out-velocity of the figure at small but finite pressures will certainly be smaller than the velocities found for freely moving particles.

The experimentally obtained values of the velocity must therefore, at low pressures, be supposed to have a limiting value considerably lower than the one determined by equation (5); in fact, hardly more than half that value. We therefore put this limiting value to be

$$U_{m,\, p \to 0} = 7 \cdot 10^5 \sqrt{\frac{z}{M} \cdot V_0}. \qquad (6)$$

Fig. 42 in L. F. I shows the results of a series of such measurements. The limiting value found is about $5.2 \cdot 10^7$ cm sec.$^{-1}$ and the *p. d.* used was $V \cong 7000$ volts. By inserting these values in (6) we get

$$\frac{z}{M} = 0.79.$$

For H^+-particles or protons $\frac{z}{M} = 1$, for α-particles this ratio is $\frac{1}{2}$, and for all other known positive particles considerably smaller.

We are therefore led to the supposition that the front-particles are protons.

In the negative figures, where the active outward-travelling particles are electrons, there exists no such limiting value for the velocity at decreasing pressures, or more

correctly, the limiting value is so high that it falls outside the range here considered. This is in complete agreement with experiment, which shows that at decreasing pressures the spreading out velocity of the negative figures may attain very high values, see f. inst. fig. 8 above and L. F. I, fig. 38.

3. The Start of Positive and of Negative Discharges.

(a) The Start of Negative Discharges.

The start of a negative figure presents no remarkable features. With a needle-point as electrode placed directly on the photographic plate the range of the figure will, at low potentials, be proportional to the *p. d.*, and this holds right down to a few hundred volts, when the figure becomes so small that it cannot be seen with the naked eye. The explanation is obvious. In the immediate vicinity of the electrode-point the field has, even at small potentials, such a value that the ionization by collision sets in, i. e. figure formation starts. But at these low potentials the electrode must neccessarily be point-shaped or have sharp edges, and must further be clean in the sense defined elsewhere by the author[1]. If the electrode is unclean, greasy, for example, the air does not come in direct contact with the sharp edges or points, and ionization by collision will thus not occur at low potentials.

There is thus no difficulty in explaining the experimental results, that negative figures start most easily from a clean point, that at low potentials their range is proportional to the *p. d.*, and that no lower limit exists for the effective potential.

[1] P. O. PEDERSEN: Vidensk. Selsk. Math.-fys. Medd. Vol. IV, No. 10. Copenhagen 1922; Ann. d. Physik (VI) Bd. 71, p. 317—376, 1923.

(b) The Start of the Positive Discharges.

The start of a positive figure, however, presents very peculiar features, as appears from chap. III 3 (b). We shall now proceed to discuss these features in the light of the hypothesis already set forth, and further defined in the preceding section, where we stated that the front particles must be protons.

We will for the present assume that these protons originate from hydrogen molecules, and we will put their number N per cm^3 equal to

$$N = N_0 \cdot p, \tag{1}$$

where p is as usual the air pressure.

The volume of that space near the electrode within which the electric field has sufficient strength to split off protons from hydrogen molecules we will call A. The total number of hydrogen molecules available for the possible giving up of protons is consequently

$$n = AN_0p. \tag{2}$$

The probability s that a hydrogen molecule will give up a proton, depends upon the field, and therefore also upon the potential V. We put

$$s = s(V), \tag{3}$$

and the number n_p of protons available is consequently

$$n_p = sAN_0p. \tag{4}$$

We shall next discuss under what conditions an available proton becomes active, that is, causes the start of a positive spreader. These conditions are undoubtedly rather complicated. However, it is excluded from the chance of becoming active if it is first rendered "hors de combat"

by any means: for example it may adhere to the first neutral molecule it strikes, thus giving rise to a positive ion, or it may be neutralized by an electron from the molecule with which it collides. The conditions that are neccessary to prevent such occurrences cannot be stated with any certainty, but the probability that the proton remains free after a collision is the greater the greater its velocity. We assume for simplicity that the proton remains free if — and only if — its velocity at the collision is greater than that corresponding to V' volts. Denoting the distance travelled by the proton in the direction of the field since its liberation by x, and the electric field strength by E, the proton will remain free after the first collision if

$$Ex > V'. \tag{5}$$

In order to simplify the calculations we take a mean value of E in the active space A by putting

$$E = \frac{V}{L}, \tag{6}$$

where L is proportional to the thickness of the active space.

Then equation (5) will read

$$x > \frac{L}{V} \cdot V'. \tag{5'}$$

The mean value of the free path l of the proton is inversely proportional to the pressure, that is

$$l = \frac{l_0}{p} \tag{7}$$

and the probability S that the first free path of one of the available protons is greater than x is

$$S = e^{-\frac{x}{l}} = e^{-\frac{LV'}{l_0 V} \cdot p} = e^{-c\frac{p}{V}}, \quad c = \frac{L}{l_0} V_0. \tag{8}$$

The total number n^0 of active protons is consequently

$$n^0 = np \cdot S = sAN_0 pe^{-c\frac{p}{V}}. \tag{9}$$

Until anything is stated to the contrary, we shall assume that we have the same electrode and the same kind of gas; in that case A and N_0 are constants and (9) may be written

$$n^0 = sKpe^{-c\frac{p}{V}}. \tag{9'}$$

We will further assume quite provisionally that $s = s(V)$ is a constant. This assumption is, no doubt, not justified, but it will simplify the following considerations, and we shall investigate later the effect of the dependency of s on V.

We therefore write provisionally

$$n^0 = K_0 \cdot p \cdot e^{-c\frac{p}{V}}, \tag{9''}$$

where K_0 is considered a constant.

A positive discharge starts only if $n^0 \geqq 1$. This is the case when

$$\frac{1}{p} \cdot e^{c\frac{p}{V}} \geqq K_0. \tag{10}$$

Here we do not know — and we are unable to calculate beforehand with sufficient accuracy — the value of K_0, but we may try to find out under what conditions the left hand term of (10) is independent of the air pressure. We will write this condition in the form

$$lg\, p - c\frac{p}{V} = \text{constant}. \tag{11}$$

Now the question is: are we able to select such a value of $c = \frac{L}{l_0} V'$ that a (p, V)-curve determined by means of

(11) shows with sufficient accuracy a relation between p and V corresponding to the relation found by experiment? Further, will the value of c applied in such a case be a reasonable one?

In fig. 18 are shown by crosses the corresponding values of potential and air pressure obtained in atmospheric air and with a plate thickness of about 1.4 mm.

The thin curve in fig. 18 represents the equation

$$lg\, p - \frac{12}{V} \cdot p = 3.04\,. \qquad (12)$$

We see that equation (12) does not give any very good representation of the experimental results since — especially at higher pressures — the experimentally determined potentials have somewhat lower values than the calculated potentials. Equation (12), on the other hand, represents values of the right order of magnitude for the relation between p and V over a wide range, and it may, therefore, be of some interest to see whether the value given for c is also of the right order of magnitude. If in (7) the free path is given in cm and the pressure in mm, then $l_0 \cong 2.6 \cdot 10^{-2}$ cm. For electrodes resting directly on the photographic plate the value of L in (6) will presumably be about 0.025 à 0.05 cm. V' must presumably have a value of about 10 volts. The values of c corresponding to this are between 9.6 to 19.2, and these limiting values agree very well with the value 12 in equation (12).

It is obvious why equation (12) can give only a comparatively rough approximation. The probability $s(V)$ that a hydrogen molecule gives up a proton is not constant, as we have assumed in the equations (9″) to (12), but must, on the contrary, increase quite rapidly with increasing values of the potential. However, we do not know this relation in any detail, and for the sake of simplicity we therefore replace (9′) by the following equation:

$$n_0 = sKpe^{-c\frac{p}{V}} = K^0 \cdot p \cdot e^{-c^0\frac{p}{V^2}}. \qquad (13)$$

This expression is, no doubt, not theoretically correct but — as compared with (9″) — has the advantage that the value of the probability s increases with increasing value of the potential.

In fig. (18) the heavy curve corresponds to the equation

$$lg\, p - 32 \cdot 10^3 \cdot \frac{p}{V^2} = 2.12\,, \qquad (14)$$

and we see that this curve furnishes a representation of the experimental results as satisfactory as may be expected when we take into account the considerable uncertainty in the experimental determination.

Fully in agreement with the considerations here set forth is the fact that the positive figure, at potentials near the critical minimum value, often consists of only one single or a few spreaders. But from this it again follows that it is a matter of chance whether or not a figure is formed with potentials near the critical value.

According to (9) the number of active protons is proportional to the volume of the active space A. It is difficult to state a definite value for this, but it is obvious that of the four different forms of electrodes shown in figs. 13 and 16 the spherical one will have the greatest value of A, the pointed one the smallest value and the rounded rod a value between the two. This explains the fact that within the critical interval the spherical electrode shows a greater tendency to produce figures than the point-electrode. The

tube-formed sharp-edged electrode shown in fig. 16, however, shows an ability to produce figures, at least equal to the spherical one. For this electrode, not only is the field very strong at the sharp edge, and consequently the probability s great, but also the active space has a considerable volume owing to the considerable length of the edge.

Uncleanness (grease or the like), will cause a slight diminution in the active space immediately around edges and points, but if the uncleanness is only small, its influence in this respect will be insignificant. For positive discharges the electrode will therefore be very little sensitive to contaminations even within the critical interval.

The difference between positive and negative electrodes in sensitiveness to contaminations is quite analogous to the peculiar relations which have been stated with regard to retardation of spark-formation as dependent upon the state of the electrodes[1]. This question will, however, be treated in more detail elsewhere.

In chapt. III 3 (b) we have mentioned that the spherical electrode, within the critical interval, if placed on a not too thick plate, shows a tendency to produce abnormally short spreaders, while sharp-edged electrodes do not show this tendency. This is easily understood from the considerations set forth above, section 2 (c), according to which for spherical electrodes the electric field will have a powerful vertical component at the starting points of the spreaders, which drives the protons down into the plate.

A final consequence of the hypothesis here set forth is that the front-particle must have a certain, rather high velocity if a discharge of the kind here considered shall

[1] P. O. PEDERSEN: "Vid. Selsk. Math.-fys. Medd." IV, 10. Copenhagen, 1922; "Ann. d. Phys." (IV). Bd. 71, p. 317—376, 1923.

be started. The positive spreaders must consequently attain at all events a certain, finite length, if they start at all.

There then remains the question of the origin of the protons. It is well known that protons are set free in discharge tubes containing even the smallest trace of hydrogen[1], and in many cases also H-atoms in considerable numbers[2]. In an apparatus such as that by means of which Lichtenberg figures are produced there will be found — even in cases where the use of pure gases as f. inst. N_2 or O_2 is aimed at — a not insignificant number of hydrogen molecules, and these are also present in considerable numbers in the ordinary air of the laboratory. Even if we reckon with an admixture of only 0.0001 pCt. hydrogen there will be present — at atmospheric pressure — $3 \cdot 10^{13}$ hydrogen molecules per cm^3. Hydrogen molecules in sufficient numbers will consequently always be at hand.

Another feature may possibly seem peculiar at first sight. The formation of positive figures ceases — as we have seen — because the number of spreaders approaches zero. It is comparatively seldom, however, that figures are obtained having only 1 or 2 spreaders, generally there will be f. inst. 5—10. On the other hand, the number will not exceed f. example 30—40, according to the existing conditions, even if we raise the potential or diminish the pressure very greatly. The above calculated probability increases, however, to a very great extent, and accordingly the number of spreaders should increase highly.

There are, however, other causes which automatically set a limit to the number n of the spreaders. Out of a probable number of spreaders, the individual members will

[1] J. J. THOMSON: "Rays of Positive Electricity", see f. inst. p. 15—20.
[2] K. F. BONHOEFFER: Erg. d. ex. Naturwiss. Bd. 6, p. 204, 207—8, 1927.

not start quite simultaneously and those first started will consequently come ahead of the others. When so many have started that at some distance from the electrode they cover practically the entire circumference, then — on account of their charge — they will counteract the formation of further new spreaders, or at least stop any such in their growth.

If we are far outside the critical interval, the number of spreaders will therefore not be determined by the available number of protons, but simply by the available space.

At not too high pressures we therefore often observe also a number of small spreaders which are stopped in their growth by the electrical charge of those first formed, see for example plates 12 V—VII and IX, 13 I—II and 14 I—II.

According to the hypothesis set forth, it may be expected that the number of available protons will be the greatest in hydrogen or in compounds of hydrogen and nitrogen, smaller in nitrogen, still smaller in compounds of nitrogen and oxygen and the smallest in gases having great electron-affinity as for example oxygen.

From the foregoing it will be understood that this difference will not make itself apparent by the number of spreaders of the normal figures, but it manifests itself quite clearly by the number of side-branches and smaller side-spreaders. The greater the number of available protons the greater number of these will be observed. A look over the figures shown in plates 4, 5 and 6 I, which are taken in various gaseous compounds will verify this fact.

The small side-spreaders and branches are presumably formed in this manner: The original spreaders, which are in the process of formation, act as electrodes with a potential somewhat lower than that of the main electrode,

but still of a value sufficient to start available protons with the necessary velocity.

Inside the spreaders protons will generally be set free to a great extent and these will be driven by the electric field to the surface of the spreader, so that here there will always be available protons. Spreaders will, however, be formed only if the electric field in the surrounding air is of sufficient value to give the protons the necessary velocity. The field outside in the air will be strongest at the edge of the spreader immediately on the surface of the photographic film. The protons driven out here will therefore also have the greatest probability of becoming active. If the spreader is formed in a narrow space between two planes — for example if there is a second photographic plate as shown in plate 8 I—II — then the lateral spreading out will be small but both the field as well as the proton-density will be great at the edges and therefore the tendency to form side-spreaders will be great.

If the side-spreaders start in directions which are nearly the same as that of the original spreaders, they will be squeezed in between these, and if they start perpendicular to the original ones, they will become very short as they are stopped by the neighbouring spreaders. Such short side-spreaders are observed in great numbers in hydrogen-nitrogen compounds. (In pure hydrogen this phenomenon is very difficult to study because the luminosity is so small). In some cases these side-spreaders may point inward — in the direction of the electrode — if there is more free space in that direction, see for example plate 5 XVI.

In cases where the spreaders are stopped abruptly by an opposing field as f. inst. at the meeting line in velocity-

measurements, the potential at the tip of the spreader will become comparatively high and the tendency to form side-spreaders will therefore also be great. This conclusion is also verified by experiments, see for example plate 14 I, especially just above the dividing line some little distance outside both ends of the lower electrode.

The hypothesis set forth thus explains in a simple manner all the peculiar features of the start of the positive figures.

4. Conductivity of Positive and of Negative Spreaders.

(a) Conductivity of Negative Spreaders.

In fig. 29, A represents a negative electrode resting on a photographic plate P, while $a\,b$ represents, schematically, a negative spreader which at the point b runs into a free — or earthed — electrode B, the potential of which is zero to begin with.

There will be present in the spreader positive ions as well as negative ions and electrons. The sum of the two last named will be greater than the number of positive ions because the spreader has a negative charge. Since the electrons have a much greater mobility than the ions only electrons are shown in I and II of fig. 29.

We assume the conductivity of the spreaders to be so high that at a point just a little to the left of b there is a potential which is a considerable fraction of the value of the potential of A. There will consequently be a strong field immediately near b and this field will pull the electrons toward and into B. This results in a decrease in the negative charge near b as indicated at c in II. A strong field will then be developed near c, which will pull a

further number of electrons in the direction of B. The location of the strong field will therefore — owing to the great mobility of the electrons — move to the left with great velocity. This is indicated by the double arrow at c.

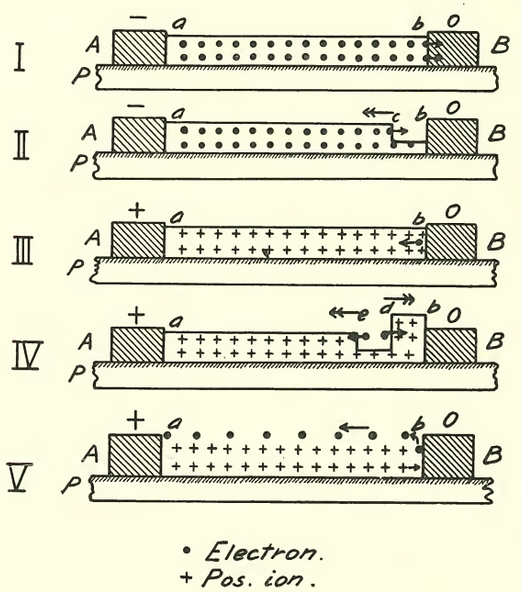

Fig. 29. Schematical Representation of the Conductivity of Negative Figures (I—II) and of Positive Figures (III—IV).

The strong field at b and later at c will cause ionization by collision, by which means the conductivity between c and the electrode B will be comparatively high, even though the negative charge between these two points will be comparatively small. From what is stated here, it appears that there will be a strong tendency to spark-formation between A and B, and the spark will begin at B. This is verified by our experiments, see chapt. III 4 (a).

(b) Conductivity of Positive Spreaders.

Here we find entirely different conditions. The spreader $a\,b$ in III fig. 29 has a positive charge, the number of positive ions being greater than the sum of electrons and negative ions. The electrons are mainly present in the upper part of the spreader.

When the spreader $a\,b$ gets near to B there will arise a strong field at b, which will drive the positive ions into the electrode B. Owing, however, to the low mobility of the ions they will move comparatively very slowly, and we will therefore consider them as insignificant at present. We might perhaps assume that the strong field at b would drive the electrons with great velocity towards A. Such a movement would, however, very soon be stopped. If f. inst. most of the electrons in the space $b\,d$ in IV are carried over to the space $d\,e$ then this would give a charge distribution as indicated in the figure. But in such a case those of the electrons within the space $d\,e$ which were near d would be carried back again with great force toward B, while those near e would be carried along in the direction of A, but with a smaller force. An "electron-wave" such as $d\,e$ will therefore be dispersed and cannot travel from B to A. Consequently no spark can be formed.

A flow of electrons may, however, very well occur from B to A i. e. an electric current passing from A to B, provided only that a suitable number of electrons are set free at B, and such a current may be quite strong without actually forming a spark. The strong field at b will cause the positive ions to impinge on B with great velocity and thus set free a sufficient supply of electrons. These will then, as shown in V of fig. 29, drift to the surface of the spreader and here be carried toward the electrode A.

If the *p. d.* between A and B is not of sufficient value to cause this current to ionize by collision, no light is emitted and no spark is initiated.

If, finally, we maintain the *p. d.* between A and B so long that the positive ions get time to move sufficient distances, then we get a discharge analogous to the one shown in fig. 28 II, except that here the moving particles are positive ions instead of electrons and in consequence the discharge moves relatively slowly.

The features explained here are in full agreement with the experimental results set forth in chapt. III 4.

A theoretical treatment of the discharge conditions in the case when the potential is maintained long enough to allow the heavier ions to play a deciding rôle in the formation of the discharge, f. inst. the question of spark formation, will be taken up elsewhere. We have mentioned these conditions in chap. III 4 (b) and (c) only to emphasize that they have nothing to do with the formation of the regular Lichtenberg figures.

5. Various Circumstances in Connection with the Formation of the Lichtenberg Figures.

(a) No Influence of an Initial Ionization.

It will be understood without further explanation that an initial ionization has no appreciable influence on the spreading-out of the positive figures as long as this ionization is not strong enough to give rise to a conductivity which will materially alter the electric field active in the formation of the figure. The hypothesis thus gives a perfectly satisfactory explanation of the features mentioned in chap. III 5 (a).

(b) The Bright Border-Line.

The bright rim-formations mentioned in chap. III 5 (b) are easily explained by means of what is set forth in 1 (d) above and in Appendix 2.

In the case of negative figures the electrons will, as is mentioned above, continue their outward movements even after the field at the edge has decreased so much that no ionization by collision takes place. The said electrons will then, however, generally combine with neutral molecules into heavier negative ions, and the outermost edge of this ion-stream will, as pointed out in Appendix 2, become comparatively sharp.

If now, simultaneously with this outward movement, a great number of electrons are set free over the area in question, then ionization by collision will occur at the sharp edge of the figure, and this ionization will cause the emission of light a little outside the edge which, owing to the former mentioned reasons, is situated a little outside the boundary of the photographic image.

Somewhat similar conditions occur in the case of positive figures, except that here the positive ions are so firmly placed that no appreciable spreading out of the figure will occur after the formation of the photographic image has stopped. A rim-formation will in this case occur close to the edge of the photographic image.

Concluding Remarks.

A theory of the formation of negative figures, which is in the main satisfactory has — as stated in the introduction — already been given earlier. When we have also treated of negative figures in the investigations described

here our object has been to throw further light upon certain features of the theory already set forth.

The theory developed above of the formation of positive Lichtenberg figures, namely, that formation of positive spreaders is due to protons which the strong field at the tip of the spreaders drive outwards with great velocity, by which means electrons are set free in sufficient number to initiate a sudden and strong ionization by collision which again sets free electrons in sufficient numbers necessary to carry away the charge towards the electrode is found to explain throughout in a satisfactory manner the many peculiar features presented by the positive spreaders.

The investigations here described further indicate that protons play an important rôle not only in the formation of positive Lichtenberg figures, but that their importance in connection with spark formation is much greater than hitherto assumed. None of the theories so far proposed for spark formation offer a satisfactory explanation of a number of peculiar spark phenomena which have been observed and pointed out during recent years[1]. The theory of the formation of the positive figures given here will presumably also be useful for the solution of those problems, but this question will be treated at a later occasion.

Presumably, also, protons play a more important rôle than has hitherto been assumed in a number of other discharge phenomena.

Finally I wish to express my cordial thanks to Carlsberg Fondet for its valuable support of these investig-

[1] P. O. Pedersen: The papers (a)—(e) mentioned p. 4.

ations. To the Rask-Ørsted Fond for contributing to the publication. And also to the various cooperators who have kindly assisted me in carrying out the experimental investigations: namely, Mr. J. P. Christensen, Mr. Chr. Nyholm and Mr. B. B. Rud who have taken most of the photographic Lichtenberg figures here used. A few of the pictures were taken by Mr. C. Schou and Mr. N. E. Holmblad while Mr. F. Nielsen has carried out the photographic enlargements. Mr. J. P. Christensen has further assisted me in preparing this publication for the press.

APPENDIX I

On Positive Particles.

Within the velocity range — $1 \cdot 10^7$ to $10 \cdot 10^7$ cm sec^{-1} — which is of particular interest for positive Lichtenberg figures only very little has been published about investigations of how the range, the ionization, and the charge etc. etc. of the positive particles depend upon the velocity.

For particles at somewhat higher velocities a number of investigations have been carried out and these we have mentioned below under sections 1—5 in so far as they are judged to be of interest for the understanding of the positive Lichtenberg figures. Finally, A. J. Dempster has recently carried out investigations with H^+ particles in hydrogen and helium at velocities within the said range, and these and a few other investigations we will discuss under section 6.

1. Range, Ionization and Velocity of Positive Particles.

The range R of high-speed α-particles is known[1] to be proportional to the third power of the velocity U that is

$$U^3 = K \cdot R = 1.076 \cdot 10^{27} R \qquad (1)$$

This relation holds good as long as the range is more than 2 cm *i. e.* at velocities above $1.3 \cdot 10^9$ cm sec.$^{-1}$.

At small ranges and velocities the range is, on the con-

[1] H. Geiger: Proc. Roy. Soc. (A) Vol. 83, p. 505—515, 1910. E. Marsden and T. S. Taylor: Proc. Roy. Soc. (A) Vol. 88, p. 443—454. 1913. Geiger und Scheel: Handbuch d. Phys. Bd. 24, p. 152, 1927.

trary, proportional to the velocity in the power $\frac{3}{2}$ as shown f. inst. by P. M. S. Blackett[1]. That is

$$U^{\frac{3}{2}} = aR, \tag{2}$$

which holds good with sufficient accuracy for ranges from 1 cm down to somewhat less than 1 mm.

The equation (2) may also be written as

$$R = b \cdot V_0^{\frac{3}{4}}, \tag{2'}$$

where V_0 is the *p. d.* through which the particle must fall to obtain the velocity U. The constant b has the value

$$b = \frac{1}{a}\left(2\frac{e'}{m}\right)^{\frac{3}{4}}, \tag{2''}$$

where m is the mass of the particle and e' its charge.

Equation (2) holds good — as shown by Blackett — not only for α-particles but also for positive atomic ions of hydrogen, argon and "atmospheric air". The corresponding values of a and some other factors of importance for the following — all based on the Blacketts measurements — are set up in the following table A.

Table A. Various properties of positive particles.

Particle	a	$\frac{a}{a_H}$	Atomic weight m	$\sqrt{m}$	Average loss of energy per unit length of track $\frac{\frac{m}{R}}{\frac{m_H}{R_H}}$	Relative charges $\eta = \frac{\sqrt{\frac{m}{R}}}{\sqrt{\frac{m_H}{R_H}}}$
H	$6.2 \cdot 10^{13}$	1.0	1.0	1.0	1.0	1.0
He (α-Part)	$3.3 \cdot 10^{13}$	1.9	4.0	2.8	2.1	1.5
"Air"	$1.94 \cdot 10^{13}$	3.2	14.4	3.8	4.5	2.1
A	$1.21 \cdot 10^{13}$	5.1	40	6.3	7.8	2.8

[1] P. M. S. Blackett: Proc. Roy. Soc. (A) Vol. 103, p. 62—78, 1923.

The table contains also the average value of the relative average loss of energy suffered by the various particles per cm of the track, which loss Blackett takes to be proportional to $\frac{m}{R}$. Further Blackett assumes this loss to be proportional to the number of pairs of ions set free per cm, and this number again with approximation proportional to the square of the effective charge of the particle. The latter he therefore takes to be proportionat to $\sqrt{\frac{m}{R}}$, and the value of this quantity is given in the last column of the table. As the charge of the particles is by no means constant over the entire track this assumption may not be quite justified but will nevertheless presumably lead to an approximately correct result.

If the average energy neccessary to set free one pair of ions is w ergs, and if the entire kinetic energy of the particle is spent in the formation of ions, then — denoting the number of pairs of ions set free per cm by I — we have the following relations:

$$wIdR = \frac{1}{2}m\left[U^2 - (U - dU)^2\right] = mUdU.$$

or

$$wI = mU\frac{dU}{dR}, \tag{3}$$

but according to (2) we have

$$\frac{dU}{dR} = \frac{2a}{3U^{\frac{1}{2}}}. \tag{4}$$

From the equations (2)—(4) we get

$$I = \frac{2ma}{3w} \cdot U^{\frac{1}{2}} = \frac{2mU^2}{3wR} = \frac{4}{3} \cdot \frac{V_0}{RV'} = \frac{4}{3} \cdot \frac{V_0^{\frac{1}{4}}}{b \cdot V'}, \tag{5}$$

where V' is the ionization-voltage of the gas in which the particle moves.

The measurements carried out by Blackett unfortunately do not go down to such small velocities and ranges as those in which we are directly interested, but until further we will assume that the law expressed by equation (2) is also applicable to velocities from $2 \cdot 10^7$ to $10 \cdot 10^7$ cm sec.$^{-1}$. In order to give an idea of the magnitude of

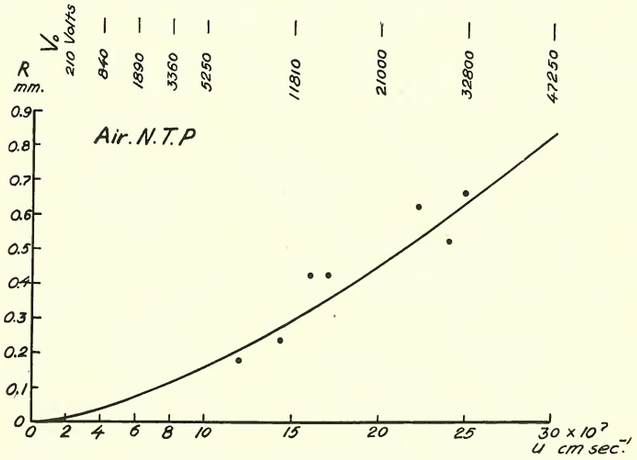

Fig. 1. Range of H^+ particles in Air N. T. P. according to Blackett.

the extrapolation thereby performed we have in fig. 1 marked by dots the corresponding values of velocity and range found by Blackett for H^+ particles in atmospheric air, while the curve shown has the equation

$$U^{\frac{3}{2}} = 6.2 \cdot 10^{13} R .$$

2. Velocity in Strong Fields.

Further we have

$$U = \sqrt{2 \frac{e'}{m} V_0} = c \sqrt{V_0} . \qquad (6)$$

From this expression and from equation (2) follows

$$\frac{dV_0}{dR} = X = \frac{2 V_0^{\frac{1}{2}}}{c} \cdot \frac{dU}{dR} = \frac{4 a V_0^{\frac{1}{2}}}{3 c U^{\frac{1}{2}}} = \frac{4 a}{3 c^2} \cdot U^{\frac{1}{2}} . \qquad (7)$$

Here X is the intensity of the electric field neccessary and sufficient to maintain the velocity U of the particle, assuming that the particle all the time has the charge e'.

In the following table B is shown among other things the value of c in equation (6) when V_0 is measured in volts for the particles investigated by Blackett. The figures given for α-particles refer actually to a helium atom with one positive charge.

Table B. Various properties of positive particles in air.

Particle	c	c^2	a	$\frac{a}{c^2}$	Relative Charge η	$\xi = \frac{4}{3\eta} \cdot \frac{a}{c^2}$	X for $U = 2 \cdot 10^7$ cm sec^{-1}
H^+	$13.8 \cdot 10^5$	$190 \cdot 10^{10}$	$6.2 \cdot 10^{13}$	32.6	1.0	43.5	$195 \cdot 10^3$ volt cm^{-1}
α-Part (H_e^+)	$6.9 \cdot 10^5$	$47.5 \cdot 10^{10}$	$3.3 \cdot 10^{13}$	69.6	1.5	61.8	$259 \cdot 10^3$ volt cm^{-1}
(Air)+	$3.6 \cdot 10^5$	$12.9 \cdot 10^{10}$	$1.9 \cdot 10^{13}$	148	2.1	94.2	$442 \cdot 10^3$ volt cm^{-1}
A^+	$2.2 \cdot 10^5$	$4.6 \cdot 10^{10}$	$1.2 \cdot 10^{13}$	263	2.8	125	$559 \cdot 10^3$ volt cm^{-1}

ξ indicates the factor by which $U^{\frac{1}{2}}$ is to be multiplied in order to obtain the intensity X of the electric field necessary to maintain the velocity of the particle in question in the gas in question, which latter in the above table is air at N. T. P. It must, however, be remembered that for this calculation of X it is assumed that the charge of the H-particle is equal to $+e$ over the entire track.

3. The Mean Value of the Charge of the Hydrogen Atom.

If l_1 is the average length of those parts of the track (in the direction of the force) along whick the H-particle

has the charge $+e$, i. e. is a proton, while l_2 is the corresponding average length of track along which the H-particle is a neutral hydrogen atom — and its charge consequently is zero — then the values found for X must evidently be multiplied by the factor

$$\mu = \frac{l_1 + l_2}{l_1} = 1 + \frac{l_2}{l_1}. \tag{8}$$

For the value of $\frac{l_1}{l_2}$ there exist a number of rather contradictory determinations. In the following we will apply only those given by E. RÜCHARDT[1]. Fig. 2 shows RÜCHARDT's

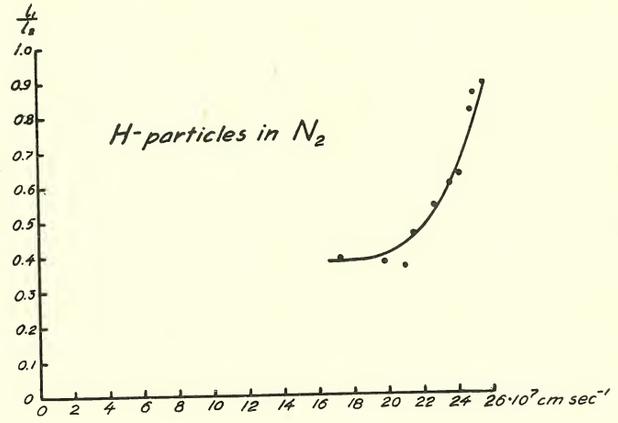

Fig. 2. Value of $\frac{l_1}{l_2}$ for H-particles in N_2 according to RÜCHARDT.

results with H-rays in N_2. For H-particles in 0_2 it seems that $\frac{l_1}{l_2}$ is somewhat smaller. Unfortunately none of the measurements deal with such relatively small velocities as those with which we have to do in the case of the Lichtenberg figures. An extrapolation must therefore be very uncertain. But RÜCHARDT's results seem to indicate

[1] E. RÜCHARDT: Ann. d. Phys. (IV). Bd. 71, p. 377—423, 1923.

that for H-particles in both H_2 and N_2 $\frac{l_1}{l_2}$ has decreased to its minimum value at velocities about $1.7 \cdot 10^8$ cm sec.$^{-1}$. Since no other information on this point is available, we will for the present assume that $\frac{l_1}{l_2}$ is constant at velocities from 10^7 to 10^8 cm sec.$^{-1}$ in which we are here interested, and we will put, for H-particles in atmospheric air

$$\frac{l_1}{l_2} = 0.4. \tag{9}$$

Although this value for $\frac{l_1}{l_2}$ is a little higher than the one found for N_2 and still more so in comparison to the one determined by RÜCHARDT for O_2, we have selected it because in all the cases in which we are particularly interested the particle will move in an exceedingly strong electric field which will tend to increase the relative velocity between the H-particle and the electrons set free by its collisions. This increase in relative velocity will decrease the probability that an electron is again captured by an H^+-particle, and consequently l_1 will be greater than it is without such a strong field, compare RÜCHARDT's work dealing with this question.[1]

4. The Value of the Ratio $\frac{l_1}{l_2}$ depends upon the Intensity of the Electric Field.

An exact treatment of this question is not possible at present owing to insufficient knowledge of the ionization — and recombination — processes. But in order to form an idea of the influence of a strong field on these pro-

[1] E. RÜCHARDT: Zeitschr. f. Phys. Bd. 15, p. 164—171, 1923. E. RÜCHARDT: Ann. d. Phys. (IV). Bd. 73, p. 228—236, 1924.

cesses we will subject the matter to some simple considerations based upon the ideas outlined by Rüchardt.

At first we assume the electric field to be zero. The particle having the charge $+e'$ moves with the velocity U_0 while the electrons are assumed to be at rest. With regard to the question of recombination we may as well consider the particle to be at rest and the electrons to move with the velocity U_0 relatively to the particle. The electrons that in a given moment are set free with the velocity zero — relative to the particle consequently with the velocity U_0 — and that are located around the particle within a sphere having the radius ϱ_0, will all move in eliptical orbits around the particle provided that ϱ_0 satisfies the following conditions.

$$\frac{1}{2} m U_0^2 = \frac{e \cdot e'}{\varrho_0}, \tag{10}$$

m denoting the mass of the electrons and $-e$ their charge.

Electrons set free outside this sphere will move in hyperbolic orbits and will consequently not be captured by the particle, while all those set free inside the sphere will be captured.

If we put $e = e' = 4.774 \cdot 10^{-10}$ E. S. E. and $m = 9 \cdot 10^{-28}\, g$ then

$$\varrho_0 = \frac{5.05 \cdot 10^8}{U_0^2}. \tag{10'}$$

For

$U_0 = 1 \cdot 10^7 \quad 2 \cdot 10^7 \quad 3 \cdot 10^7 \quad 4 \cdot 10^7 \quad 5 \cdot 10^7\ \mathrm{cm\,sec^{-1}}$

we get

$\varrho_0 = 5.05 \cdot 10^{-6}\ 1.26 \cdot 10^{-6}\ 5.6 \cdot 10^{-7}\ 3.16 \cdot 10^{-7}\ 2.02 \cdot 10^{-7}$ cm.

We will next consider the case where a constant field X (E. S. E.) acts parallel to the velocity U_0. Here an exact

treatment is very difficult, we will therefore take only a simple approximation.

Referring to figure 3, the particle is at a given moment located at P and an electron is set free at A. To begin with the electron has — in relation to the particle — the velocity U_0 in the positive direction of the X-axis. It is further acted upon by the electric field X which tends to

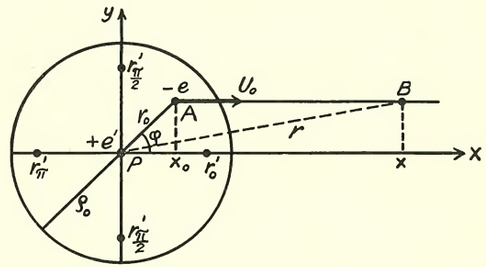

Fig. 3. Recapture of Electrons in Strong Electric Field.

increase the relative velocity. We now assume that the electron is continually moving out along the line AB which is parallel to the X-axis. This is of course not correct, since the track will be curved. But we are here not interested in the shape of the track itself but only whether the electron will infinitely continue its movement away from the particle, or return to its vicinity. In the latter case we consider it to be captured, in the first case not.

If the starting point A were located on the x-axis then the electron would remain there and would only be captured if at some distance or other its velocity decreases to zero. If this occurs then the electron will return to the particle, in the reverse case it would travel away. The conditions are quite analogous if the electron is bound to move along the line AB.

At the point B the velocity U_x of the electron is determined by

$$\begin{aligned}\frac{1}{2}mU_0^2 &= \frac{1}{2}mU_0^2 - \frac{ee'}{r_0} + \frac{ee'}{r} + eX(x-x_0)\\ &\cong \frac{1}{2}mU_0^2 - \frac{ee'}{r_0} + \frac{ee'}{x} + eX(x-x_0)\\ &= ee'\left(\frac{1}{\varrho_0} - \frac{1}{r_0} + \frac{1}{x}\right) + eX(x-x_0). \end{aligned} \tag{11}$$

The velocity U_x will be zero for $x = x'$ if

$$e'\left(\frac{1}{\varrho_0} - \frac{1}{r_0} + \frac{1}{x'}\right) + X(x'-x_0) = 0 \tag{12}$$

or when

$$x'^2 - x'\left[x_0 + \frac{e'}{X}\left(\frac{1}{r_0} - \frac{1}{\varrho_0}\right)\right] + \frac{e'}{X} = 0 \tag{13}$$

and consequently for

$$x' = \frac{1}{2}\left[x_0 + \frac{e'}{X}\left(\frac{1}{r_0} - \frac{1}{\varrho_0}\right)\right] \pm \sqrt{\frac{1}{4}\left[x_0 + \frac{e'}{X}\left(\frac{1}{r_0} - \frac{1}{\varrho_0}\right)\right]^2 - \frac{e'}{X}}. \tag{14}$$

A necessary condition for the velocity to become zero at all is that the value of x' as determined by (14) is real, that is, we must have

$$x_0 + \frac{e'}{X}\left(\frac{1}{r_0} - \frac{1}{\varrho_0}\right) \geqq 2\sqrt{\frac{e'}{X}}. \tag{15}$$

In the limiting case, to which the lowest sign of equation (15) applies, we have

$$x' = \sqrt{\frac{e'}{X}} \quad \text{or} \quad X = \frac{e'}{X'^2}, \tag{16}$$

so that the electric force in the point x' is zero. If the velocity has not gone quite to zero when the electron has attained this point then the velocity can never be zero.

Since $x_0 = r_0 \cos\varphi$ then the equality in (15) gives the following equation for the determination of the maximum value r' of r_0, for which the electron will return to the vicinity of the particle:

$$r'^2 - r'\frac{2}{\cos\varphi}\left(\sqrt{\frac{e'}{X}} + \frac{e'}{2\varrho_0 X}\right) + \frac{1}{\cos\varphi}\cdot\frac{e'}{X} = 0 \tag{17}$$

and therefore

$$\begin{aligned} r' = &\left[\frac{1}{\cos\varphi}\cdot\left(1 + \frac{1}{2\varrho_0}\sqrt{\frac{e'}{X}}\right)\right.\\ &\left.\pm\sqrt{\frac{1}{\cos^2\varphi}\left(1 + \frac{1}{2\varrho_0}\sqrt{\frac{e'}{X}}\right)^2 - \frac{1}{\cos\varphi}}\right]\cdot\sqrt{\frac{e'}{X}}. \end{aligned} \tag{18}$$

For $\varphi = 0$ we have

$$r' = \left[1 + \frac{1}{2\varrho_0}\sqrt{\frac{e'}{X}} - \sqrt{\frac{1}{\varrho_0}\sqrt{\frac{e'}{X}} + \frac{1}{4\varrho_0^2}\cdot\frac{e'}{X}}\right]\cdot\sqrt{\frac{e'}{X}} = r'_0,$$

and for $\varphi = \frac{\pi}{2}$ we have

$$r' = \frac{\frac{1}{2}\sqrt{\frac{e'}{X}}}{1 + \frac{1}{2\varrho_0}\sqrt{\frac{e'}{X}}} = r'_{\frac{\pi}{2}},$$

and for $\varphi = \pi$ we have

$$r' = \left[-\left(1 + \frac{1}{2\varrho_0}\sqrt{\frac{e'}{X}}\right) + \sqrt{2 + \frac{1}{\varrho_0}\sqrt{\frac{e'}{X}} + \frac{1}{4\varrho_0^2}\cdot\frac{e'}{X}}\right]\cdot\sqrt{\frac{e'}{X}} = r'_\pi. \tag{19}$$

The space within which the electrons return and are captured may then with approximation be reckoned to be a sphere having the radius ϱ' determined by

$$\varrho' = \frac{1}{4}\left(r'_0 + 2r'_{\frac{\pi}{2}} + r'_\pi\right). \tag{20}$$

The electric field has thus decreased the space within which capturing occurs in the ratio

$$\nu = \left(\frac{\varrho'}{\varrho_0}\right)^3. \qquad (21)$$

In table C below are given values of ν calculated for a series of velocities from $1 \cdot 10^7$ to $1 \cdot 10^8$ cm sec.$^{-1}$ assuming there is a field intensity $X = 10^3$ E. S. U. $= 3 \cdot 10^5$ Volt cm^{-1}.

Table C. Values of ν for various velocities and for $X = 3 \cdot 10^5$ volts cm^{-1}; $\sqrt{\frac{e'}{X}} = 6.9 \cdot 10^{-7}$ cm.

U_0	ϱ_0	r'_0	$r'_{\frac{\pi}{2}}$	r'_π	ϱ'	$\nu = \left(\frac{\varrho'}{\varrho_0}\right)^3$
	cm	cm	cm	cm	cm	
$1 \cdot 10^7$	$5.05 \cdot 10^{-6}$	$4.82 \cdot 10^{-7}$	$3.23 \cdot 10^{-7}$	$2.70 \cdot 10^{-7}$	$3.50 \cdot 10^{-7}$	0.00033
$2 \cdot 10^7$	$1.26 \cdot 10^{-6}$	$3.34 \cdot 10^{-7}$	$2.71 \cdot 10^{-7}$	$2.39 \cdot 10^{-7}$	$2.79 \cdot 10^{-7}$	0.011
$3 \cdot 10^7$	$5.6 \cdot 10^{-7}$	$2.38 \cdot 10^{-7}$	$2.14 \cdot 10^{-7}$	$1.96 \cdot 10^{-7}$	$2.15 \cdot 10^{-7}$	0.057
$4 \cdot 10^7$	$3.13 \cdot 10^{-7}$	$1.72 \cdot 10^{-7}$	$1.63 \cdot 10^{-7}$	$1.52 \cdot 10^{-7}$	$1.62 \cdot 10^{-7}$	0·137
$5 \cdot 10^7$	$2.02 \cdot 10^{-7}$	$1.31 \cdot 10^{-7}$	$1.27 \cdot 10^{-7}$	$1.24 \cdot 10^{-7}$	$1.27 \cdot 10^{-7}$	0.262
$1 \cdot 10^8$	$5.05 \cdot 10^{-8}$	$4.83 \cdot 10^{-8}$	$4.43 \cdot 10^{-8}$	$4.14 \cdot 10^{-8}$	$4.14 \cdot 10^{-8}$	0.69

For small velocities, l_1 must accordingly be many times smaller with the strong field than without such a field, while l_2 will presumably be nearly independent of the field. This relation will, however, hardly be so pronounced as appears from the above table, because the density of the electrons will presumably be the greatest near the particle. In the table we have reckoned with a uniform density of released electrons.

A H^+-particle will presumably need less energy in order to penetrate the air than a H-atom. Since the strong field increases the value of $\frac{l_1}{l_2}$ it tends to reduce the energy

necessary to maintain a certain velocity for a H-particle as compared to the value arrived at by calculations based upon Blackett's investigations where no field was employed.

5. Relation between the Intensity of the Electric Field and the Velocity of Positive Particles.

According to table B and the formulae (8) and (9) the field intensity necessary to maintain the velocity $U_0 = 2 \cdot 10^7$ cm sec.$^{-1}$ should be

$$X = 195\,000 \left(1 + \frac{1}{0.4}\right) = 683\,000 \text{ volts cm}^{-1}. \qquad (22)$$

Considering the influence of the strong field on the ability of the H^+-particle to capture electrons it will presumably be reasonable to reduce the value given for the necessary field intensity, and as a rough estimate we put it at

$$X = 300\,000 \text{ volts cm}^{-1} \text{ for } U_0 = 2 \cdot 10^7 \text{ cm sec.}^{-1}. \qquad (23)$$

Although this value is only based upon a rough estimate it may presumably be of the right order of magnitude.

6. Collisions between Slow Positive Particles and neutral Molecules.

It may certainly be considered doubtful whether positive ions having a velocity less than that corresponding to 20—30 volts are able to ionize common gases at all. The ionizing ability of these slow positive ions is at all events extremely small[1]. W. J. Hooper (l. c.) is furthermore of the opinion that even at velocities corresponding

[1] J. Franck und P. Jordan: Handb. d. Phys. Bd. 23, p. 730—733, 1926. W. J. Hooper: Phys. Rev. (II) vol. 27, p. 109, 1926.

to 925 volts, positive ions in hydrogen at low pressures (0.012 mm) produce very little or no ionization at all, while at this velocity the ionization seems to be quite considerable at higher pressures.

From experiments carried out by W. Aich[1] it appears that the cross-sectional area of hydrogen molecules, determined for movements of protons in hydrogen, is very nearly the same as the gas-kinetic cross-sectional area if the proton is considered to have infinitesimal dimensions.

Similar relations presumably exist in connection with slow protons in other gases.

From investigations with protons having a velocity corresponding to about 900 volts A. J. Dempster[2] draws the conclusion that the effective cross-sectional area of hydrogen- and helium-molecules in case of collisions with protons of this velocity is very nearly equal to zero, and the protons therefore — just as electrons — should show the Ramsauer-effect if their velocity is about $4 \cdot 10^7$ cm sec.$^{-1}$. In that case also, no alternations should occur in the charge of the proton.

It will hardly be possible to take a definite stand-point with regard to these questions at the present time.[3] There is at all events hardly any reason to assume that nitrogen, oxygen, carbonic acid, and other gases that do not show the Ramsauer-effect in connection with electrons, should do so in connection with protons, and what we have set forth above in Chapt. IV indicates, in our opinion definitely, that this will not be the case.

[1] W. Aich: Zeitschr. f. Phys. Bd. 9, p. 372—378, 1922.

[2] A. J. Dempster: Proc. Nat. Acad. Sc. Amer. vol. 11, p. 552—554, 1925; vol. 12, p. 96—98, 1926.

[3] Compare for example: E. Rüchardt in Handb. d. Phys. Bd. 24, p. 99—101, 1927 and W. Wien: Handb. d. Experimentalphysik Bd. 14, p. 527, 1927.

The conditions are different with the noble gases which we have had no opportunity to investigate in a perfectly pure state. Here our investigations are not decisive, but some observations in connection with helium indicate that the results found for this gas by Dempster are correct.

7. Resume.

Even though the material of experimental results at hand is very incomplete we are, no doubt, on the safe side when we assume that:

At velocities which are smaller than that corresponding to 20—30 volts, the positive ions — including the protons — will only in an extremely small degree have an ionizing effect on those gases referred to in the investigations here discussed, while the molecules of those gases, for collisions with positive ions, show nearly the same cross-sectional area as they should have according to the kinetic gas-theory.

At velocities corresponding to more than 10 000 volts, any kind of positive ions have a strongly ionizing effect in any kind of gas.

At velocities corresponding to more than a few hundred volts all positive ions — except the protons — will have a strongly ionizing effect in any kind of gas.

At velocities corresponding to more than a few hundred volts the protons will also have a strongly ionizing effect in all gases except the noble ones and possibly hydrogen. In the noble gases — and possibly in hydrogen — the protons do not cause ionization up to velocities corresponding to about 900 volts.

APPENDIX II

1. Dispersion of Positive or Negative Charges.

We put the velocity v of the ions equal to

$$v = kE, \tag{1}$$

where E is the electric field intensity and where k may be considered to be constant within very wide limits; for example for air at N. T. P. from $E = 0.1$ to $E = 20\,000$ volts cm.$^{-1}$.[1] Within very wide limits, k is inversely proportional to the air pressure p, so that we may write

$$k = \frac{k_0}{p}, \tag{1'}$$

where k_0 is a constant independent of the air pressure.

If we are not taking into account the mutual repulsion between the single particles, then the density of these will not be varied by their movement in an outer electric field. To understand this, we may just consider a space-element, the outer boundaries of which are a thin tube of lines of force representing the outer field, and two equipotential surfaces (1) and (2) having the areas f_1 and f_2 (see fig. 1). The electric field at these surfaces are respectively E_1 and E_2. We then have:

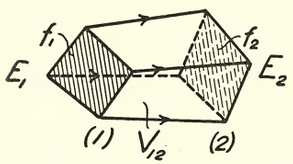

Fig. 1. Element of space having for boundaries a tube of lines of force as shown, and the two equipotential surfaces having the areas f_1 and f_2.

[1] See L. B. Loeb: "Kinetic Theory of Gases", p. 440, 1927.

$$f_1 E_1 = f_2 E_2. \tag{2}$$

During the time dt the volume of the element of charge at the area (1) will, owing to displacement of the charge be reduced by $f_1 v_1 dt = f_1 k E_1 dt$, and at the area (2) be increased by $f_2 v_2 dt = f_2 k E_2 dt$, but since according to equation (2) $f_1 v_1 = f_2 v_2$ the volume of the element of charge will remain unaltered. Variations in the volume — and consequently also in the density — can therefore be due only to the repulsive forces within the element of charge in question, and we shall therefore proceed to discuss the effect of this repulsion.

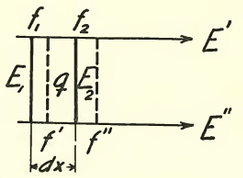

Fig. 2. E' and E'' denotes lines of force; f_1 and f_2 equipotential surfaces.

The two equipotential surfaces of which f_1 and f_2 are sections, are separated by the infinitesimal distance dx, and for the areas f_1 and f_2, circumscribed by the tube of lines of force, we therefore have that $f_1 = f_2$. During the time dt, f_1 covers the volume $f_1 v_1 dt$ while f_2 covers the volume $f_2 v_2 dt = f_1 v_2 dt$.

The element of space is consequently increased from $f_1 \cdot dx$ to $\left(f_1 \ (dx + \frac{v_2 - v_1}{dx} \cdot dx\, dt\right)$.

The relative increase in volume is consequently

$$\frac{dV}{V} = \frac{v_2 - v_1}{dx} \cdot dt, \tag{3}$$

where V is the volume of the space-element.

If the electric density at the point in question is q, then we have

$$\frac{v_2 - v_1}{dx} = k \frac{E_2 - E_1}{dx} = 4\pi q k. \tag{4}$$

We consequently get

$$\frac{1}{V}\cdot\frac{dV}{dt} = 4\pi qk, \qquad \text{(I)}$$

or

$$\frac{dV}{dt} = 4\pi kQ, \qquad \text{(II)}$$

where $Q = q \cdot V$ is the total charge of the space-element V.

Since $Vdq + qdV = 0$ then (I) may be written

$$-\frac{dq}{dt} = 4\pi kq^2. \qquad \text{(III)}$$

From this equation we see that if the density was originally constant, $q = q_0$, then the density will always have the same value all over but this value itself will decrease at the rate

$$\frac{1}{q} - \frac{1}{q_0} = 4\pi kt. \qquad \text{(IV)}$$

For an infinitely long cylinder, no movement occurs in the direction of the axis of the cylinder and consequently in (II) we can replace V by the cross-sectional area A of the cylinder, if at the same time instead of Q we insert the quantity of charge per cm length of the cylinder, Q_1.

$$\frac{dA}{dt} = 4\pi kQ_1. \qquad \text{(II')}$$

If we put $A = \pi R^2$ then equation (II') will be

$$R\frac{dR}{dt} = 2kQ_1 \qquad \text{(II'')}$$

or $R^2 - R_0^2 = 4kQ_1t$, where R_0 is the radius for $t = 0$.

If mn (fig. 3) is a plane surface on which the charge q is distributed, and if the ordinates to the curve $abcd$ are equal to the corresponding values of q, then the electric strength acting out along the surface will be smaller

at the point d than at the point c' at which latter point the charge-curve is assumed to have a point of inflection. If we draw a curve $d'c$ symmetrical to cd with regard to $c'c$ then the outwardly directed field in c' will originate

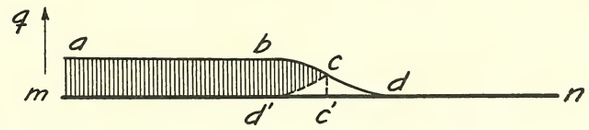

Fig. 3. The spreading out of a charge q along a plane surface mn.

from the shaded part of the front of the charge. The electric strength will therefore have very nearly its highest value at the point of inflection c'. The charge at c' will consequently move outward with greater velocity than will the charge outside this point. The steepness of the outermost front will consequently gradually increase as the charge is spreading out.

Near the centre of a large, plane charge — see fig. 4 — we shall have

$$D - D_0 = 4\pi kq_1t. \qquad \text{(V)}$$

At the edge, the charge will disperse with a somewhat smaller velocity, so that after a while its outer boundary will have the form shown by the dotted line, and then it will gradually approach a spherical form.

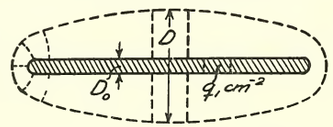

Fig 4. The spreading out of a plane electric charge.

In order to form an idea of the tendency of an originally flat front of an electric charge to assume a steeper form we will treat a couple of geometrically simple cases where the calculations offer no difficulty. The first one is a spherically distributed charge in which the density q

depends only on the time and on the radius r from a fixed centre. In the second case — a charge having cylindrical form — q depends only on the distance r from the straight line representing the axis of the cylinder.

According to (III) the charge-density q at a distance r decreases during the time dt from q to $q - 4\pi k q^2 dt$ while the charge-density $\left(q + \frac{dq}{dr} \cdot dr\right)$ at a distance $r + dr$ during the same time interval decreases to $(q+dq) - 4\pi k (q+dq)^2 \cdot dt$.

The difference Δq between the charge-densities, (which originally was $\Delta q_{(t=0)} = dq$), is after the time dt.

$$\Delta q_{(t=dt)} = dq\,(1 - 8\pi k q\, dt). \tag{5}$$

In case of the spherical charge we have according to (1)

$$v = k \cdot \frac{Q_r}{r^2}, \tag{6}$$

where Q_r is the total charge within the sphere of radius r.

During the time dt the distance $\Delta r_{(t=0)} = dr$ between the two charge-particles will change to

$$\Delta r_{(t=dt)} = dr + \frac{dv}{dr} \cdot dt = dr\left(1 + 2k\,\frac{2\pi q r^3 - Q_r}{r^3} \cdot dt\right). \tag{7}$$

From (5) and (7) we get

$$\left(\frac{\Delta q}{\Delta r}\right)_{(t=dt)} = \frac{dq}{dr} \cdot \left[1 - 2k\left(6\pi q - \frac{Q_r}{r^3}\right) dt\right]. \tag{8}$$

In the preceding the products $(k \cdot Q_r)$ and $(k \cdot q)$ are always positive (compare equation (1)), and from equation (8) it therefore appears that the steepness of the front will remain unaltered for

$$6\pi q = \frac{Q_r}{r^3} = \frac{4}{3}\pi \cdot q_0 \quad \text{or for} \quad q = \frac{2}{9} \cdot q_0, \tag{9}$$

where q_0 is the mean density of the charge within the sphere of radius r.

From (8) and (9) appears that the steepness of the charge-curve increases for $q < \frac{2}{9} \cdot q_0$ and decreases for $q > \frac{2}{9} \cdot q_0$.

For the cylindrical charge distribution we get, in a corresponding manner,

$$\left(\frac{\Delta q}{\Delta r}\right)_{(t=dt)} = \frac{dq}{dr} \cdot \left[1 - 2k\left(6\pi q - \frac{Q_r}{r^3}\right) \cdot dt\right], \tag{10}$$

so that the steepness of the charge-curve increases when

$$6\pi q < \frac{Q_r}{r^2} = \pi q_0 \quad \text{or} \quad q < \frac{1}{6} q_0, \tag{11}$$

while in the opposite case it decreases.

These calculations confirm the fact that the moving front of an electric charge will have a tendency to increase in steepness.

We shall further give some examples where the results from the foregoing may be applied.

Examples:

(1) A homogeneous sphere has a radius R and the total charge Q. We have

$$\frac{dR}{dt} = k \cdot E = k\,\frac{Q}{R^2} \tag{12}$$

and

$$\frac{dV}{dt} = \frac{d\left(\frac{4\pi}{3} R^3\right)}{dt} = 4\pi k Q,$$

which agrees with equation (II).

(2) For a homogeneous circular infinitely long cylinder having the radius R and the charge Q_1 per cm of length we have

$$\frac{dR}{dt} = k \cdot \frac{2\,Q_1}{R}$$

and

$$\frac{dV}{dt} = \frac{d(\pi R^2)}{dt} = 4\,\pi\,k\,Q_1\,. \qquad (13)$$

2. Dispersion of Positive and Negative Charges.

If there are ions of both signs present, and if the charge-densities are respectively q_+ and q_- then the resultant density will be $q = q_+ - q_-$.

In the preceding, we have assumed that only ions of the one sign were present, but the results found are of course also valid with approximation in the case when ions of both signs are present, provided that those of the one sign are extremely few compared to those of the op posite sign.

Finally, if q_+ and q_- have such great values that the ionized area may be considered to have infinitely good conductivity, then the surplus of charge Q will collect on the surface of the area, and a further extension of the area can then be determined by means of simple electrostatic considerations.

A sphere or a cylinder of such a conductivity will thus expand in accordance with the formulae (5) and (6) above.

Also in this case, the outer boundary of the charge will have a tendency to become sharp, since stray ions found outside the charge, but being of the same sign as this, will move more slowly than the surface of the charge.

APPENDIX III

1. The Shape of the Positive and Negative Spreaders at the Meeting Point.

There is still a single phenomenon — appearing quite peculiar at first sight — which we will just touch upon, although it does not directly belong to the regular Lichtenberg figures the theory of which has been our sole object in the preceding. Our purpose is to prevent that some readers should find the phenomenon in question to be contradictory to the above evolved theory of the formation of the positive Lichtenberg figures.

If, in the arrangement outlined in fig. 23, the conditions are so selected that the positive and the negative spreaders only just reach each other, very peculiar features are often observed at the place where the two figures meet. An example is shown in L. F. I, fig. 63 and enlarged reproductions of others are shown on plate 24. Of these latter, we will first discuss the upper meeting point in part II.

From the end of the positive spreader, a strongly luminous thread projects over to the edge of the negative figure, where it ends in a strongly luminous spot at the outer end of a negative spreader. This luminous thread has the same characteristics as the subsequent negative discharges in — or along — positive spreaders. (See for example plates 12 VIII, 18 I and 20 I). A closer inspec-

tion of the examples reproduced in plate 24 shows that those negative spreaders which have come into contact with the positive ones are more luminous than those that have no connection. There can be no doubt that in the cases considered negative electricity flows over to the end of the positive spreaders. So far the phenomenon is clear enough.

A number of peculiar features may, however, be observed on this link between the positive and the negative

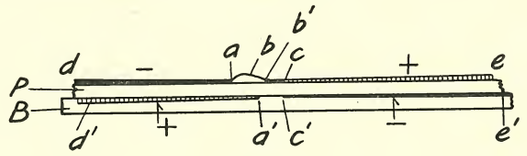

Fig. 1.

spreaders. All of the four junctions on plate 24 show such a strongly luminous spot at the end of the respective negative spreaders, but in all of the four cases the luminosity is comparatively faint in the immediate vicinity of the spot and this is so on both the positive and the negative side. Something similar is apparent on the other figures shown in plate 24.

In order to explain the faintness in luminosity on the positive side of the spot we may, by referring to fig. 1, propose the following. The regular negative figure *da* has just reached the point *a* at the same moment when the regular positive figure has reached the point *c*, and would normally have stopped here but for the negative figure which exerts an attraction on it. Under this influence, the positive spreader proceeds to *b'*. The electric field extending from the negative charge is here still stronger than at *c* and the positive spreader will proceed further, but the

field has here a slightly different direction because the induced positive charge *d'a'* on the metal plate *B* at *a'* projects a little beyond the edge *a'* of the negative discharge. This positive charge at *a'* changes the direction of the electric field at the tip of the positive spreader from the usual downward to a somewhat upward direction at the point *b*. A little further forward near the point *a* the electric field from the negative spreaders will predominate and the positive spreader will "strike down" in the end-point *a* of the negative spreader.

In the case where the positive and negative figures are placed nearer together, so that near the meeting line both of the figures are still moving on at a considerable velocity, the positive spreaders will be held down against the photographic plate all the way until where they join with the negative ones. Examples of this are shown plate 24 I. The positive spreaders are in this case of no greater luminosity than usual although the corresponding negative spreaders show that a flow of negative electricity has taken place in the direction of the positive electrode, but this circumstance is quite analogous to what is mentioned in chap. III 4 (a) (see also fig. 20).

This terminates our discussion of the relations shown by positive figures where they join with negative ones.

2. Distribution of the Photographic Intensity at the Meeting Point.

In this connection also we observe certain peculiarities, as for instance the formation of luminous wings, stretching out from the point of junction. A satisfactory and thorough explanation of this light distribution can hardly

be given at present, although the main features may be explained without difficulty.

The luminous effect is in the main due to three different causes. It is partly due to the comparatively strong light emitted from the luminous thread $abb'c$ (fig. 1) and especially from the part abb' which is raised a little above the photographic film; and partly to the light emitted by the recombination of the positive and negative ions which are present immediately at the surface of the film. The most active factor here is presumably the recombination of electrons with positive ions, while the recombination between positive and negative atomic or molecular ions seems to occur without the emission of any great amount of actinic light.

We shall next discuss some particulars concerning the distribution of the light. In those cases where the positive and negative spreaders just get into contact with each other, a strongly luminous junction-point is visible in the outer faint part of the negative spreader; see for example the upper point of junction in part II and the two middle ones in part III plate 24. This feature is less pronounced in the cases where the positive and negative eleetrodes are placed nearer to each other; see for example the lower points of junction in II and III and all of the points of junction in IV plate 24.

In the first mentioned cases the formation of the negative figure is completed before the positive figure reaches over to it. The junction will then occur at the edge of that area outside the strongly luminous negative figure to which the charge has further moved after the photographic figure was in reality completed, and at a moment when the electrons have already combined with oxygen-, water- or other

molecules to form molecular ions. In this case the point of junction will be located outside the strongly luminous part of the negative spreaders.

If, on the contrary, the electrodes are placed so near each other that the positive spreaders reach the negative ones before the formation of the latter is completed, then the point of junction will be located in that part of the negative figure where ionization by collision occurs and where light is consequently produced.

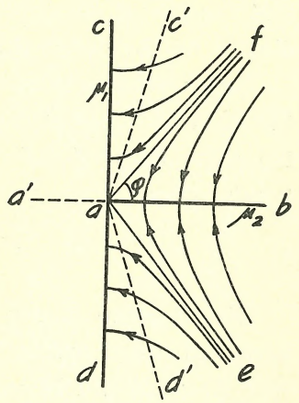

Fig. 2. Charge- and field-distribution after the joining of a positive spreader ba with a negative spreader $a'a$.

At the moment the positive spreader has joined with the negative one at a, electrons will start out along the positively charged spreader where they will cause ionization by collision, which is followed by recombinations which will produce the strongly luminous tracks visible in the figures, while the charge of these tracks will simultaneously change from positive to negative.

The charge- and the field-distribution thus obtained are outlined in fig. 2. The line cad marks the boundary of the negative charge at the moment when the positive spreader reaches the point a. The track ab will then, as mentioned, rapidly become negatively charged, whereupon we shall have the field-distribution shown.

We may with approximation assume the field from the negative figure to be produced by a charged line cad having the charge density $-\mu_1$, since the influence of

that part of the charge which is located to the left of *cad* is mainly compensated by the influence of the induced positive charge on the plate B below (see fig. 1). We will further assume the charge density along *ab* to be equal to μ_2. For the sake of simplicity we will further assume that the charge along *ba* projects to the left from *a* as indicated by the dotted line *aa'*.

Under these assumptions the lines of force will take the form of hyperbolae with the axis *ab*, *ac* and *ad* while the asymptotes *af* and *ae* with *ab* form the angle φ determined by

$$tg\ \varphi = \sqrt{\frac{\mu_2}{\mu_1}}.$$

The negative charge at great distances from *a* will move on with practically unaltered velocity, while its spreading out will be completely stopped at *a*. The boundary line of the negative charge will consequently acquire a bend at *a* and after a while it will follow the dotted line *c'ad'*. If this line is reached by the negative charge at the moment when the light from the luminous track *abb'* (fig. 1) is releasing a considerable number of electrons by photoelectric effect, then a strong ionization by collision will occur along the line *c'ad'* since here, according to appendix 2, the charge-density changes quite suddenly and therefore a strong field will exist. The subsequent recombination will then produce the luminous "wings".

CONTENTS

CHAPTER I

CHAPTER II

CHAPTER III

The Properties of the Positive Figures.

CHAPTER IV
The Formation of the Positive Figures.

APPENDIX I
On Positive Particles.

APPENDIX II

APPENDIX III

Forelagt paa Modet den 20. Januar 1928.
Færdig fra Trykkeriet den 28. Maj 1929.

MATHEMATISK-FYSISKE MEDDELELSER

UDGIVNE AF

DET KGL. DANSKE VIDENSKABERNES SELSKAB

7. BIND (Kr. 17,70):

1. Bohr, Harald: Unendlich viele lineare Kongruenzen mit unendlich vielen Unbekannten. 1925 ..... 1.40
2. Hartmann, Jul., and Trolle, Birgit: On Beat-phenomena in Cylindrical Tubes exposed to Sound-waves. With three plates. 1925 ..... 2.85
3. Pauli, W. jr.: Ueber die Intensitäten der im elektrischen Feld erscheinenden Kombinationslinien. 1925 ..... 0.65
4. Hardy, G. H. and Littlewood, J. E.: A theorem concerning series of positive terms, with applications to the theory of functions. 1925 ..... 0.90
5. Steffensen, J. F.: On a Generalization of Nörlund's Polynomials. 1926 ..... 1.00
6. Hartmann, Jul., and Trolle, Birgit: New investigation on the air jet generator for acoustic wawes. 1926 ..... 2.40
7. Mollerup, Johs.: Sur l'approximation d'un nombre irrationnel par des carrés rationnels. 1926 ..... 0.80
8. Nielsen, Niels: Sur certains développements d'une fonction holomorphe. 1926 ..... 0.75
9. Bjerrum, Niels: Untersuchungen über Ionenassoziation. I. Der Einfluss der Ionenassoziation auf die Aktivität der Ionen bei mittleren Assoziationsgraden. 1926 ..... 2.00
10. Nielsen, Niels: Recherches sur les fonctions cylindriques et sur certaines fonctions analogues. 1926 ..... 1.35
11. Hevesy, G.: On the Missing Element 87. 1926 ..... 0.60
12. Kuhn, W.: Die Stärke der anomalen Dispersion in nicht leuchtendem Dampfe von Thallium und Cadmium. 1926 .... 3.75
13. Sugiura, Y. and Urey, H. C.: On the Quantum Theory explanation of the Anomalies in the 6th and 7th Periods of the Periodic Table. 1926 ..... 1.15
14. Burrau, Øyvind: Berechnung des Energiewertes des Wasserstoffmolekel-Ions (H_2^+) im Normalzustand. 1927 ..... 0.90
15. Knudsen, Martin: The Hot-wire Manometer. 1927 ..... 0.80
16. Juel, C.: Om v. Staudt's Definitioner. 1927 ..... 0.85
17. Pólya, G.: Über die algebraisch-funktionentheoretischen Untersuchungen von J. L. W. V. Jensen. 1927 ..... 1.40

8. BIND (Kr. 17,20):

1. Hille, Einar: On the Logarithmic Derivatives of the Gamma Function. 1927 ..... 2.40